Evaluation and optimisation of photovoltaic (PV) plant designs

by

Tafadzwa L. Gurupira

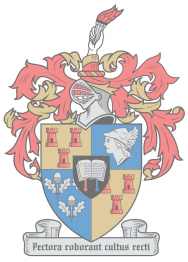

Thesis presented in partial fulfilment of the requirements for the degree of Master of Engineering (Electrical) in the Faculty of Engineering at Stellenbosch University

Supervisor: Dr. A. J. Rix

March 2018

Declaration

By submitting this thesis electronically, I declare that the entirety of the work contained therein is my own, original work, that I am the sole author thereof (save to the extent explicitly otherwise stated), that reproduction and publication thereof by Stellenbosch University will not infringe any third party rights and that I have not previously in its entirety or in part submitted it for obtaining any qualification.

Date: March 2018 .....

Abstract

Evaluation and optimisation of photovoltaic (PV) plant designs

T. L Gurupira

Department of Electrical and Electronic Engineering,
University of Stellenbosch,
Private Bag X1, Matieland 7602, South Africa.

Thesis: MEng (Electrical)

December 2017

Factors such as the increasing energy demand, the depletion of fossil fuels and the push for more sustainable, less polluting energy sources have resulted in increased interest and investments in renewable energy sources worldwide. Among these renewable energy sources is solar photovoltaics (PV). PV is, however, riddled with several challenges of its own such as a lack of an efficient, integrated and holistic approach to the PV system design optimisation. Towards this end, the PV system design process is reviewed, and two optimisation frameworks are formulated and presented as potential solutions. Of particular interest was how applicable these frameworks would be in a South African context so two existing plants in the Northern Cape province of South Africa were adopted as test cases; one for the fixed tilt investigations and the other for the single-axis tracking investigations. A constrained minimisation algorithm was used to simultaneously evaluate various design variables to maximise the system total annual energy output, maximise the system's performance ratio and minimise system losses in the single objective optimisation problems. On the other hand, several design variables and objectives were simultaneously evaluated in the multi-objective optimisation cases and a multi-criteria decision making (MCDM) procedure was used to rank the various alternative optimal PV system layouts to help select the most suitable layout for the given design scenario. The successful integration of the optimisation algorithms and a reputable solar PV system design tool led to faster execution of optimisation procedures and a more holistic approach to system design while ensuring PV system modelling accuracy, expansiveness and adaptability to several design scenarios.

Uittreksel

Evaluation and optimisation of photovoltaic (PV) plant designs

T. L Gurupira

Departement Elektriese en Elektroniese Ingenieurswese,
Universiteit van Stellenbosch,
Privaatsak X1, Matieland 7602, Suid Afrika.

Tesis: MIng (Elek)

Desember 2017

Daar is wêreldwyd 'n toenemende belangstelling in hernubare-energiebronne as gevolg van 'n hoër en stygende aanvraag na energie, asook die potensiële finansiële-winsgewendheid wat hierdie bronne aanbied vir beleggers. Verder voorsien hernubare-energie bronne ook die geleenthied om ons afhanklikheid vanaf besoedelende fossielbrandstowwe te verminder. Fotovoltaïese energie is onder andere een van hierdie hernubare energie bronne. Die proses van energieverskaffing, deur middel van fotovoltaïese aanlegte, bied egter nog na 'n paar uitdagings, soos byvoorbeeld 'n gebrek aan 'n optimale ge- ïntegreerde en holistiese benadering tot die ontwerp van fotovoltaïese stelsels. Met hierdie doel voor oë, word die ontwerp van die fotovoltaïese stelsel hersien, tesame met die verdere toepassing van twee optimerings-metodes. Dit was verder van groot belang om die toepassing van hierdie metodes in die konteks van Suid-Afrika te ondersoek. Daarom is twee bestaande Fotovoltaïese aanlegte in die Noord-Kaap as toetsgevalle gebruik; een aanleg is gebruik vir die ondersoek van 'n stasionêre-uitleg en die ander vir die ondersoek van 'n enkel-as-volger-uitleg. 'n Beperkte optimerings-algoritme is gebruik om gelyktydig verskeie ontwerpsveranderlikes te evalueer, sodat die totale jaarlikse energie gelewer, asook die stelsel se prestasieverhouding gemaksimeer word. Hierdie doelwitte, tesame met die vermindering van stelselverliese, is in ag geneem vir die enkel-doelwit-optimerings-probleme. Aan die ander kant was daar verskeie veranderlikes en doelwitte gelyktydig geëvalueer in die multidoelwit-optimerings-gevalle. 'n Multi-kriteria-besluitnemings-prosedure is gebruik om 'n rangorde toe te ken aan die verskillende optimale Fotovoltaïese stelsel uitlegte, om die mees geskikte uitleg vir die gegewe ontwerpsgevalle te vind. Die suksesvolle integrasie van die optimeringsalgoritmes, asook 'n betroubare Fotovoltaïese-stelsel-ontwerps-program, het gelei tot die spoedige uitvoering van die optimeringsproses, tesame met 'n meer holistiese benadering tot stelselontwerp. Die doelwitte gestel is almal beriek, asook die effektiwiteit aangaande die ontwerp van die fotovoltaïese modellering, skalering en aanpasbaarheid vir verskeie ontwerpsgevalle is aangespreek.

Acknowledgements

I would like to express my sincerest gratitude to the following people and organisations:

- God almighty for the opportunity, the gift of life and blessings that have seen me get this far,
- Dr Arnold Rix, my supervisor, for his assistance and guidance,
- Scatec Solar for the funding my studies,
- My family and friends for their support, prayers and encouragement,
- My friends and fellow office mates: Brian De Beer, JP Botha and the rest of the PV and Media Lab guys for their wisdom, the memories we made and the endless banter that made the masters work more bearable. A special mention out of this group goes to Warren Farmer and Armand Du Plessis for their help with the translation of this thesis' abstract to Afrikaans.

Dedications

I would like to dedicate this thesis to my family. You did all you could to see me get this far and I will continue to do all I can to represent you and make you proud.

Contents

List of Figures

List of Tables

Nomenclature

AC	Alternating Current
AHP	Analytical Hierarchical Processes
AM	Air Mass
Ambtemp	Ambient temperature
AOI	Angle Of Incidence
ASCI	American Standard Code for Information Interchange
BoS	Balance of system
BW	Bid Window
CdTe	Cadmium Telluride
CF	Capacity Factor
CIS	Copper Indium Silinum
CM	Circuit Mismatch
CSP	Concentrated Solar Power
CSV	Comma Separated Values
DC	Direct Current
DHI	Diffuse Horizontal Irradiance
DISC	Direct Insolation Simulation Code
DNI	Direct Normal Irradiance
EQT	Equation Of Time
E-W	East-West
EMF	Electromotive Force
GCR	Ground Cover Ratio
GHI	Global Horizontal Irradiance
G*inc*	Global Incident Irradiance
GW	Gigawatt
GW_p	Gigawatt peak
IAM	Incidence Angle Modifier
IPP	Independent Power Producer
ISO	International Organisation of Standardisation

LCOE	Levelized Cost Of Energy
LID	Light Induced Degradation
LST	Local Solar Time
MCDM	Multiple Criteria Decision Making
MLPE	Module Level Power Electronics
MPPT	Maximum Power Point Tracking
MW	Megawatt
MW_p	Megawatt peak
MWh	Megawatt hour
NASA	National Aeronautics and Space Administration
NIS	Negative Ideal Solution
NOD	Number Of Days
NREL	National Renewable Energy Laboratory
N-S	North-South
PIS	Positive Ideal Solution
POA	Plane Of Array
PR	Performance Ratio
PV	Photovoltaic
PVGCS	Photovoltaic Grid Connected System
REFIT	Renewable Energy Feed in Tariff
REIPPPP	Renewable Energy Independent Power Producer Procurement Program
SAW	Simple Additive Weighting
SAM	System Advisor Model
SAURAN	South African Universities Radiometric Network
SQP	Sequential quadratic programming
SODA	Solar radiation data
STC	Standard Test Conditions
TMA	Total Module Area
TOPSIS	Technique for Order Preference by Similarity to the Ideal Solution
WindVel	Wind Velocity

Chapter 1

Introduction

1.1 Background

There is a strong case being made worldwide for the adoption of renewable energy sources. The global energy sector is grappling to manage the increasing energy demand. This increase in demand is mainly driven by global population growth and the economic development of some of the world's emerging economies. To make matters worse, fossils fuels, which curently account for the majority of the global primary energy production are facing depletion due to their finite nature[9],[10] and [11]. Renewable energy sources are, therefore, ideal in this situation as they will be able to provide a more sustainable and diversified energy supply. Adoption of renewable energy sources over fossil fuels is also vital to the reduction of carbon emissions globally [12]. These emissions, from the burning of fossil fuels, trap heat and contribute to the global warming phenomenon which has harmful effects on our climate, environment and health [13]. According to a special report compiled by the International Panel on Climate Change (IPCC), the life-cycle global carbon emissions associated with renewable energy are minimal compared to those produced by fossil fuels as shown in Figure 1.1.

Some of the common renewable energy sources, as shown in Figure 1.2, include:

- solar, which harnesses energy from sunlight,
- wind, where energy is captured by turbines as the wind blows,
- biomass, which turns organic matter into electricity or transportation fuel,
- geothermal, which uses the earth's internal heat for a wide range of uses such as electricity production and heating and cooling,
- ocean, which can be harnessed as mechanical energy from the tides and the waves or even thermal when the sun's heat meets the water and
- hydro-power, where flowing water is harnessed using turbines to generate electrical energy.

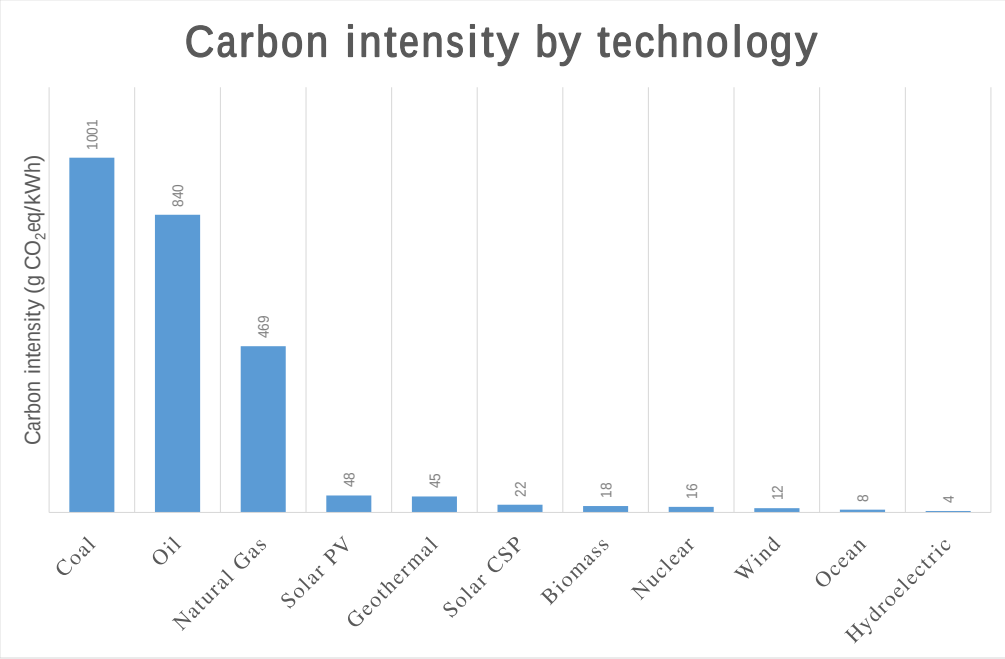

Figure 1.1: Carbon intensity of electricity generation technologies given in grams of carbon emitted per kWh of electricity generated from the respective technology [1].

Figure 1.2: Renewable energy sources.

1.1.1 Solar Energy

Solar energy can be further broken down into several technologies:

- Photovoltaics (PV) in which absorbed solar irradiation is directly converted into electrical energy using collectors. These collectors are usually made of semi-conductor material which operates on the principle of the photoelectric effect to generate electricity. There is also a different type of photovoltaics known as Concentrated Photovoltaic (CPV) which uses a large amount of solar irradiation focussed onto a highly efficient multi-junction solar cell using lenses and curved mirrors. This technology is usually used in areas with high Direct Normal Irradiance (DNI).
- Concentrating Solar Power (CSP), where sunlight is reflected and concentrated onto receivers and the solar energy is converted into heat through a medium, usually water, and the steam produced is used to turn turbines. This technology is also ideal in regions with high DNI.
- Solar Thermal technologies which are used for water heating, space heating and space cooling, as well as process heat generation.
- Solar energy for architecture and urban planning, where buildings are oriented towards the sun's azimuth to provide light and warmth.

1.1.1.1 Solar Energy Worldwide

Several sources, including the 'Snapshot of Global PV Markets :2016' [14], state that the total installed PV capacity at the end of 2016 was at least 303 GW. 265 GW of the 303 GW were contributed by the 25 International Energy Agency Photovoltaic Power Supply (IEA PVPS) countries alone. This was a direct result of a global expansion of about 75 GW in 2016 which equals a growth rate of about 50% from the 50.9 GW installed globally in 2015. Figure 1.3 shows the progression of global PV installations, in gigawatts, from the year 2000 to the year 2016. An additional 85 GW is projected to be installed by the end of 2017 and the growth in the photovoltaic industry is anticipated to continue. There is an estimated capacity of between 3000 GW and 10000 GW expected to be installed by the year 2030 [2]. Most of this expansion is not only linked to the urgency in trying to solve the global energy and pollution crisis, but it is also directly linked to the technological advancements and industry re-structuring in the PV industry over the past couple of years. The consequent price reductions and expansion of the knowledge base in the industry will potentially also continue to influence the cumulative number of solar installations worldwide.

On the PV technology side of things, a look at the price and cost evolutions related to solar cells shows that the average price per watt has dropped over the past few decades. The price of crystalline silicon solar cells, for instance, has dropped from approximately $77 per watt in 1977 to as low as $0.27 per watt as gazetted by the Energy Trend Company [15]. Since PV modules are more expensive than any other PV system component in the Balance of System (BoS), most current PV system designs are done for better value for money by optimally installing te modules. Recent research has, however, come to light indicating that optimising the BoS costs is becoming increasingly important due to decreasing module prices. This, in turn, is also beginning to influence PV system design decisions [16].

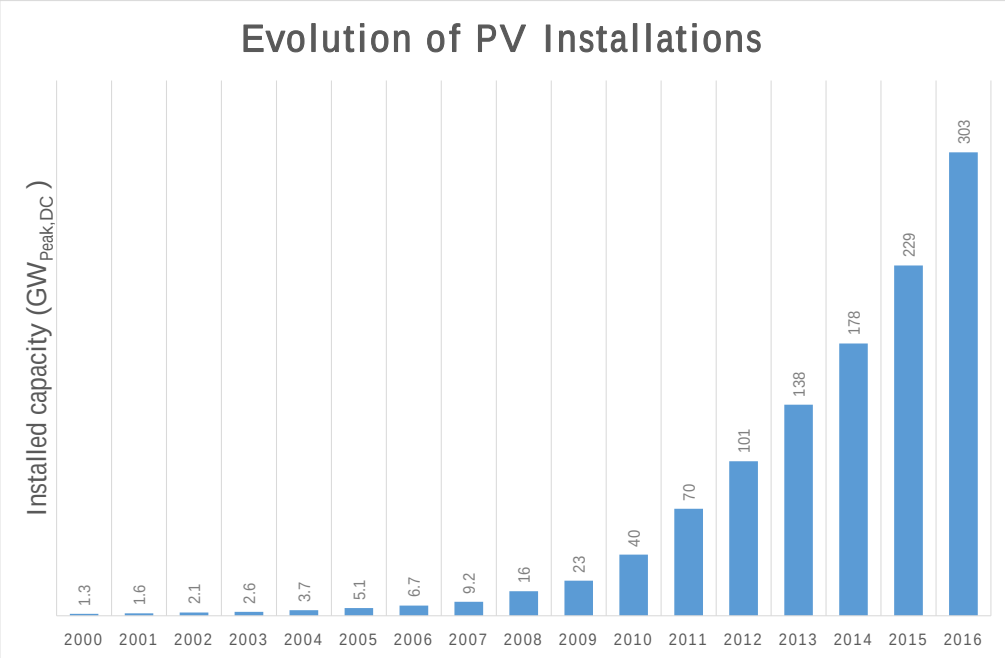

Figure 1.3: Evolution of PV installations from the year 2000 to the year 2016 [2].

1.1.1.2 Solar Energy in South Africa

Solar energy is one of the most readily accessible renewable energy resources in South Africa. This can be seen in Figures 1.4a and 1.4b showing the distribution of the solar resource in South Africa. The Northern Cape Province offers the most favourable levels of solar irradiation and this explains why, as shown in Figure 1.5, most of the solar PV plants are located in this province.

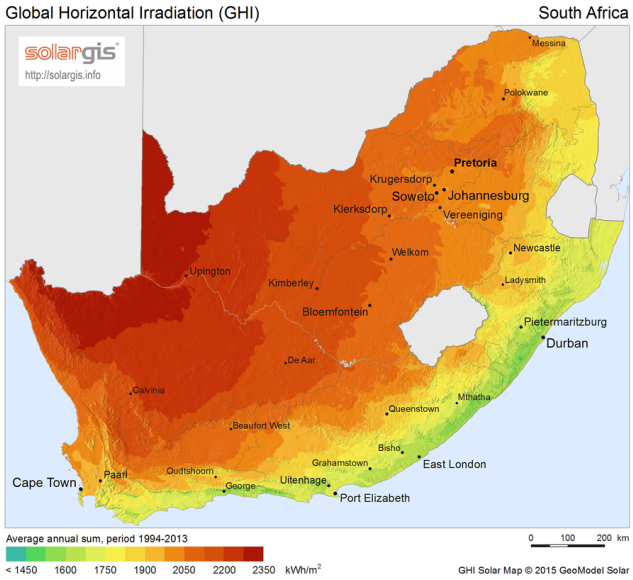

(a) Distribution of GHI

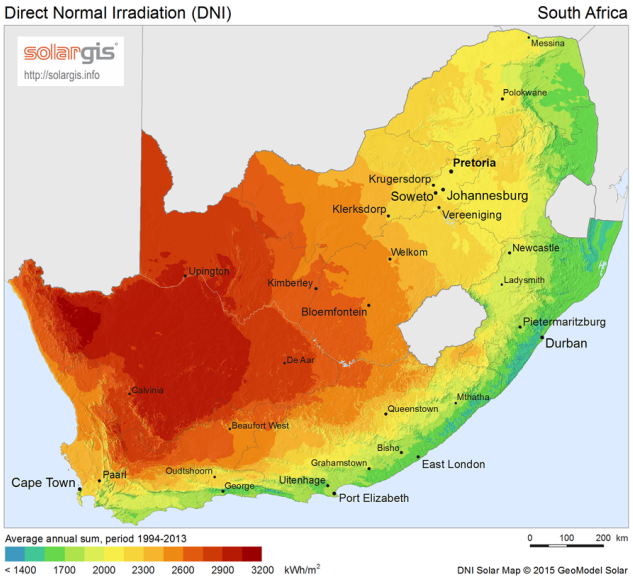

(b) Distribution of DNI

Figure 1.4: Solar resource distribution in South Africa [3].

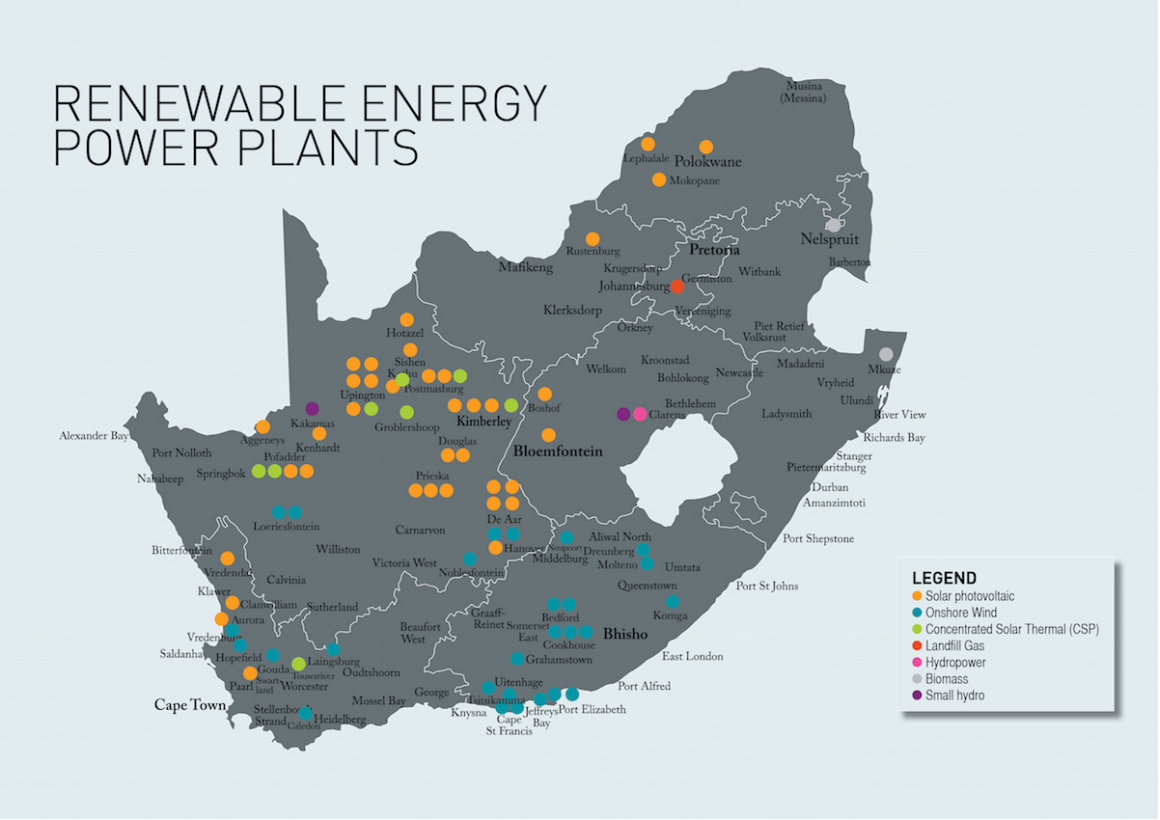

Figure 1.5: Map showing the distribution of 79 renewable energy power plants from the first four rounds of the REIPPP in South Africa [4].

Over the years South Africa, like the rest of the world, has also seen growth in the number of PV installations. This is believed to be due to the rising costs of electricity, constraints in the electricity supply system, technological advancements and price structure improvements in the alternative energy sector in the country [17]. In addition to that, the adoption of solar energy sources has also been expediated by government and municipal incentives. For instance, a tax incentive was implemented by the government in January 2016 through the South African Revenue Service (SARS) for renewable energy systems under the amended Income Tax Act No. 58 of 1962. This fiscal incentive essentially allows for a reduction on movable assets used in renewable energy production on a 50|30|20 basis over the course of three years, for systems greater than 1 MWp, if the asset is being put to use for the first time by the taxpaying entity [18]. For systems smaller or equal to 1 MWp, a discount of 28% is granted to the taxpaying entityin year 1 [19]. Several metropolitan municipalities have implemented feed-in-tariffs and net-metering as incentives for residential and commercial customers. These include the City of Johannesburg Metropolitan Municipality [20], City of Cape Town Metropolitan Municipality [21], and eThikwini Metropolitan Municipality [22] with feed-in-tariff programs and Nelson Mandela Bay Metropolitan Municipality with an already established net metering guideline document [23].

Efforts are being made on several other fronts to unlock more of South Africa's solar potential such as developing and growing more credible solar resource databases. SAURAN [24], which stands for Southern African Universities Radiometric Network, is one such initiative. SAURAN is spearheaded by the Centre for Renewable and Sustainable Energy Studies (CRSES) at the University of Stellenbosch and the Group for Solar Energy Thermodynamics (GSET) at the University of KwaZulu-Natal. Its aim is to provide high-resolution ground-based radiometric

data from stations in locations in the Southern African region. Furthermore, the Department of Energy (DOE) and the Department of Science and Technology have a joint initiative known as the Solar Energy Technology Roadmap (SETRM). STERM's main goal is to foster the development of solar energy technologies locally, within the confines of relevant policies and national initiatives [17]. These are but a few of the examples showing the growth and the development of the solar PV market in South Africa.

1.2 Project Description

1.2.1 Problem Statement

Despite all the notable progress on the national and international front, there is still a lot of work to be done towards attaining the South Africa's sustainability goals [25] and tackling some of the drawbacks in the global solar industry. One of the biggest of these drawbacks is the high capital costs of PV systems and it is a problem too big for any single entity to try to solve on its own. Therefore, while the government, municipalities and policy makers play their role in facilitating the process of finding solutions to this, PV system designers also have an important role to play in their own rite. This includes researching and implementing optimisation techniques that will enable them to deploy solar projects at lower costs without sacrificing plant performance [26] and [27]. Optimisation can be defined as the process of making a design or system more effective or functional [28]. With regards to the PV system design in our context, it means revisiting the design process to find areas of improvement that could result in higher energy production, better system performance and lower system losses and operation costs.

PV system design tools play a significant role in the design optimisation process. For designers to have an idea of how the PV system they will be designing is likely to perform in a specific location under specific conditions, they make use of simulation software. The software takes weather and site data as inputs and runs simulations and reports back the expected plant yield and performance based on the proposed PV system design layout. This is an indispensable step in the design phase as important decisions will be made based on the simulation results so it requires software that can accurately model PV system behaviour and enable the desisn of a PV project that is bankable. Bankability is essentially an index of the financial strength and stability of a project. Bankability is influenced by factors such as the quality of the PV system components in the PV system, which can be directly linked to the manufacturing companies[29] and [30]. Other important factors taken into account are the reliability of the simulation results, the simulation software and the datasets used as well as the experience of the system designers. This therefore means that even the selection of the simulation software cannot be taken lightly. Simulations and optimisation process may require several iterations and evaluations based on a number of plant performance parameters so robustness, modelling flexibility and the extent of functionality of the software also need to be taken into account. The unfortunate limitation with most PV system software tools is that their focus is mostly on:

- PV module selection, interconnection and behaviour in the operating conditions,
- inverter selection, interconnection and behaviour and
- the influence of mounting structures.

However, cables and other BoS components are seldom taken into account, save for accounting for when their losses are estimated.

Moreover, each PV project comes with its own constraints and objectives that sets it apart from other projects. As such, there is hardly ever a one-size fits all design procedure that can cater for all types of projects [26] and [31]. There are also, often, numerous design parameters and objectives that need to be designed for and this could lead to:

- numerous iterations being needed to reach a decision,
- some objectives being incommensurate and therefore difficult to compare with each other, and
- some objectives and parameters being antagonistic, therefore necessitating some sort of compromise or trade-off for the selection of the optimal layout selection.

1.2.2 Goals and Objectives

The goal with this project was to investigate the optimisation strategy currently being implemented by some plant designers in order to identify areas of improvement. The current method involves calculating the ideal pitch and tilt angle of a PV system in a particular location, varying these two parameters together with other design variables till the system is optimised for maximum energy output and then implementing financial modelling to optimise for levelised cost of energy. This is done for the three different module technologies, monocrystalline, polycrystalline and thin film, and the technology and layout that makes the most financial sense is selected. This method is therefore investigated for improvement potential.

The first step was to understand and evaluate the current trends and then formulate optimisation frameworks that would be more effective and beneficial to the designers. Particular attention was paid to ensure the relevance and applicability of the optimisation frameworks to the South African context. Three key desired outcomes were identified and laid out as follows:

(a) The frameworks would have to be suitable for constrained optimisation, as each design space is defined by certain constraints that the system designers have to adhere to. In addition, the optimisation frameworks would have to be easily adaptable to diverse design objectives and parameters since as stated before, different projects come with different goals and requirements.

(b) The number of iterations needed to find an optimal layout from the design space becomes increasingly large when the search space is widened and/or when the design parameters or objectives to be investigated simultaneously are increased. Robust mathematical models that can handle such high computational requirements would, therefore, be required. These models would also have to come with or be easily incorporated with reliable PV system design tools to ensure system modelling accuracy and bankability.

(c) Multi-objective optimisation was identified as a possible approach to the design process. This would, however, possibly lead to designers having to compare and contrast incommensurable parameters and dealing with antagonistic objectives. As such, methods for dealing with parameters in different units and decision making schemes suitable for multiple criteria would have to be implemented.

1.2.3 Significance of Research

Solving this problem will lead to frameworks that:

- replace or complement the current arduous and redundant plant design procedure,

- are easily adaptable to various design scenarios, with regards to constraints, parameters and objectives,
- provide a faster and well-rounded approach to the PV system design process and
- yield accurate and bankable PV system designs.

This will, as a result, be a step towards improving plant productivity, reducing system costs and ensuring investor confidence and reducing investment risks. In the long run, this could lead to more profitability for the independent power producers (IPPs) while at the same time improving the prospects of adequate and affordable electrical energy for the consumers in South Africa.

1.3 Thesis Outline

The researcher aims at coming up with frameworks for optimally designing utility-scale grid connected PV systems taking multiple variables into account simultaneously, in a constrained design space. The organisation of the rest of this thesis is as follows:

- **Chapter 2:** In this chapter, the fundamentals behind solar PV systems are presented. Conditions favourable for solar PV projects are discussed first, followed by a breakdown of the PV system as a whole, with particular focus being drawn to the modules, the inverters and the mounting systems. Thereafter, system performance parameters are briefly examined and the basics of PV system design are discussed, together with the role of simulation software in the design and evaluation process.
- **Chapter 3:** The preliminary design optimisation process is discussed in this chapter. First, the current conventional design optimisation procedure that is supposedly in need of improvement is presented, and thereafter, a literature review is conducted to discuss other optimisation procedures that are also being implemented elsewhere in the PV industry. Criteria for the optimisation process in the form of design parameters and design constraints are touched on as well as several investigations into some of the optimisation strategies found in literature. This then forms the basis on which our final optimisation frameworks are formulated.
- **Chapter 4:** In this chapter, the optimisation frameworks are presented and discussed in more detail. First a literature review is performed to analyse the algorithms that have been used in PV system design to date; their strengths, their weaknesses and their applicability to this context. The optimisation methodology implemented in this project is then broken down into the software used for the PV system design aspect of the process and the algorithms implemented for the optimisation process and how the two processes are integrated. In subsequent sections the algorithms used to perform the constrained multi-variable optimisation for single and multiple design objectives are presented and then conclusions drawn from the design methodology presented.
- **Chapter 5:** In this penultimate chapter, the formulations of the optimisation problems are presented together with the optimisation results generated from the implementation of the optimisation frameworks discussed in Chapter 4. The problems are presented as cases representing the fixed tilt design scenarios as well as the single-axis tracking scenarios and for each case, three investigations are undertaken to perform the same optimisation for the three PV module technologies - monocrystalline, polycrystalline and thin film. Comparisons are then drawn from the trends in each individual PV technology's

investigation as well as across all three technologies to find the best technology and its corresponding optimal layout.

- **Chapter 6:** In this final chapter, all the conclusions drawn from each of the former chapters are brought together and final conclusions and relevant recommendations are made.

Chapter 2

Theoretical Background

2.1 Introduction

PV systems can be generally classified as grid-connected or stand-alone systems based on how the system is connected to electrical loads and, in addition to that, the configuration of their components and their operational requirements [32] and [33]. The main differences are found in:

- whether they provide either alternating current (AC) or direct current (DC) power to the loads,
- whether they are connected to energy storage media such as batteries or not and
- whether they are connected to the grid or operate independent of it.

2.1.1 Stand-alone PV Systems

This type of PV system operates independent of the electric utility grid and that is why it is often referred to as the off-grid system. Stand-alone systems come in two types: one that makes use of battery storage and one that is directly coupled to an electrical load.

- **Directly coupled systems** are usually very simple in nature. The PV module is directly connected to a load that matches the current and voltage output of the module. This type of stand-alone system is typically used on devices and appliances that need to run during the day since it only produces electricity when the sun is up. Common uses of such systems are ventilation and water-pumping.
- **Stand-alone systems with battery technology** can be connected directly to the load and battery storage to ensure that excess energy is stored and made available for use in times when the sun is not shining. This type of system is expected to supply all the energy needed by the load and other sources of energy are sometimes used to supplement the solar energy such as fuel generators and wind or hydro turbines to form what is referred to as hybrid PV systems [32], [34] and [33].

2.1.2 Grid-connected PV Systems

This type of system is also referred to as grid-tied, inertified or utility-interactive system. As the name suggests, grid-connected systems are meant to operate in parallel with and tied with the electric utility grid. The primary component in this type of system is the DC-to-AC inverter. The inverter converts the DC power produced by the PV modules into AC power

that is synchronous with the voltage and power quality requirements of the utility grid. The parameters to be satisfied to ensure safe and secure functioning of the electric power system are supplied in the particular country or regions's grid code [32], [34] and [33]. A grid code is a document that specifies the technical requirements that a facility, such as an electricity generating plant, has to meet in order to connect to a public electric network [35].

A variation of this grid-tied system is one that comes with battery backup in order to power selected backup loads when the grid is down. This type of system usually comes with a bi-directional interface between the AC output circuits and the utility network. This interface enables excess power to be fed back into the grid when the AC power output is more than the load demand and enables the grid to supplement the PV system output when the load demand is greater. As can be noted from the extra features, this type of grid-tied system is the more complex and less cost-effective [36].

2.2 Solar Resource and Site Selection

2.2.1 Chapter Overview

In this section the focus will focus on the basics of PV system design, particularly that of the grid-connected battery-less type. The layout of the sections will be as follows: in Section 2.2 the solar resource and site selection process are described, in Section 2.3 PV system components are discussed, in Section 2.4 system performance parameters are discussed, in Section 2.5 PV system design tools are described and in Section 2.6 plant design fundamentals are discussed.

Solar resource collectively refers to the various solar radiation parameters which together with other meteorological parameters such as ambient temperature and wind speed can be used to characterise a site. The solar and weather data along with the sun's position, relative to the earth, can be used to model system performance and perform energy yield predictions. PV system performance estimation is a crucial step in determining whether a potential solar PV project will be feasible and viable in a particular location and it is heavily dependent on the accuracy of these three elements that are used in the modelling process.

The solar resource and weather conditions of a place are often intermittent and prone to vary from one year to another so the datasets need to be compiled over a number of years, typically ten, to create historical site data with a reasonable degree of confidence for use in yield prediction. The position of the sun, however, is predictable and sets of equations and algorithms are usually used to pin-point the sun's position relative to the earth at any given time.

2.2.2 The sun's position relative to the earth

The sun's position can be described in terms of two main angles, the altitude (elevation) angle, β, and the azimuth angle, ϕ_s as shown in Figure 2.1. Equations 2.1 and 2.2 allow us to compute the solar altitude and solar azimuth angles from the latitude, L, day of the year, represented by the declination angle, δ, and time of the day, represented by the hour angle, H. All the angles involved can be described as:

- **Solar azimuth angle,** ϕ_S, - the angle between the north-south axis and the direction of the sun.

- **Solar altitude angle,** β, - the angle between the horizontal plane and the geometric centre of the sun. Its complement is called the zenith angle and it features in several other solar related calculations.
- **Declination angle,** δ, - the angle drawn between the plane of the equator and the line between the geometric centre of the sun and the centre of the earth. This angle changes throughout the year as a result of the earth's orbit and the sun's apparent up and down movement through the seasons as shown in Figure 2.2 (see Equation 2.24).
- **Hour angle,** H, - the angular representation of time where time is quantified as the number of degrees the earth must rotate to be directly over the line of longitude which happens at solar noon (see Equation 2.26).

$$\beta = sin^{-1}(cosLcosHcos\delta + sinLsin\delta) \tag{2.1}$$

$$\phi_s = sin^{-1}\frac{sinHcos\delta}{cos\beta} \tag{2.2}$$

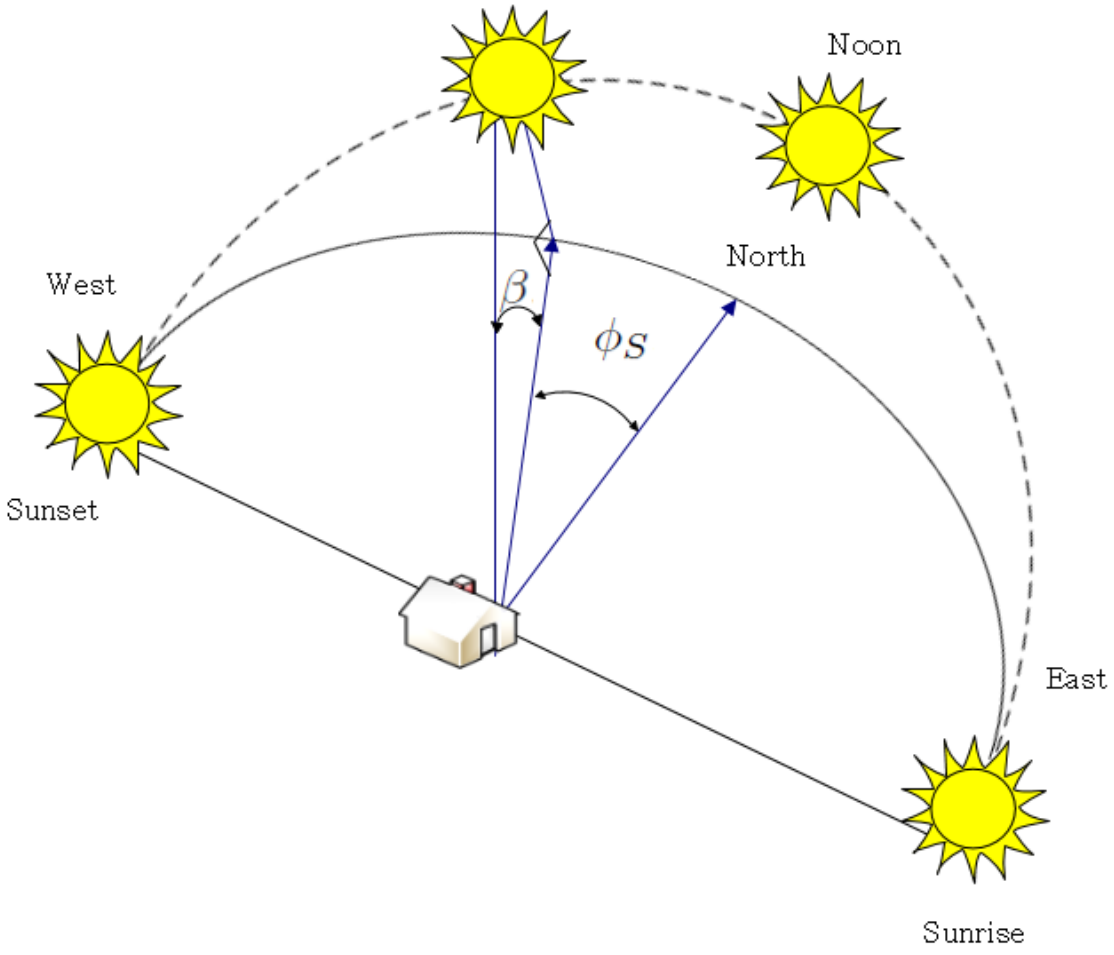

Figure 2.1: Illustration of the sun's altitude and solar azimuth angles β and ϕ_s, respectively.

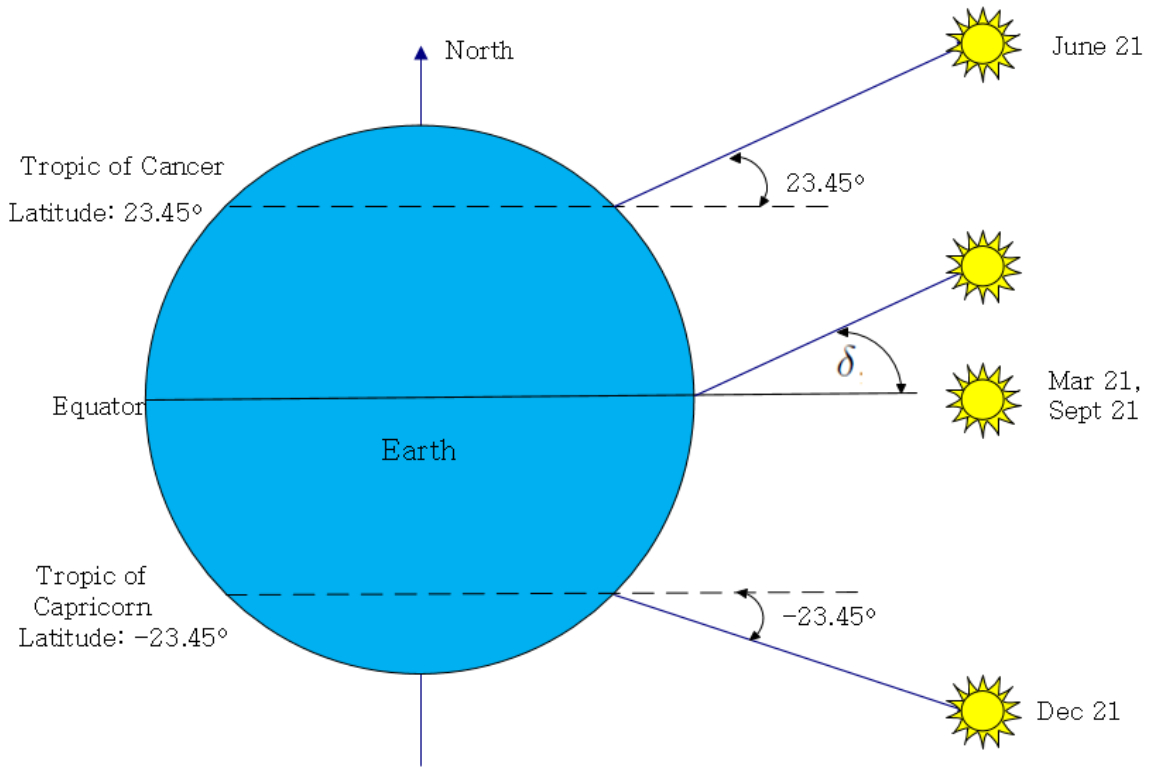

Figure 2.2: Illustration of the solar declination angle.

2.2.3 Solar radiation parameters

The solar resource of a location is usually defined using three main measured terrestrial solar radiation (solar radiation within the earth's atmosphere) parameters. These are:

- Global Horizontal Irradiance (GHI)
- Direct Normal Irradiance (DNI)
- Diffuse Horizontal Irradiance (DHI)

2.2.3.1 Global Horizontal Irradiance (GHI)

Global Horizontal Irradiance (GHI) refers to the total amount of solar power that is received by a unit area of a horizontal surface. GHI is made up of diffuse and direct beam components of solar irradiation which are explained in the next subsections. Figure 2.3 shows some of these solar irradiation characteristics.

2.2.3.2 Direct Normal Irradiance (DNI)

The Direct Normal Irradiance (DNI) is also referred to as the beam component because it is the beam power component received on a unit area of a surface normal to the direction of the sun. Solar PV tracking systems and concentrating solar power technologies mainly seek out to maximise their collectors' reception of this component of the solar irradiation. If (measured) values of the DHI and GHI are available, equation 2.3 can be used to estimate the values of the DNI.

$$G = G_{diff} + G_{dir}cos(\theta_Z), \tag{2.3}$$

where:
G is the GHI,

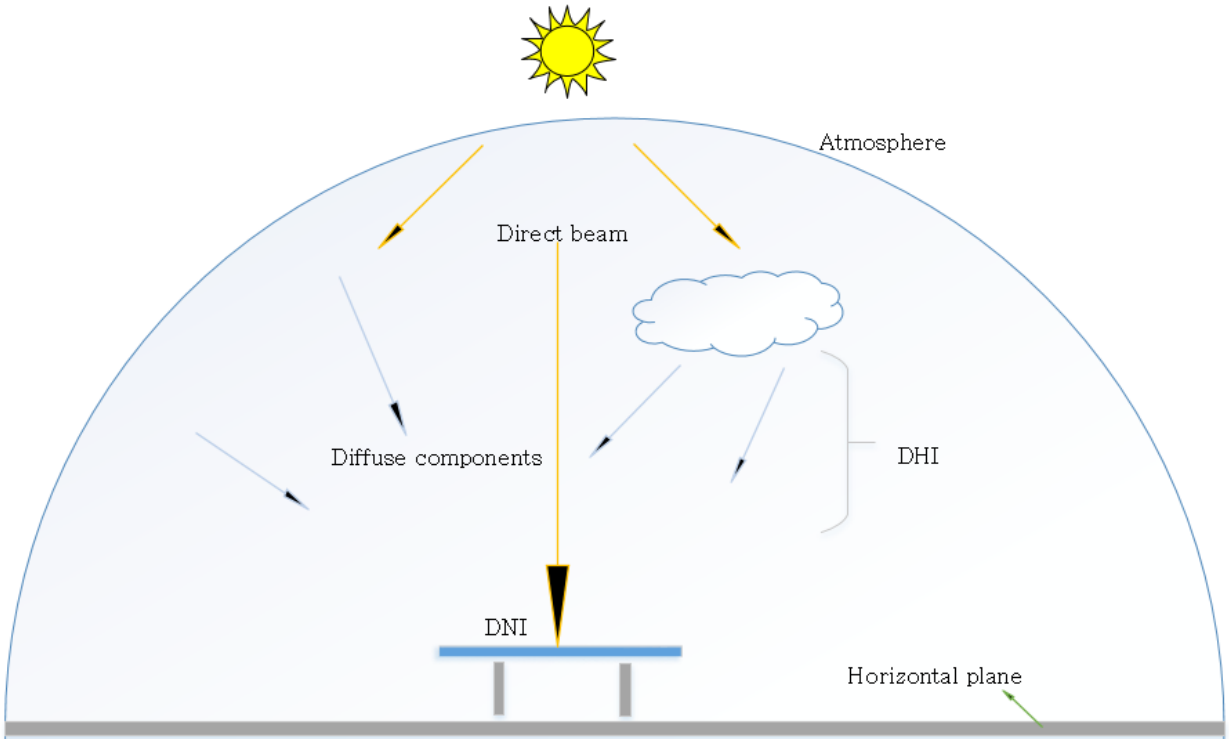

Figure 2.3: Terrestrial solar irradiation characteristics

G_{diff} is the DHI,
G_{dir} is the DNI and
θ_Z is the zenith angle of the sun.

Fitted models known as decomposition models can also be used to approximate the values of the DNI of a particular area by approximating the relationship between the clearness index, k_t, and the diffuse fraction, k_d . k_t is the ratio of the GHI to the extraterrestrial irradiance, G_{extra}:

$$k_t = \frac{G}{G_{extra}}, \tag{2.4}$$

while k_d is given as the ratio between the DHI and the GHI:

$$k_d = \frac{G_{diff}}{G}. \tag{2.5}$$

The relationship between k_t and k_d is approximated differently by different decomposition models, sometimes using additional parameters such as the variability of the clearness index, Δk_t, the solar elevation angle, α_s and the dew point temperature, T_{dp}. Table 2.1 shows some of the common decomposition models and the input variables they make use of.

2.2.3.3 Diffuse Horizontal Irradiance (DHI)

Diffuse Horizontal Irradiance (DHI) refers to the solar power received per unit area of a horizontal surface from the irradiation that is scattered by particles in the atmosphere and does not arrive on the surface on a direct path from the sun but from several other directions.

To maximise on energy production solar panels are often oriented to face the equator and tilted at an angle, θ_T, usually set to equal the latitude, to try and maximise the normal irradiance incident on the solar panel's surface. The orientation angle of the PV module is

Table 2.1: Decomposition model

Model	Input variables
Orgill and Holland (1977)[37]	k_t
Erbs (1982) [38]	k_t
DISC (1987) [39]	k_t, α_s
Reindl 1 & 2 (1990) [40]	k_t, α_s
Louche (1991) [41]	k_t
DIRINT (1992) [42]	Δk_t, α_s, T_{dp}

referred to as the collector/surface azimuth angle, ϕ_c, and is defined as the angle between the horizon and the direction normal to the surface of the PV module. There are different conventions for defining surface azimuth but the more commonly used one is the north-clockwise convention. According to this convention north is the origin and the positive direction is clockwise therefore making east 90°, south 180° and west, 270°. The other convention is just the reverse and takes south as the origin. To quantify the amount of irradiance incident on a tilted module surface, irradiance data needs to be transposed into the plane of the array (POA).

2.2.3.4 Global Plane of Array (POA) Irradiance

Otherwise known as the Global Tilted Irradiance (GTI), it refers to the total solar power received per unit area of a tilted surface. Ideally PV system designers aim for designs that maximise the average, long-term Global POA Irradiance, G_{POA}, value and due to the fact that the sun's position relative to the module position is ever-changing, a crucial step in estimating PV plant performance is determining G_{POA} as a function of time, if reliable measured G_{POA} data is not available. The G_{POA} depends on various factors such as:

- the position of the sun
- the mounting structure and orientation of the PV array
- the direct beam and diffuse irradiance components
- the ground reflectance (albedo)
- the presence of obstructions that could cause shading (both near and far),

and is calculated mathematically as:

$$G_{POA} = G_{beam} + G_{ground,ref} + G_{Sky,diff} \tag{2.6}$$

$$G_{beam} = G_{dir} * cos(\theta_{AOI}) \tag{2.7}$$

$$G_{ground,ref} = G * \alpha_\lambda \frac{1 - cos(\theta_T)}{2} \tag{2.8}$$

where:
G_{beam} is the direct beam component of irradiance in the plane of the array,
$G_{ground,ref}$ is the ground-reflected component of irradiance in the plane of the array,
$G_{Sky,diff}$ is the sky diffuse component of irradiance in the plane of the array,
θ_{AOI} is the angle of incidence of the irradiance on the tilted PV module surface,
α_λ is the ground albedo and
θ_T is the tilt angle of the PV module.

Calculation of incident irradiance on a tilted surface from horizontal irradiance data is facilitated by transposition models, and each model differs from the others due to the assumptions it is based on and the input variables it depends on. Table 2.2 shows some of the common transposition models.

Table 2.2: Transposition models

Model	**Input variables**
Isotropic [43]	DHI, θ_T
Klucher [44]	DHI, GHI, θ_T, θ_{AZ}, θ_Z, α_s
Reindl [40]	DHI, GHI, DNI, θ_T, θ_{AZ}, θ_Z, α_s
Perez [45]	DHI, DNI, G_{extra}, θ_T, θ_{AOI}, airmass
Hay-Davies [46]	DHI, DNI, G_{extra}, θ_T, θ_{AZ}, θ_Z, α_s

2.2.4 Solar radiation data sources

Solar resource data is usually obtained either by collecting actual ground measurements at the location of interest or from satellite data. Ground measurements are obtained by using equipment such as pyranometers and silicon sensors to collect hourly and sometimes sub-hourly data onsite. To obtain long-term irradiance datasets the measured data is sometimes put through the process of interpolation since extensive historical data from ground-based stations is seldom available [47]. The other challenges presented by data obtained from ground measurements include variable standards of calibration, maintenance and measurement periods and uncertainties in the interpolated data.

Satellite data sources, on the other hand, usually have a wider geographical and historical coverage. They are also not susceptible to most of the uncertainties and challenges that ground-measured data sources are prone to. A list of some of the more globally applicable sources of solar resource data is given in Table 2.3 [47], [48] and [49].

Table 2.3: Sources of solar resource datasets

Data Source	Type	Coverage	Access
SolarGIS	satellite data	Regions between 60° North and 50° South latitude angles; from 1994, 1999 or 2006 (depending on region) to date	paid
SoDa Helioclim	satellite data	Mainly Europe, Africa and the Middle East; from February 2004 to date	paid
Meteonorm	ground data	global; from 1981- 2010 for most regions	paid
3Tier	satellite data	global; from 1997, 1998 or 1999, depending on region, to date	paid
PVGIS	depends on region and time frame	global; between 1981 and 2011, depending on region	free
NASA-SSE	satellite data	global; from 1983 till 2005	free

2.2.5 Site selection

The process of selecting a site for a PV plant has an influence on the PV project's financial and technical viability. Although there are no hard and fast rules when it comes to site selection, especially considering the fact that viable projects have been developed in areas with steep slopes and waste disposal sites [47], there are several factors worth considering. These factors include:

- Climate and solar resource - these have a direct bearing on the irradiation that the solar PV modules receive and consequently, the plant energy output.
- Topography and ground conditions - these determine how factors such as far-shading, mounting system selection and the ground cover reflectivity affect the PV module performances.
- Land, especially the area available and policies for land-use in the region - this determines how modules are laid out on the field and in turn, their performance.
- Availability and accessibility of a grid connection from the site - the grid needs to be within reach such that energy losses are not incurred due to the use of longer cables during transmission.
- Environmental and social aspects - the effect of setting up a PV plant in the region needs to be evaluated for its potential positive and negative impacts on the environment and the area's inhabitants.
- Costs and financial incentives - this helps determine whether a PV project will be financially viable or not.

2.3 PV System Components

PV systems are made up of different components and each component serves a specific purpose. Some of the major components of Photovoltaic Grid-Connected Systems (PVGCS) are:

- PV modules
- Inverters
- Mounting structures and other balance of system (BOS) components such as wiring, overcurrent and over earth fault covering, surge protectors, instrumentation and control systems (Scada or DCS) and disconnect devices.

2.3.1 PV modules

2.3.1.1 Photovoltaic effect

PV modules are responsible for the conversion of solar irradiation into electricity by means of the photovoltaic effect. The photovoltaic effect is facilitated by semiconductor materials such as silicon (Si), gallium arsenide (GaAs) and copper sulphate (Cu2S). Semiconductors are specialised materials with conductivity that depends on the temporary availability of energy to activate electrons in the crystal lattice. When photons are absorbed on the surface of a solar cell, they raise the electrons in the lattice structure of the cell to a state of higher energy that enables the the electrons move freely in the semiconductor. When electrons move from their original positions, they create positive charges known as holes and this movement is facilitated by two thin regions made by dopants. Dopants are specially added impurities that alter the electrical properties of the semiconductors and help create regions of excess electrons, known as type-n regions, and regions with an excess of positive holes, known as type-p regions. Where these two regions meet they create what is known as a p-n junction which produces an internal electric field. When the photons create free electrons and holes close to the p-n junction, the electric field makes the electrons move towards the n-side and the holes towards the p-side thereby creating an electromotive force (EMF) between the n and p regions. Wires are then used to connect the n and p sides to supply electric current to an external circuit.

2.3.1.2 PV module technology

There are curently several types of PV modules available on the market and they all differ in terms of their electrical and optical properties. These differences cause certain types of modules to perform better in certain environments or scenarios than others. PV modules can be generally classified into crystalline silicone modules and thin film modules with other minor subdivisions as shown in Figure 2.4.

- **Monocrystalline silicon (Mono-c-Si) solar cells**
  Also referred to as single-crystalline solar cells, these solar cells are made from cylindrical silicon ingots. Using the Czochralski process, four sides are cut out of the ingots to make silicon wafers and this is what gives Mono-c-Si PV modules their characteristic look. The solar cells of Mono-c-Si modules exhibit a dark uniform and evenly coloured look as shown in Figure 2.5a because they are made from a single seed crystal of high-purity silicon. Mono-c-Si solar panels have the highest efficiency, typically ranging from 15% to 20% [50] and [51], due to their high-grade silicon content and tend to last the longest,with a typical warranty of 25 years, compared to other types of modules. One of their major downsides is the fact that they are the more expensive than polycrystalline and thin film modules.

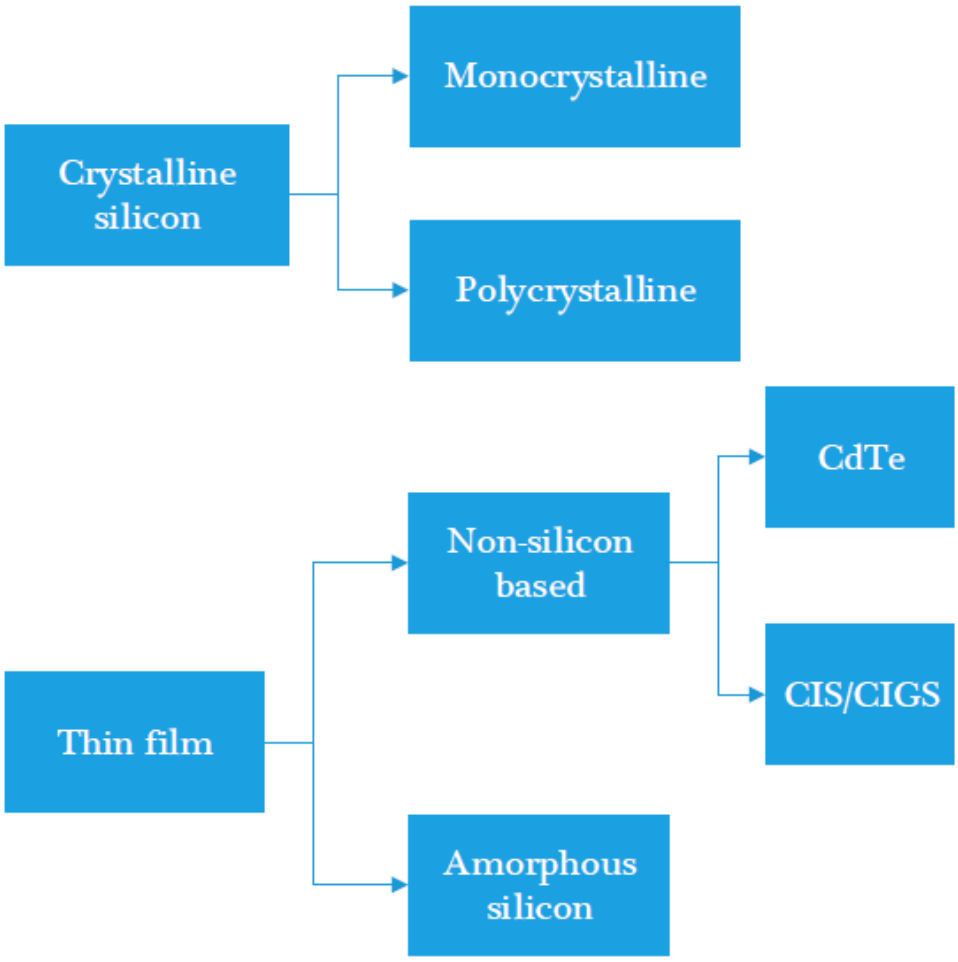

Figure 2.4: PV Cell Technologies

- **Multi-crystalline silicon (multi-c-Si) solar cells**
  This cell technology is also referred to as Polycrystalline silicon (p-Si). Multi-c-Si cells are produced when raw silicon is melted and poured into a square mould and then cooled and cut into rectangular wafers. This process creates variable shades in multi-c-Si cells due to the visible edges and grain boundaries as shown in Figures 2.5c and 2.5d. Multi-c-Si modules do not cost as much as Mono-c-Si modules, because their method of production is cheaper than the Czochralski process, but the modules are just as durable so they typically also carry a warranty of about 25 years as well. Their efficiency is slightly lower than Mono-c-Si module efficiency, typically between 13% and 16%, but higher than that of thin film technologies [50] and [51].

- **Thin film solar technology**
  Thin film modules are produced by depositing thin layers of PV material on a substrate like glass, metal or plastic. The types of thin film photovoltaic (TFPV) solar cells commonly used commercially include cadmium telluride (CdTe), copper indium gallium selenide (CIGS) and amorphous thin-film silicon (a-Si), which is silicon-based. TFPV modules often have lower efficiencies [50] and [51], compared to their crystalline counterparts but are often easier to mass-produce and are generally less sensitive to high temperatures and shading. This type of PV modules is, however,generally considered to be susceptible to slightly faster degradation and has a shorter lifetime compared to the crystalline silicon

modules [51]. That explains why thin film modules usually come with shorter warranties. Figure 2.5b shows a Thin Film solar cell.

(a) Monocrystalline solar cell

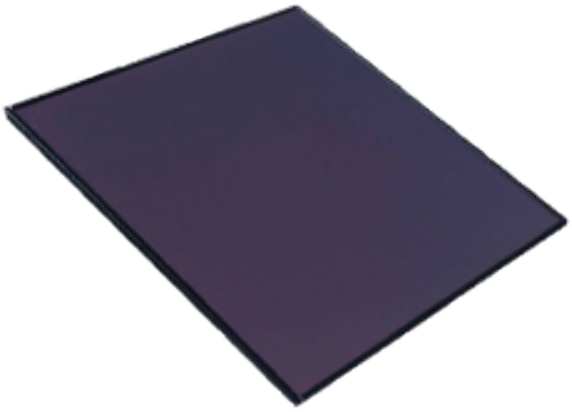

(b) Thin Film solar cell

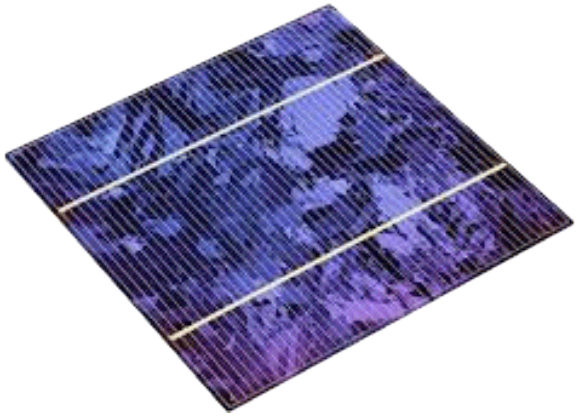

(c) Multicrystalline solar cell

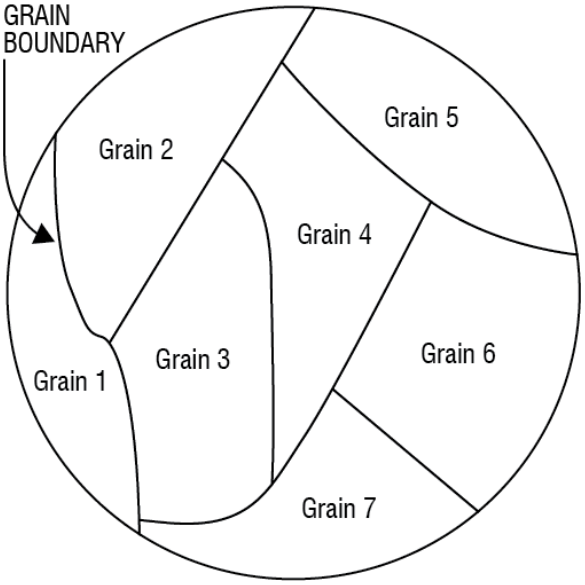

(d) Grain boundaries in multi-c-Si cells

Figure 2.5: Types of PV modules

With several module manufacturers operating in the solar PV industry today, it is essential to know what else to look out for when it comes to PV module selection. One of the most important criteria used for module selection is industry acceptance and towards this end, PV system designers usually refer to the tier system. While tiers do not directly guarantee module quality, they are considerably good at indicating it. Tier rankings may also vary in certain criteria, depending on the entity that compiles the list but they are quite similar in several respects. In general, most PV system designers and investors prefer Tier 1 module manufactures, for bankability reasons. Tier rankings are, however, not ordinarily available to the public but organisations such as Bloomberg New Energy Finance (BNEF) are working towards bridging that gap. BNEF also has a solar insight service [52] that provides more information about the tier system.

2.3.2 Inverters

Solar power inverters are responsible for the conversion of the DC electricity produced by solar PV modules into AC electricity. This is so that the electricity can be used by other appliances on-site or fed into the grid and transmitted to other end-users. Inverters also go beyond just that one application and are often typically useful in:

- performing maximum power point tracking (MPPT) to maximise the energy harvest from the PV system,
- connecting the PV system to the grid in compliance with the grid-code and
- providing basic monitoring and ancillary services.

There are several topologies of inverters and each one differs in architecture and capacity and in turn exhibits strengths and weaknesses that make it more suitable for certain PV systems than others are.

- **String inverters**
  The name of these inverters comes from the fact that they are connected to a string or a couple of strings of PV modules. This type of setting ensures that there is a lower risk to the entire system because if one inverter fails or has to be disconnected during maintenance routines, the system can still supply power from the remaining functional string inverters in the topology. The set up of a system with string inverters also means that different string designs can be supported which is ideal for sites where multiple orientations and variable numbers of modules per string are warranted. This type of inverters is mostly used for residential or commercial PV plants because they often have capacities ranging from 1 kW to 8 kW. String inverters have advantages such as lower balance of system (BOS) and ongoing maintenance costs and simpler design due to modularity. The downsides of this type of inverter include higher DC watt unit costs and also an increased number of inverter connections and AC cabling.
- **Central inverters**
  Central inverters are similar to string inverters, but they are much bigger and therefore capable of supporting more strings. Unlike in string inverter setups where strings run directly to the inverter, in central inverter setups strings are first connected together in a common combiner box that then runs the DC power to the central inverter input side. Central inverters generally require fewer component connections and lower DC watt unit costs, but they tend to cost more to install and have a higher DC wiring and combiner costs. They also tend to require larger spaces for inverter pads. Capacities of such inverters usually range between 50 kW and 1000 kW and they are, therefore, mostly suitable for commercial and utility scale PV plants.
- **Microinverters**
  Microinverters, as the name suggests, are a much smaller version of solar inverters that convert DC to AC power right at the solar panel. Microinverters are part of the module level power electronics (MLPE) family, together with power optimisers. They monitor the performance of each PV module rather than a whole string or groups of strings. They are increasingly becoming a popular choice of inverters for residential and commercial PV systems, but they are usually regarded as less practical for utility scale PV systems due to their higher costs per unit watt and the vast number of microinverters that will be needed for such large PV plants. Microinverters are already being integrated into PV

modules by some manufacturers to make what are known as AC modules. This makes the modules relatively more expensive but ensures that the installation is cheaper and relatively easier.

2.3.3 Mounting Systems

How the modules of a system are installed also has a bearing on the performance of the system as well as its cost. Generally, ground-mounted systems can be classified into three main categories, namely:

- **Fixed tilt** - where the subarray is , mounted at fixed tilt, θ_T, and azimuth, ϕ_c, angles. As a rule of thumb, most designers use the latitude angle of the site as the optimal tilt angle, and the azimuth as the direction facing directly towards the equator; north for places in the southern hemisphere and south for places in the northern hemisphere.
- **Single-axis** - where the subarray is mounted at a fixed tilt angle and tracks the movement of the sun from east in the morning to west in the evening about the north-south axis. How far the subarray rotates towards the east and the west is determined by the tracker rotation limit, θ_R. Some single-axis tracking systems employ a method known as backtracking which adjusts the orientation of the rows of modules tracking the sun to prevent them from shading each other.
- **Azimuth tracking** - where the subarray is at a fixed tilt angle but rotates in a horizontal plane, tracking the daily movement of the sun and disregarding the azimuth angle.
- **Dual-axis** - where the subarray rotates from east to west following the sun's daily movement just like a single-axis tracking system and also tracks the sun's seasonal movement throughout the year in the north to south direction.

Tracking systems use specialised algorithms that can pinpoint the sun's position with respect to the site at any given time of the day and allow the subarrays to be oriented such that they directly face in that particular direction to maximise solar irradiance incidence on the modules' surfaces. Figure 2.6 shows the diagramatic representation of the above-mentioned mounting methods.

2.4 PV System Performance Parameters

Several metrics used to evaluate a plant's operation to give an indication of a plant's financial and technical performance will be discussed in this section. These plant performance indicators are used across the entire energy production chain in the PV system to identify opportunities to improve its performance and reliability and consequently its yield and profitability.

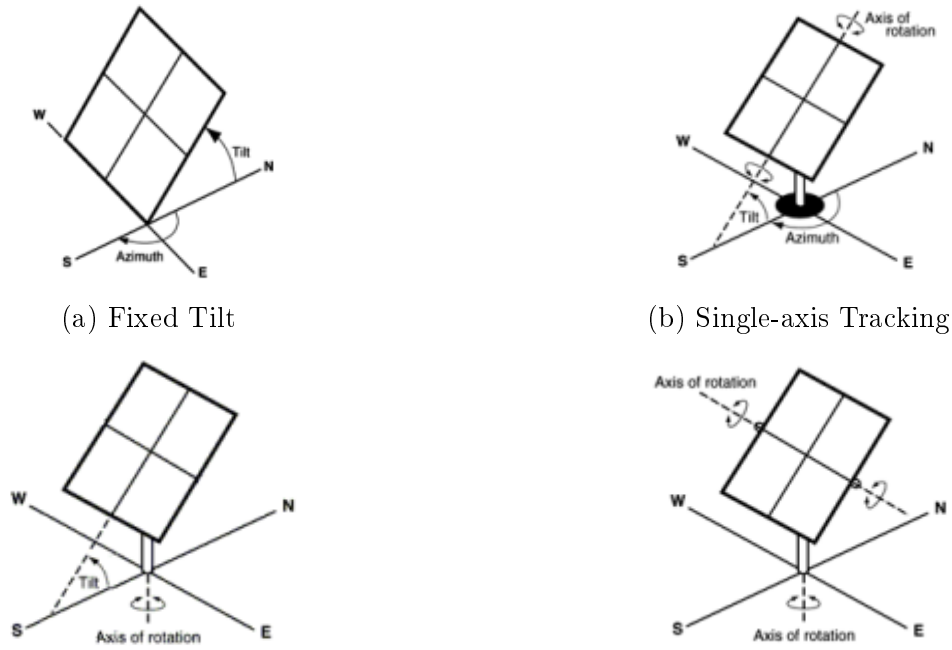

(a) Fixed Tilt

(b) Single-axis Tracking

(c) Azimuth Tracking

(d) Dual-axis Tracking

Figure 2.6: Mounting methods as illustrated in the System Advisor Model documentation[5].

2.4.1 Energy production

The electrical energy output of a PV system is one of the most common ways by which the performance of a plant can be measured. Energy output is usually set as a design goal and the plant is regarded as performing really well if the production is greater or equal to the set threshold or at least reasonably close to it. Factors that influence energy production include the amount of irradiance incident on the surface of the PV module, the module temperature, the efficiency of the PV modules and the inverters and the losses in the generation and transmission of the energy. Theoretically, the energy production is calculated as the product of the total system power output (usually given as kilowatts) and the time period of in question (usually measured in hours):

$$Total\ Energy\ (kWh) = Total\ Power(kW) * Time(h). \tag{2.9}$$

2.4.2 Specific Yield

Specific Yield is a way of measuring plant performance by stacking its energy production against its peak installed capacity. It is often used to compare the operating results of PV systems designed with different technologies or layouts on a standardised scale. Specific Yield is calculated as:

$$Specific\ Yield\ (kWh/kWp) = \frac{Total\ Energy\ (kWh)}{Peak\ Capacity\ (kWp)}. \tag{2.10}$$

2.4.3 Performance Ratio

The performance ratio (PR) is also known as the quality factor (Q) because it is a measure of the quality of a PV system. Another way of looking at the PR is as a measure of a plant's energy efficiency and reliability. PR illustrates the the relationship between the actual plant yield and the theoretical energy output and it is usually expressed as a percentage as shown in

Equation 2.11:

$$Performance\ Ratio\ (\%) = \frac{Total\ Plant\ Output\ (kWh)}{Calculated\ Nominal\ Output\ (kWh)} * 100, \tag{2.11}$$

where the nominal energy plant output is calculated using the total annual incident solar irradiation at the generator surface of the PV plant, Annual POA Irrad., and the relative efficiency of the PV plant modules, η_{Module}, as:

$$Nominal\ Output\ (kWh) = Annual\ POA\ Irrad.\ (kWh) * \eta_{Module}. \tag{2.12}$$

2.4.4 Capacity Factor

Capacity factor (CF) is a measure of the amount of energy produced by a PV plant compared to its maximum possible output. It is calculated as a fraction or percentage, generally by dividing the total energy the plant produces under normal operating conditions in a given period of time by the total amount of energy the plant would have produced if it ran at its full capacity during that period as given in Equation 2.13:

$$Capacity\ Factor\ = \frac{Total\ Energy\ Produced\ (kWh)}{Maximum\ Possible\ Energy\ Output\ (kWh)}, \tag{2.13}$$

2.4.5 Levelised Cost Of Energy (LCOE)

The levelised cost of energy (LCOE) is the cost, per kilowatt-hour (kWh), of an operating plant over an assumed financial life. LCOE indicates a measure of the overall competitiveness of energy generating technology as it takes into account all the costs incurred during the lifetime of the generating technology and the units of energy produced during that same time frame. It is a convenient way to also compare projects from different technologies, lifetimes and/or capacities and this is particularly useful in assessing grid competitiveness and proximity to grid parity (which occurs when an alternative source of energy can generate power at a LCOE that is less than or equal to the price of purchasing power from the electricity grid). The simplified formula for calculating LCOE is:

$$LCOE = \frac{\sum_{n=0}^{N} \frac{C_n}{(1+d)^n}}{\sum_{n=1}^{N} \frac{Q_n}{(1+d)^n}} \tag{2.14}$$

where:
N is the analysis period,
C_n are the annual project costs in year n,
Q_n is the amount of electricity generated by the system in year n, in kWh and
d is the discount rate which can be $d_{nominal}$ or d_{real} for nominal (including inflation) or real (without inflation) discount rates respectively.

The annual cost summation starts from $n = 0$ to include the investment costs in the calculations, while the total energy production summation only starts from $n = 1$, because that is when the system starts producing energy.

2.4.6 Losses

Loss analysis is an integral part of measuring the performance of a PV plant. Poor operating conditions on a PV plant and the non-ideal nature of PV system components are usually the chief causes of losses in a PV system. These losses are explained in more detail in the following subsections.

2.4.6.1 Shading losses

Shading losses are usually a result of obstructions in the vicinity of a PV system casting shadows on the solar PV modules or the modules in adjacent rows casting shadows on each other some time during the day. In the case of most utility scale PV plants, trees, buildings and other nearby obstructions can be avoided through a due diligence process when selecting the site. The biggest shading challenge is, therefore, due to the inter-row shading of PV modules, especially on space-constrained sites. To minimise these self-shading losses, PV system designers rely on finding the optimum tilt angle and spacing of rows of PV modules. Equation 2.27 in subsection 2.6.1.4 deals with the calculation of the ideal row spacing such that the derate factor due to shading does not go beyond 2.5% in a PV system, but there are several other methods and algorithms used by system designers to quantify and mitigate shading losses [53] and [54].

2.4.6.2 Incidence angle modifier (IAM) losses

The incidence angle modifier losses are characterised by a decrease in the irradiance reaching the PV module surface with respect to the irradiance under normal incidence due to reflectance caused by incidence angles that are not normal to the plane of the module surface. The reflectance phenomenon is consistent with the Fresnel's Laws of transmission and reflections at an interface of two transparent materials of different refraction indices, n_1 and n_2. Although in reality there are multiple and sometimes complex calculations that need to be taken into account, in practice the irradiance effectively reaching the PV cell surface is often closely estimated using the ASHRAE model which depends on only one PV module parameter, b_o, as:

$$L_{IAM} = 1 - b_o * (\frac{1}{cos\theta_{AOI}} - 1), \tag{2.15}$$

where θ_{AOI} is the incidence angle on the plane.

2.4.6.3 Soiling losses

When dirt accumulates on the surface of PV modules it can adversely affect the amount of irradiance that reaches the PV cells for conversion into electrical energy. This accumulation of dust, dirt and other contaminants is known as soiling and several studies are being currently undertaken to find better methods of quantifying the losses that arise from it. An alternative way of estimating soiling losses without using expensive equipment or intricate methods is by using precipitation levels. Monthly precipitation levels, in millimetres, can be used to approximate soiling losses as shown in Table 2.4 derived from a study by ARUP which involved module performance comparisons for locations in South Africa in [53].

2.4.6.4 PV losses due to irradiance levels

Losses due to irradiance are a result of the reduction of the efficiency of a PV module in conditions of low irradiance. This is because a PV module's efficiency increases at high light intensity and decreases at low light intensities relative to the PV modules' rated standard irradiance conditions of 1000 W/m^2. Figure 2.7 shows the variation of module efficiency with irradiance at different temperature levels.

Monthly precipitation (mm)	Soiling loss
0 - 20	3%
20 - 50	2%
> 50	1%

Table 2.4: Soiling Loss Scale

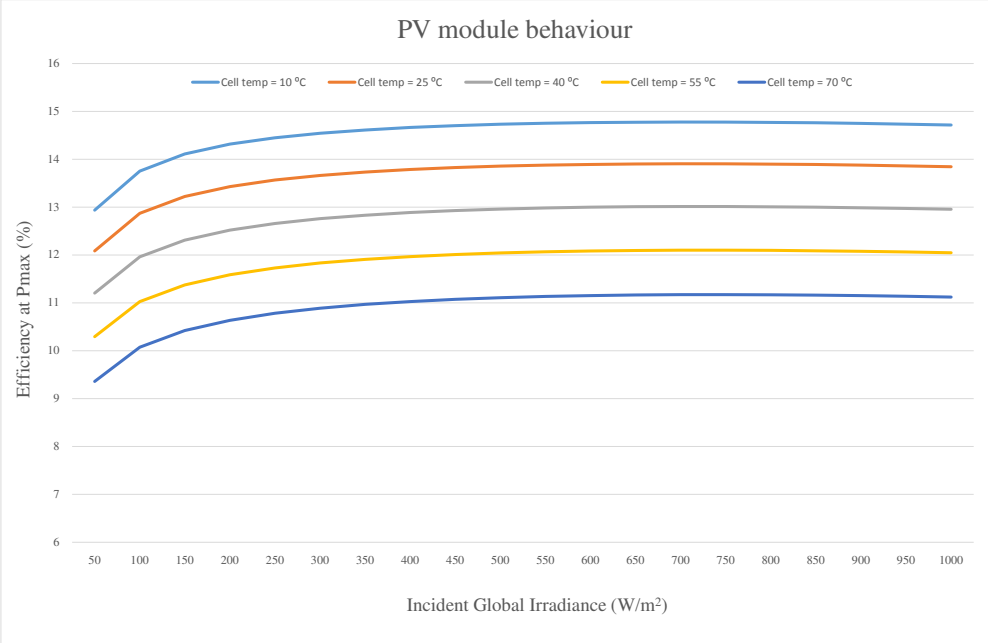

Figure 2.7: Variation of module efficiency with irradiance at different cell temperature levels

2.4.6.5 Thermal losses

Standard rated temperature conditions for PV modules are pegged at 25°C, but in reality, PV modules operate mostly in temperature conditions higher than that. When modules operate at higher temperatures their efficiency tends to decrease and the losses associated with that are referred to as thermal losses or PV losses due to temperature levels. Thermal losses are calculated using an energy balance between the cell temperature readings from modules under operating conditions and the prevailing ambient temperature. Figure 2.8 shows the variation of module efficiency with irradiance at different temperature levels.

$$U * (T_{cell} - T_{amb}) = \alpha * G_{inc} * (1 - \eta_{module}) \tag{2.16}$$

where:
U is the thermal loss factor dependent on the mounting mode of the modules and wind velocity,
T_{cell} is the temperature of the PV cells,
T_{amb} is the ambient temperature,
α is the absorption coefficient of solar irradiation,
G_{POA} is the global irradiance incident in the plane of the array, and
η_{module} is the efficiency of the module.

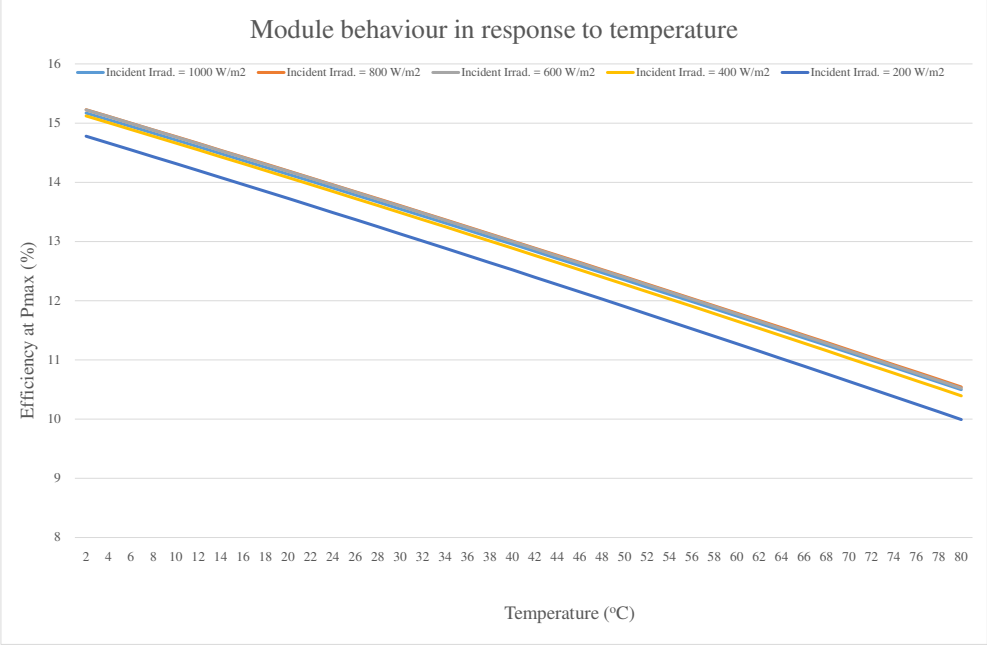

Figure 2.8: Variation of module efficiency with temperature at different irradiance levels

2.4.6.6 Mismatch losses

Mismatch losses are mainly due to varying current drives in modules connected in a string. Electrical properties such as the current-voltage (IV) characteristics of PV modules, even ones of the same PV module model, are never exactly the same. In the case of a series connection, the module with the lowest current drives the whole string and the corresponding power loss is what is referred to as mismatch loss or circuit mismatch (CM). Mismatch losses are not that easy to quantify so one of the ways that are used to estimate them is statistical sampling, especially when being evaluated by simulation software [55]. A more common way, however, is to derive the mismatch losses by calculating the difference between the expected total power of a string or array and the actual power realised by that particular string or array as follows:

$$CM = \frac{\sum_{n=1}^{N} P_{m,max} - P_{a,max}}{\sum_{n=1}^{N} P_{m,max}} \tag{2.17}$$

where:
$P_{m,max}$ is the maximum output power of each module,
$P_{a,max}$ is the maximum output power of the entire array, and
n is the number of modules in an array.

2.4.6.7 DC Ohmic losses

DC Ohmic losses are mainly caused by the resistance in the cables that interconnect PV modules, but they are also caused by transition resistance in fuses and terminal connections. The DC ohmic power losses are, therefore, usually calculated as:

$$P_{DC,ohmic} = I^2 R, \tag{2.18}$$

where I is the average DC array current and R is the resistance in the cables.
Differences in cable lenghts and sizes among parallel strings can lead to voltage drops, $I * R$,

thereby contributing to mismatch losses, so it is not unusual for DC ohmic losses and mismatch losses to be combined and given as one loss value [56].

2.4.6.8 Inverter losses

Losses in inverters are mainly due to ohmic and switching losses in semiconductors. Collectively, all these losses are referred to as inverter losses. The efficiency of an inverter, η_{inv}, is calculated as the ratio of the the power available at the inverter output terminal, $P_{inv,out}$, to the power at the inverter input terminal, $P_{inv,in}$. Consequently, the inverter losses, $P_{inv,loss}$, are given as:

$$P_{inv,loss} = 100 * (1 - \frac{P_{inv,out}}{P_{inv,in}}) = 100 * (1 - \eta_{inv}). \tag{2.19}$$

2.4.6.9 AC Ohmic and external transformer losses

The distribution and transfer of AC power from the inverter output terminals to the utility meter usually lead to energy losses in the AC wiring and a reduction in the energy that enters the transformers. Furthermore, hysteresis and eddy current losses as well as resistive and inductive losses in the transformers also lead to a further reduction in the energy that gets injected into the grid from the PV system. Ideally, field data should be used to quantify the ohmic losses and the transformer losses separately, but where measured field data is not available, these losses, $P_{AC+transf}$, can be combined and calculated as:

$$P_{(AC+transf)} = 100 * (1 - \frac{P_{grid}}{P_{inverter,out}}), \tag{2.20}$$

where P_{grid} is the power supplied to the grid.

2.5 PV System Simulation Tools

Performance and financial modelling are regular and essential processes in the design of PV systems. Performance models are used to estimate the expected energy output of a given PV system, while financial models are used to approximate the costs involved in the process of the energy production, including the construction and maintenance of the PV plants and in some cases the proceeds expected after the energy is sold off to other users by the power producers. This process is usually facilitated by the use of simulation software packages. Typical PV simulations involve the prediction of plant performance and estimation of cost of energy based on cost and design parameters specified for the site in question.

The procedure for modelling a PV system and predicting its energy yield, using hourly or sub-hourly time-steps, in simulation software typically consists of the following steps:

- Sourcing weather data, such as irradiance, wind speed and temperature from sources such as the ones described in Section 2.2. Some simulation software comes with weather data libraries, with an option for users to import data for sites the libraries do not cater for.
- If DNI data is missing in the set, decomposition models can be used to approximate it from the available irradiation datasets.
- Using transposition models to calculate the irradiation incident on the plane of the tilted array.

- Designing and sizing the PV system and modelling its performance and energy yield under the site's operating conditions.
- Applying the relevant losses or loss models.
- Generating the plant performance report using the various system performance parameters.

There are several solar PV simulation software packages that one can choose from; some available free of charge and others at a cost. The different software packages also come with features that make them more suitable for certain tasks than others [57]. It is important for PV system designers to select the right kind of design tool that serves their desired purpose, on a platform suitable for them and at a cost that is within their budget. We came across several design tools and they could basically be classified under five categories:

- **Free** - examples include SAM, PVLib, RETScreen, HOMER Legacy v.2.68, SKELION and HYBRID2
- **Paid** - examples include PVSyst, PVComplete, PVscout 2.0 Premium, SolarPro, Plan4Solar PV, PV F-Chart PV Sol Premium, Homer, PolySun, EasySolar, HELIOS 3D Solarparkplanung and Solarmapper
- **Online** - examples include SISIFO, PV-GIS, PVWATTS, PV*SOL, DIAFEM and EASY-PV for the free applications and Helioscope, SOLARPlus, Focus Solar, SolarDesignTool, Aurorasolar, Solar Analytics, SolarGis PV Planner, PolySun, EasySolar and Solarmodel for the paid applications.
- **Tools from inverter manufacturers** - examples include ABB (Power One), Mastervolt, Kaco, Fronius, Ingecon Sun Planner, SMA Sunny Design, Samil Power Design, SolarInfo Design Software, Goodwe EZDesigner and Satcon Configurator.

Investigation of three of these software packages for the purposes of our design optimisation will be discussed in the the following chapter.

2.6 Plant Design Fundamentals

2.6.1 Layout Design and Optimisation

This stage of the design process deals with the general layout of the PV plant so that the PV system performance is at its best, operations and maintenance (O&M) procedures are not inconvenienced and the design and full operation of the plant is all done at a reasonable cost. Typically, the objectives for the layout design include:

- selecting the tilt, orientation and configuration that optimises energy yield,
- designing for a row-spacing (pitch) that minimises self-shading losses, while at the same time maximising utilisation of the available land area,
- creating access routes and leaving enough room between rows to allow for operations and maintenance (O & M) procedures, and
- laying out the PV modules to minimise cable lengths so that electrical losses are minimised.

Our focus on the layout design covers the tilt, azimuth, configuration and spacing of the rows of PV modules to satisfy some of these objectives as given in the following sections.

2.6.1.1 Configuration

The configuration of PV modules is mostly related to how the modules experience electrical shading effects. There are typically two types of configurations of PV modules, portrait and landscape, and they are as shown in Figure 2.9. Most PV modules currently on the market come with bypass diodes to mitigate shading losses and, depending on how these diodes are connected on the modules, their bypassing mechanism may or may not be fully utilised in the one configuration compared to the other. Most bypass diodes are connected along the length of the module so landscape configuration will mean smaller electrical shading losses in design scenarios where inter-row spacing is limited so as to minimise the self-shading losses. The portrait configuration, on the other hand, may be considered in cases where east and west horizon shading losses are prevalent. Several rooftop installers also recommend portrait configurations mainly to avoid running mounting rails parallel to the roof trusses. Different PV module technologies have also been known to respond differently to partial shading losses, with some thin-film module technologies emerging as the least affected, compared to mono and polycrystalline technologies. All things considered, the decision of whether to mount your modules using a landscape or portrait configuration is mostly determined by the module manufacturing company's recommendation as well as site-specific constraints.

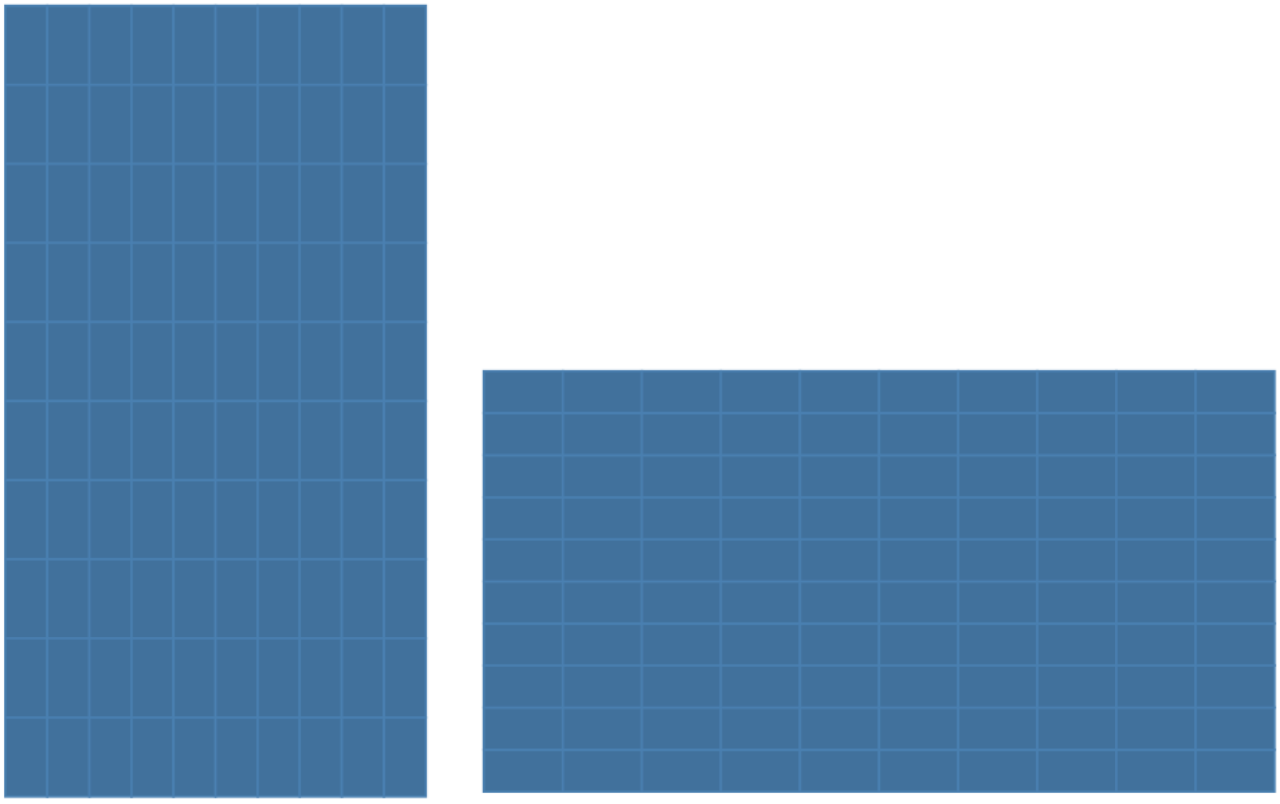

(a) Portrait (b) Landscape

Figure 2.9: Module configurations

2.6.1.2 Tilt

The highest energy output from PV arrays is achieved when the solar rays have a 90° incident angle with the module surface [58]. To achieve this, in fixed tilt systems, PV modules are tilted at a certain angle from the horizon, which is typically equal to the latitude angle of the site. This angle enables the PV modules to capture the highest amount of total annual

irradiation. This optimal tilt angle based on the rule-of-thumb (ROT) might, however, be subject to adjustments as a result of site-related constraints. These constraints that need to be considered include:

- **Shading**: higher tilt angles often lead to higher amounts of total irradiation captured, but they can also lead to higher levels of inter-row shading.
- **Soiling and snowing**: higher tilt angles tend to suffer from dirt and snow accumulation less, compared to lower ones, simply because the sharp incline of the panels makes snow slide off them easily and rain and dew which wash the panels also gets to do so easily.
- **Wind loads**: in regions that experience strong winds, lower tilt angles will be preferred for their ability to withstand the wind speeds without needing too many reinforcements on the mounting structures.

2.6.1.3 Azimuth

The ideal PV module surface azimuth angle, ϕc, is based on a rule-of-thumb (ROT) which stipulates that the optimum orientation of a fixed tilt PV system for the highest total energy production is towards the equator. This means that for a site in the northern hemisphere, the modules should face the true south direction and in the southern hemisphere, the modules should face true north. It is not uncommon for designers to have to deviate from this ROT in response to factors such as limitations in the design space or differences in design objectives. Time-of-Day (TOD) energy production preferences are one way in which design objectives can have such an influence on the selection of the azimuth angle. In such a design scenario, the objective would, for instance, be to design a system that helps meet energy demands during a specific time of the day and not necessarily the highest total energy output. Figure 2.10 shows an example of how the power output profile of a system changes in response to the change in the surface azimuth angle.

2.6.1.4 Row space (Pitch)

Pitch is essential to ensure that there is enough room for access to PV modules for O&M purposes and that rows of PV modules do not shade each other. The distance left between rows should also not be too large otherwise it leads to wasteful use of land. Two of the most commonly used methods for calculating the pitch on a PV plant, using Figure 2.11 as a complementary reference figure, are:

- **Using shadow analysis** to predict and avoid shading problems between adjacent rows during a certain window period [6] in the day. With this method, the winter solstice day is selected as the worst case scenario to work from to calculate the ideal row-spacing, d:

$$d = L_s \cos \Phi_s \tag{2.21}$$

$$L_s = \frac{\gamma}{\tan \beta} \tag{2.22}$$

$$\delta = 23.45[\frac{360}{365} * (n - 81)] \tag{2.23}$$

$$\sin \beta = \cos(L)\cos(\delta)\cos(H) + \sin(L)\sin(\delta) \tag{2.24}$$

$$\Phi_s = \frac{\cos(\delta)\sin(H)}{\cos(\beta)} \tag{2.25}$$

$$H = 15 * N_h \tag{2.26}$$

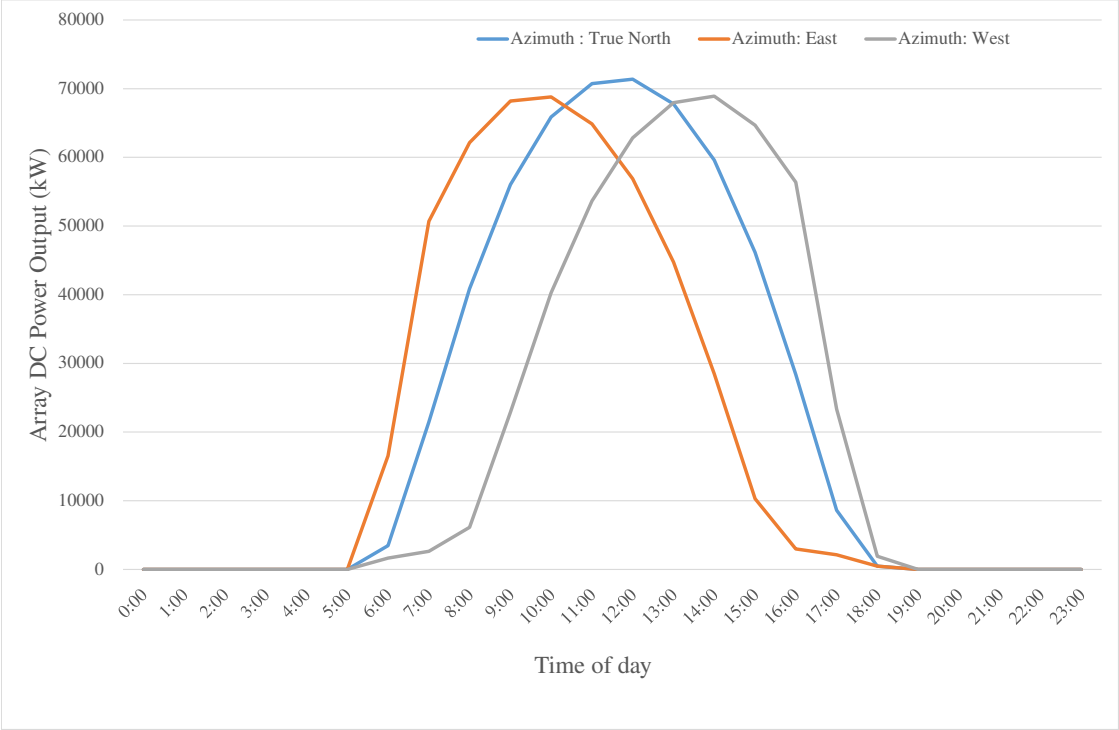

Figure 2.10: Effect of changing the azimuth on the power output profile of a PV system (in the southern hemisphere)

where
β is the altitude angle,
γ is the height of the uppermost tip of the PV module measured vertically from the ground,
L_s is the length of the shadow,
L is the latitude of the location,
δ solar declination angle,
H is the hour, in solar time,
Φ_s is the azimuth angle of the shadow,
N_h is the number of hours before solar noon and
n is the day number from the very first day of the year.

The winter solstice is chosen because it is the day that experiences the longest north-south shadows in a year due to the sun's position with respect to the site's location.

- **Using the ground cover ratio (GCR)** to calculate the row space, d, so as to minimise shading and improve the shading derate factor. The goal is to find d such that the resulting GCR leads to a desired derate factor using the equations:

$$GCR = \frac{CollectorArea, A_c}{TotalGroundArea, A_{tot}} = \frac{w * l}{(w * cos\theta + d) * l}, \tag{2.27}$$

where w and l are module dimensions.

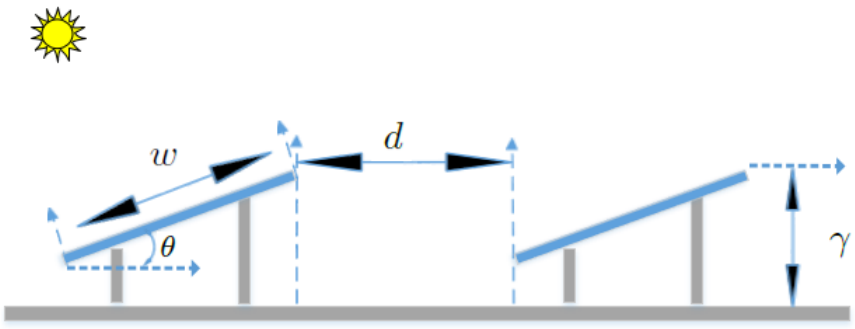

Figure 2.11: Reference figure for shading loss calculations

The approximate GCR can be selected using the corresponding mounting method and desired shading derate factor according to the plot shown in Figure 2.12. PVWATTS suggests that it is common industry practice to optimise land use on PV plants by using a GCR value that corresponds to a shading derate factor of 0.975 which translates to 2.5% shading losses [6].

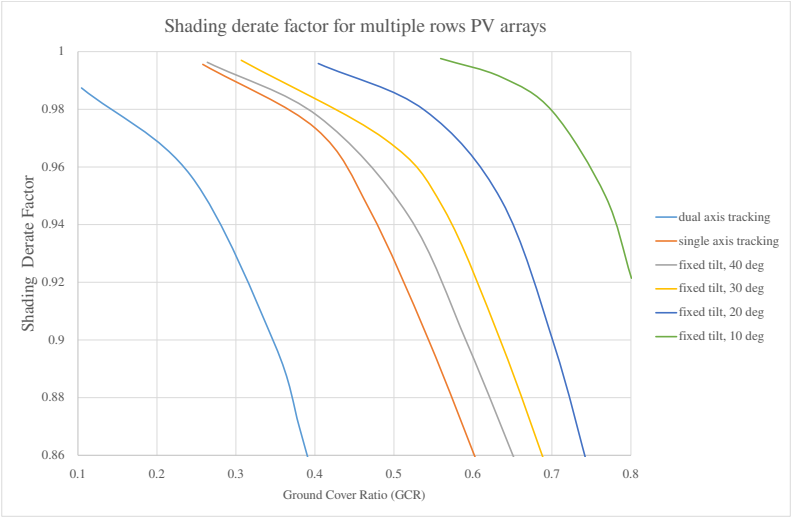

Figure 2.12: Shading derate factors for different PV module configurations adapted from [6]

2.6.2 System sizing

Sizing the PV system refers to calculation of the number of PV modules and inverters that will be able to meet a particular energy demand or performance objective. The whole process goes beyond determining the number of PV modules needed to how many of them ought to be connected in series and in parallel in order to match the inverter ratings under general operating conditions. System sizing can be summarised in the following steps and can be executed by the designer manually or using design tools. This process is usually initiated by first selecting the PV module and inverter models and then implementing the three fundamental steps:

(a) **Determine number of PV modules per string**: The designer typically chooses an initial number of PV modules that leads to a maximum power voltage closest to the average of the inverter's minimum and maximum MPPT voltages. If the string open circuit voltage exceeds the inverter's maximum DC input voltage, the number of modules per string is decreased by one and this continues until the open circuit voltage is below this limit.

(b) **Calculate the number of parallel strings**: The number of parallel strings of PV modules to meet the desired array capacity is determined using the formula:

$$N_{parallel} = \frac{P_{array}}{N_{series} * P_{module}} \tag{2.28}$$

where:
$N_{parallel}$ is the number of parallel strings of PV modules,
P_{array} is the total maximum DC power of the array,
N_{series} is the number of series modules, and
P_{module} is the module maximum DC power.

(c) **Calculate the number of inverters needed**: The number of inverters of the chosen model required to match the preferred DC to AC ratio as;

$$N_{inverters} = \frac{N_{parallel} * N_{series} * P_{module}}{Ratio_{DC:AC} * P_{max,AC}} \tag{2.29}$$

where:
$N_{parallel} * N_{series} * P_{module}$ gives the total DC capacity of the system,
$N_{inverters}$ is the number of inverters,
$Ratio_{DC:AC}$ is the desired DC-to-AC ratio, and
$P_{max,AC}$ is the inverter maximum AC power.

Figure 2.13 shows the algorithm that summarises the array sizing calculation.

2.7 Chapter Summary

In this chapter, the fundamentals behind solar PV systems were presented. This covered conditions favourable for solar PV projects, a breakdown of the PV system, system performance parameters, the basics of PV system design and the role of simulation software in the design and evaluation process. The purpose of this chapter was to highlight the key elements that make up the PV system and its design procedure as a form of background for the design optimisation procedures implemented in the thesis.

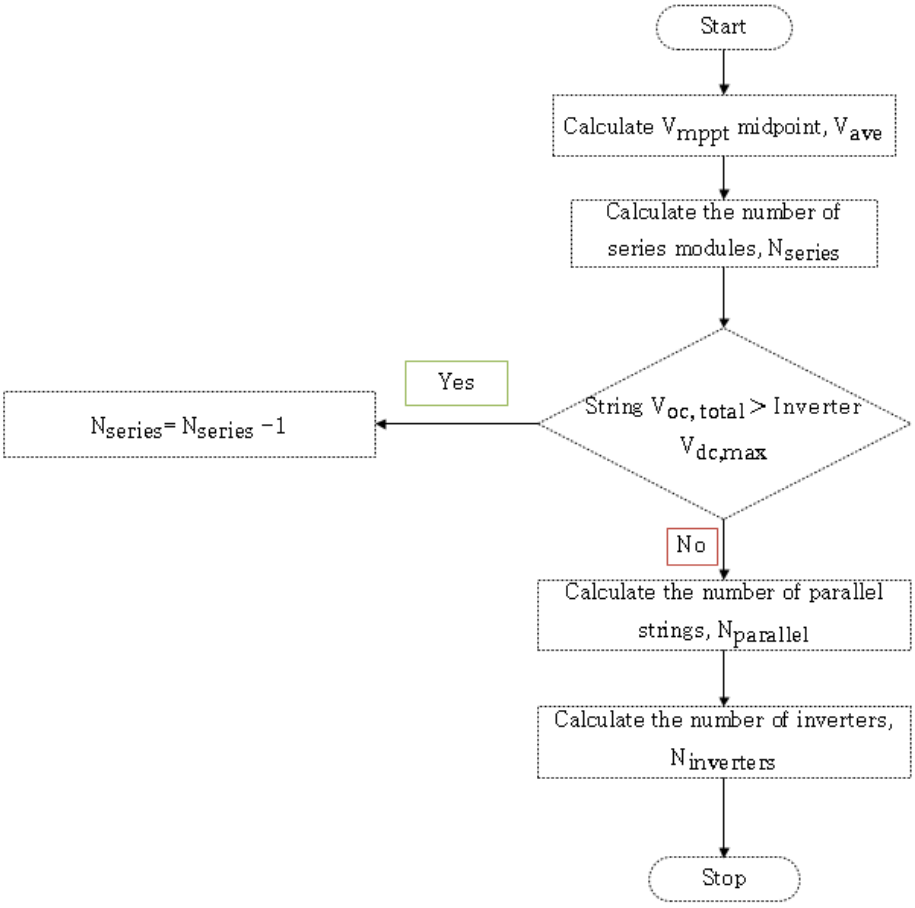

Figure 2.13: System sizing algorithm

Chapter 3

Preliminary Design Optimisation

3.1 Introduction

This chapter is the first step towards formulating an optimisation framework and it involves establishing the right kinds of design tools and optimisation strategies for the layout design. The process of optimally designing PV system layouts can go a long way towards improving system perfomance and lowering the corresponding system losses and in turn reducing system and operation costs [27]. Layout optimisation, however, goes beyond just picking the ideal module tilt and azimuth angles. There are several other design parameters that might also need to be taken into account as well as practical and site-related constraints that influence the design decisions for PV systems [47]. Some of the common PV system design constraints include:

- area constraints
- energy value
- costs
- PV technology and
- incentives and policies.

In this chapter, a bit of background on work that has been done in the PV industry to investigate plant layout optimisation is given in Section 3.2. This is followed by a brief discussion of some of the optimisation criteria in Section 3.3 and then case study investigations of the various strategies in Section 3.4.

3.2 Literature Review

In this section, several sources are highlighted for the purpose of shaping the optimisation framework formulation process. The studies described in this section not only shed more light on the work that has been done in this particular field of study but also help develop a deeper understanding of all the aspects involved in the design optimisation process.

K. Joyce, in 'Optimizing PV Plant Design to Achieve a Low Levelized Cost of Energy (LCOE)', discusses some of the optimisation tools and methods that Black & Veatch [59] implements to optimally design PV systems for a minimised LCOE by means of parametric analyses [27]. Through an investigative approach to design parameter selection in constrained design spaces, the study reveals the interdependence of design considerations that affect the

LCOE, and the importance of understanding their relationships and influence on system costs and performances to achieving a minimised LCOE. The significance of constrained multivariable optimisation is one of the main lessons that can be drawn from this article.

In the article, 'The 3 Best Ways to Optimize a Commercial PV System', authors P. Grana and P. Gibbs review and suggest methods of optimisation for commercial PV system designers [26]. The authors highlight how transformative and crucial some optimal design decisions are, especially with all the technological advancements being experienced in the solar industry and how that is affecting the prices of the PV components and in turn the focus of the PV system design process. They go on to identify the three elements:

(a) module (row) spacing and tilt angle

(b) azimuth angle

(c) inverter and module level power electronics (MLPE) and shade tolerance,

as the best ways to optimise commercial PV systems. The connection they make between the current trends in the solar industry and the effect the trends have on the focus of PV system design optimisation is quite insightful and relevant to our work.

In 'A study into the optimisation and calculation of electrical losses in renewable energy generation,' the author investigates calculation and optimisation of electrical losses in renewable energy generation technologies [60]. The electrical losses are reviewed and the data collected in the process is used as an empirical method to design a tool that can quickly and accurately predict losses in future projects. This then forms a new way of obtaining bankable data to assess the risks involved in future renewable energy projects. Although the work itself was not directly linked to our particular focus in its entirety, there were certain elements in the methodology that fit in well with the focus of this chapter's focus that were drawn from it.

B. Goss, in 'Design process optimisation of solar photovoltaic systems,' is embedded in a rooftop PV system project to analyse and identify opportunities for improvements in the design procedures [10]. From the study, the author creates a design framework to accurately model the performance of a PV system with special attention to three key areas, namely:

(a) safety assurance,

(b) design process integration and

(c) financial optimisation.

The observations he makes particularly in the lack of design integration and financial optimisation in most commercially available design tools could be vital to our optimisation framework.

Authors, Louazene et al, Gong etal and Del Vecchio all have work that looked into the layout optimisation of PV arrays [61], [62] and [63]. The influence of the tilt angle and the various tilting methods are investigated, along with some design constraints and design considerations. These investigations are good starting points for the preliminary design optimisation formulation.

3.3 Optimisation Criteria

The criteria of our optimisation processes were broken down into two types, namely, design parameters and design constraints. Design parameters are the variables that characterise a PV system design such that when they are varied, the performance of the PV system also vary. The goal is to find and select the design variables that enable the system to exhibit its best performance. Some of the design parameters that can be investigated, either individually or simultaneously, are:

- tilt angle, θ_T,
- azimuth angle, ϕ_C,
- mounting/racking system,
- row spacing,
- DC:AC ratio (also known as the inverter loading ratio, ILR),
- the different PV module and inverter technologies.

Design constraints are limitations in the design space or the possible design parameters that can be selected. The goal is to understand fully what these constraints are and design the system optimally, while navigating the design constraints efficiently. The design constraints include, as mentioned earlier,:

- area constraints - the amount of space available for the solar installation and its characteristics, such as its terrain can heavily influence the process of the layout optimisation process.
- energy value and time of use - the desired time of use for the electrical energy generated has a direct effect on the design parameter selection and optimisation.
- costs - the cost of PV system components and the cost of energy production play a pivotal role in determining a plant's financial viability.
- PV technology - the types of modules and inverters available on the market and their attributes has an effect on the design parameters and the technical feasibility of a PV project.
- incentives and policies governing the solar industry in that particular country or region can also put certain limits on some design parameters.

3.4 Optimisation tools and strategies: Case Studies

3.4.1 Test Case

A site in the Northern Cape Province of South Africa was selected as a benchmark for our simulations. The Northern Cape is well-known for offering some of the best conditions in the world for solar PV electrical energy generation [64]. Figure 3.1 shows the renewable energy power plants in South Africa with solar PV projects mostly concentrated in the Nothern Cape province. With about 17 solar PV plants now commercially operational in the province [7] and [65], it was only fitting that we use the region for our simulations.

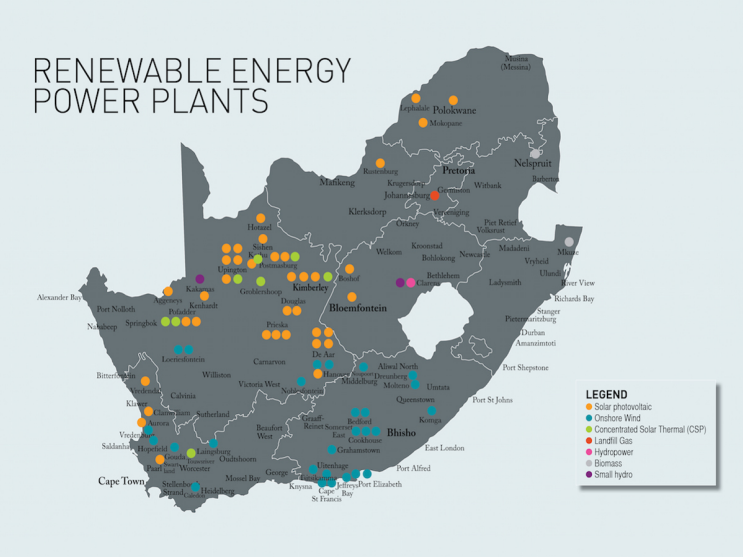

Figure 3.1: Renewable energy power plants in South Africa courtesy of [7]

The test-case was an existing 75 MWp solar PV plant made up of 84 sub-systems, each containing 3720 polycrystalline modules and an inverter. The configuration is such that there are 24 series modules per string and 155 parallel strings feeding into each of the 84 inverters. The entire system therefore consists of 312 480 modules over a total module area of 516 217 m^2. Table 3.1 summarises the configuration of the subsystems. To facilitate the PV system performance simulations, ground measured data from weather stations on the site was used. The dataset's integrity and reliability had already been checked and approved from previous work done by T. Mahachi in [56].

Table 3.1: Sub-system configuration

Variable	**Description**
Ground measurement data from site	GHI, DHI, ambient temperature,wind speed
Module orientation	0° , facing North
Inclination	30°
Type of installation	ground mounted
PV module model	BYD P6-30, 240 W
Number of modules per subsystem	3720 (24 in series in a total of 155 strings)
Inverter model	SMA Sunny Central 800CP
Total number of modules and inverters on site	312 480 modules, 84 inverters
Total module area	516 217m^2

3.4.2 Comparison of the software packages

Different software packages have different features that make them more suitable for certain tasks than others [57]. This investigation will focus on three of those packages, namely System Advisor Model (SAM), Photovoltaic systems (PVSyst) and PVLib. In this subsection SAM,

PVSyst and PVLib are described in more detail. For each program, a brief summary of the design tool will be given, closely followed by subsections in which some of their respective merits and demerits are discussed. The purpose of the exercise was to determine which one of the software packages would be the most ideal to use in the optimisation procedures to follow.

3.4.2.1 Summary of the Software Programs

Advisor Model (SAM)

SAM is a software package developed by the National Renewable Energy Laboratory (NREL) in the United States of America. SAM was originally called the Solar Advisor Model, but has since expanded its focus to also cover non-solar technologies such as geothermal power, wind power and biomass power, hence the name change. It is categorised as a financial and performance modelling software because it helps assess the operation of a proposed or actual renewable energy system and ties that in with an evaluation of the costs thereof. A typical SAM simulation consists of the following basic steps:

1. Selecting, from the interface, the required renewable energy technology and financing option.
2. Selecting the appropriate set of simulation and financing models. This is done by SAM in the background, based on the options selected in Step 1.
3. Specifying the necessary input variables such as the weather data file, site location and equipment. The supported weather files are typical meteorological year files (TMY2 or TMY3) and energy plus weather files (EPW).
4. Running the simulation. For advanced analyses, the user can configure simulations for sensitivity or optimisation before running the simulations. The user can then view the simulation results on a variety of graphs and reports generated automatically by SAM in the user interface's results section. There is also an option to export the results to a third-party software package for presentation or further analysis.

SAM's features allow it to cater to the needs of a variety of users including project developers, engineers, manufacturers, academic researchers, technology developers and policy makers and analysts [5]. Figure 3.2 shows the interface on the SAM application.

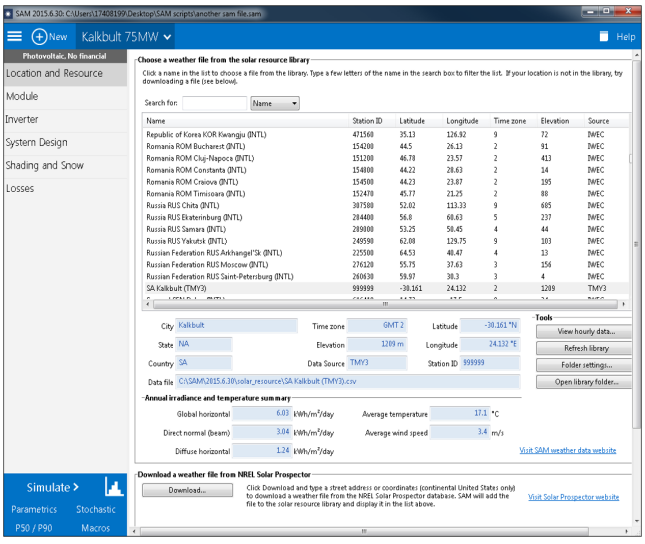

Figure 3.2: A screenshot of the SAM application user interface

Photovoltaic Systems (PVSyst)

PVSyst is a PV-centric simulation tool that was originally developed at the University of Geneva but is now a standalone company. The software package focuses on modelling, sizing, simulating and analysing PV systems. PVSyst does have some sort of financial modelling in place, but it is primarily a performance modelling software [55].

A typical simulation in PVSyst consists of the following steps:

1. Defining the project. This is where the user creates the desired project on the user interface, names it and selects the corresponding geographic location and meteo file to be used. A number of sites and meteo files are already included in the PVSyst databases but the user also has the option of importing his own. PVSyst supports several types of weather files such as TMY2, TMY3 and EPW and files from sources such as Meteonorm, Photovoltaic Geographical Information System (PVGIS), World Radiation Data Centre (WRDC), Retscreen, Helioclim and SolarGIS.

2. Creating a system variant. This is where the user creates a calculation version of the project created in step 1. On the interface, the user gets to define various input parameters such as module orientation, system configuration and loss parameters.

3. Running the simulation. The user runs the simulation and generates a variety of graphs and reports for the analysis of the PV system. PVSyst allows the user to analyse the results in the program, export them to a different program or save the variant for further evaluation.

PVSyst offers the users extensive reports and breakdowns and valuable insights into the engineering aspects of design and deployment. This allows PVSyst to cater for a wide range of users including researchers and architects. Its interface is also multilingual and available in other languages such as German, French, Spanish and Italian, in addition to English [55]. Figure 3.3 shows the interface on the PVSyst application.

Figure 3.3: A screenshot of the PVSyst application user interface

PVLib

PVLib is a product of the collaborative efforts of a group of PV professionals called the PV Performance Modelling Collaborative (PVPMC), facilitated by Sandia National Laboratories

in the USA. The PVLib toolbox is a standard repository for PV system modelling and analysis algorithms [66]. To date, it does not have any financial models implemented so it is only a performance modelling software package. The PVLib toolbox uses code-level modular programming to perform the modelling of the system. The toolbox is available in MATLAB or python programming languages. The PVLib toolboxes do not come with any graphical user interfaces so the user is expected to call the functions, set the required parameters and execute the simulation using the modules provided as building blocks. A typical simulation in PVLib comprises the following steps:

1. Setting up the location and design of the PV system. This includes importing the necessary python libraries and add-ons, collecting the weather data for the desired site and setting the orientation of the PV modules or arrays. The weather data is obtained from typical meteorological year files (TMY2 and TMY3).

2. Modelling the DC (direct current) IV (current-voltage) characteristics. This entails the estimation of the chosen module's behaviour according to its IV characteristics given in the module database, in response to the weather data given in step 1. Along with some intermediate results, the user obtains the estimated DC power yield.

3. Converting the DC power to AC (alternating current). The user makes use of a PVLib module that takes in the technical characteristics of a desired inverter as one of the parameters and models the AC power output.

4. Plotting the graphs and tables. The user also has the option of exporting the simulation results for presentation or further analysis in a third-party software package.

Access to PVLib is free and the software itself is easy to install. Its code is open-source and therefore transparent and easy to edit or modify [67]. The modular approach in PVLib allows users to draw better analyses on portions of the modelling chain separately. Because of the programming literacy that PVLib requires, the program attracts users mostly from specialised fields such as engineering and research. Figure 3.4 shows the interface on the of the PVLib-python toolbox in use on, Jupyter Notebook [68], a notebook interface.

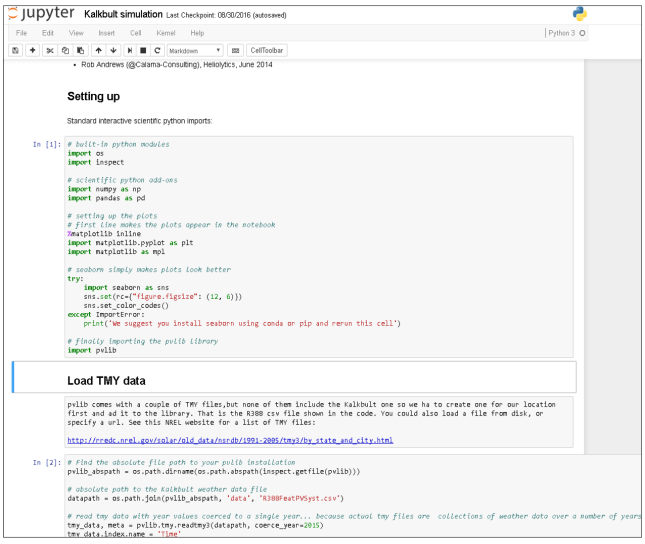

Figure 3.4: A screenshot of the PVLib-python toolbox, running on Jupyter

SAM, PVSyst and PVLib were then compared to each other according to various evaluation criteria:

(a) Cost and commercial availability

(b) Working platforms

(c) Version updates

(d) User-friendliness and ease of use

(e) Reporting and analysis options

(f) Modelling flexibility

(g) Performance and economic modelling capability

(h) Validation of simulation results with field data

3.4.2.2 Cost and commercial availability

SAM and PVLib are free to download, but you need a registration key to activate your copy of SAM. NREL provides SAM registration keys free of charge and uses your registration data merely for statistical purposes [5].

As for PVSyst, after installing it users can use it for free in the evaluation mode for 30 days during which it runs at full capacity. To enjoy the full capabilities thereafter, a user will have to purchase a license, otherwise PVSyst will automatically switch to its demo mode in which it runs with limited capabilities. The licensed mode is available in two flavours, namely Pro30, for PV systems up to 30 kW and Premium, the more expensive one which works with unlimited sizes of PV systems. A full listing of the prices for the licenses can be accessed on the PVSyst website [55]. PVSyst also supports academics with discounts on licenses bought for educational purposes. The discounts are available for schools, universities and other educational institutes on request directly from PVSyst.

3.4.2.3 Working platforms

PVSyst runs only on Windows client versions currently supported by Microsoft. The supported versions are Vista, 7, 8 and 10 on both 32 bit and 64 bit systems. Other operating systems are supported through the use of virtual machines running Windows such as VirtualBox [55].

SAM runs on Windows 7, 8 and 10 and is available in both 32 and 64 bit versions. SAM also runs on OSX and Linux operating systems, but it is only available in 64-bit versions [5].

PVLIb comes in two different types of toolboxes, namely PVLib for MATLAB and PVLib-python [67]. As the names suggest, the two toolboxes work on MATLAB and python environments respectively. PVLib-python works on platforms that have python versions 2.7, 3.4 or 3.5 and Pandas versions 0.13.1 or newer and these versions of python are available for Windows, Mac OS X and Linux [69]. MATLAB is also supported on Windows, Mac OS X and Linux.

3.4.2.4 Version updates

PVSyst is updated regularly and the PVSyst website provides information with regards to the improvements and fixed errors associated with each update and the date each update was released [70].

As is the case with PVSyst, SAM is update regularly and the NREL SAM website shows release notes for each of the updates and revisions, highlighting the improvements made and errors fixed [71].

PVLib is also being continuously improved and expanded in its functionality. All the releases are available on GitHub and are accompanied by a brief summary of the associated bug fixes, version documentation and acknowledgements of main contributors [72].

3.4.2.5 User-friendliness and ease of use

SAM comes with a graphical user interface (GUI). This makes it easy for users with no experience in computer programming or developing computer models to build PV systems and perform simulations. The GUI allows users to find their way around the program with relative ease. It provides access to input variables and simulation controls and it displays the user's selections as well as graphs and tables after running the simulation.

PVSyst also has a graphical user interface (GUI) that makes it possible for users who are not particularly experienced in computer modelling to build their own PV systems, perform basic simulations and generally navigate their way through the software program with relative ease. The interface in PVSyst allows the user to perform system designing and sizing and to obtain results in graphical or tabular form easily. For most of the tasks, the user only has to input certain required values in the appropriate fields and then execute actions by the touch of a button.

PVLib does not offer a graphical user interface. It is essentially a collection of scripts and functions that handles data, module and inverter parameters and takes in atmospheric and irradiance models. The user runs these scripts and functions sequentially to perform PV system simulations. The interface is therefore bound to present some challenges to users with no programming skills or experience in computer modelling of PV systems.

3.4.2.6 Reporting and analysis options

SAM has a default graphing tool that not only enables the display of results as sets of default graphs, but also allows the creation of custom graphs. Alternatively, the results can be presented in the form of tables or exported to other software packages for presentation or further analysis. SAM also provides a number of options for simulation results analysis, namely [73]:

(a) Parametric analysis - This enables the user to assign multiple values to input variables in order to create graphs showing the relationship between one or more input variables to a metric result. This operation is ideal for the optimisation of input variables.

(b) Sensitivity analysis - This option enables a user to investigate how sensitive an output metric is to variations in certain input variables.

(c) Statistical analysis -This analysis option allows the user to investigate uncertainties in one or more input variables on output metrics.

(d) Multi-level subsystems - This allows users to model power systems as a combination of subsystems. This could be ideal, for instance, in a situation where each subsystem is meant to be oriented in a different direction.

(e) Excel Exchange - This option allows the user to link an input variable in SAM to a cell or range of cells in a Microsoft Excel Workbook.

(f) P50/P90 analysis - This is a method of calculating the probability that a system's total annual output will exceed a certain value, for a site of which the weather data is available for many years.

(g) Exchange Variables - This option allows the user to input his own variables for use with a custom Transient System Simulation (TRNSYS) deck or Excel Exchange.

PVSyst, like SAM, documents simulation results into reports, summarising the simulation parameters, main results and system quality. The results can also be viewed as tables or exported to a third party software package like Microsoft Excel for further analysis or presentation. The only analysis option that PVSyst offers is the P50/P90 [55].

PVLib allows the user to view simulation results by plotting the respective metric's graph or exporting the results to a third-party software package such as Microsoft Excel for further analysis. The original PVLib toolbox does not offer any analysis options.

3.4.2.7 Modelling flexibility

PVSyst comes as a complete desktop application and does not have an allowance for scripting. That means that the user can only model a PV system the design of which adheres to certain predefined standards in PVSyst. It is therefore not possible for the user to introduce or modify any of the thermal, electrical or optical models in PVSyst [74]. Users can however define devices not found in the PVSyst component databases using the manufacturers' datasheets, thereby creating new devices in the database.

SAM also comes as a complete desktop application but it has a built-in scripting language, SAM User Language (SamUL). This allows the user to automate tasks and to perform more complex analyses from within SAM [5]. With SAM, a user also cannot introduce new thermal, electrical or optical models but can link and import variables from other other programs such as Microsoft Excel and TRNSYS. The user is also allowed to define devices that cannot be found in the component database using the component's datasheet. In August 2017 SAM actually became open source and one of the main reasons for that was so that users can change the code, build their own versions of SAM and add their own features and capabilities, in addition to providing more transparency in their algorithms and promoting collaborations [75].

PVLib is built on the very basis of modelling flexibility. The availability and free access to the PVLib source code makes it possible and easy for users to modify models, databases and input methods for a range of research and design goals [66] and [67].

3.4.2.8 Performance and economic modelling capability

SAM has a lot of performance models for photovoltaic systems, concentrating solar power, solar water heating, wind power, geothermal and biomass power. The photovoltaic systems in SAM are further subdivided into three categories:

(a) Flat Plate PV, which models the system using sub-models for the components (modules and Inverters) of the system. This is the model we will use for our grid-connected PV system performance model.

(b) High-X Concentrating PV, which models concentrating photovoltaic (CPV) systems.

(c) PVWatts, which models crystalline silicon-based systems and is an implementation of NREL's PVWatts model which is web-based.

SAM offers a significant number of financial models. The models calculate the cash-flows and financial metrics for different financing options chosen by the user. The financial models given in SAM are for residential projects, commercial (excluding Commercial PPA) projects, commercial projects with power purchase agreements (PPA) and utility projects [5].

PVSyst only deals with photovoltaics and it splits its performance models into four main categories:

(a) Grid-connected - This is a type of system that is made up of components constituting the PV array i.e. modules/ strings of them, inverters and everything up to the connection to the grid.

(b) Stand-alone - A system which should constitute of modules, a battery and a regulator.

(c) A water pumping system.

(d) DC Grid - A system made up of a PV-array and a load profile meant for public transport network.

PVSyst also offers economic evaluation to model project costs and investments. With the financial model, the user can project running costs and deduce the long-term profitability, especially for grid-connected systems [55].

The PVLib original toolbox has a performance model that currently only supports grid-connected systems and does not offer any financial models. There is, however, room for improvement in PVLib and for more experienced users to expand on PVLib's capabilities and add elements that will help them model other systems [66], [67] and [76].

3.4.2.9 Comparisons of Simulation results

The 75 MWp solar plant was modelled in the three programs to simulate the total energy yield for the whole year using the Hay-Davies [46] transposition model. Weather data measured on the site for the year 2014 was used in the simulations and the simulated total energy yield of each software package was compared to the total yield recorded at the test site for the year 2014. Table 3.2 summarises the losses calculated for the 75 MWp system from the plant's measured data.

Table 3.3 shows a summary of the total yield produced by the simulations in each of the software programs and their percentage differences from the actual plant yield. The percentage difference was calculated as:

$$Diff(\%) = \frac{Yield_{actual} - Yield_{simulated}}{Yield_{actual}} \cdot 100\% \tag{3.1}$$

In Figure 3.5, the three simulated annual yields are compared to the plant's actual yield for the year 2014 and in Figure 3.6, a similar comparison is drawn based on the energy profiles on randomly selected clear sky and cloudy days. The results show consistency and that PVSyst simulated the yield more accurately, with a calculated percentage difference of 3.4%, followed

Table 3.2: Summary of plant losses

Loss	**Value (%)**
Shading	-2.5
Reflection	-2.5
PV loss due to irradiance level	-0.45
Module mismatch and DC ohmic	-1.77
Soiling loss	-1.75
PV loss due to temperature	-6.3
Inverter loss	-2.6

Table 3.3: 2014 Total Annual Yield Comparison

Source	**Total Yield (MWh)**	**Difference (%)**
Actual yield	149868.2	-
PVSyst	144813.6	3.37
SAM	144046.4	3.86
PVLib	142276.8	5.07

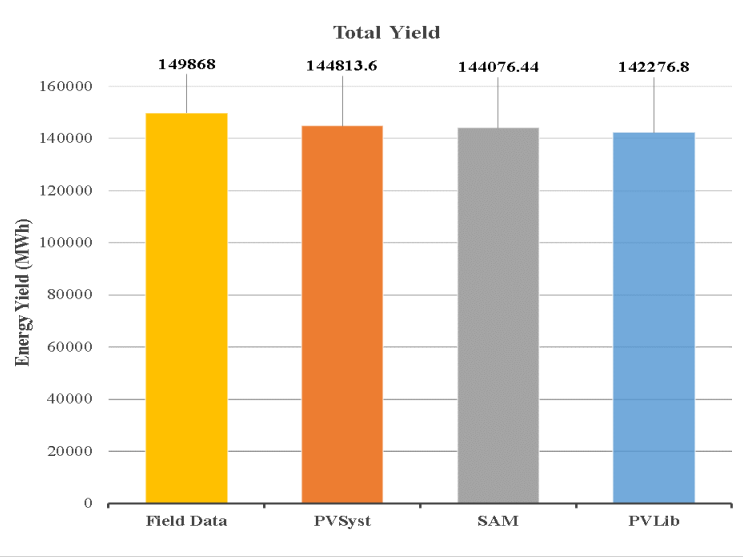

Figure 3.5: Total energy yield for the year 2014

by SAM with 3.9% and then lastly PVLib with approximately 5.1%. The results also show that the three software programs were generally conservative in their yield predictions and this is probably because of the overestimation of losses in some of the programs' default losses. The default losses were used in some of the system modelling stages where the actual values for the losses could not be calculated from the available plant data or the design tool did not provide an option for actual values to be input for particular system losses but rather estimated them

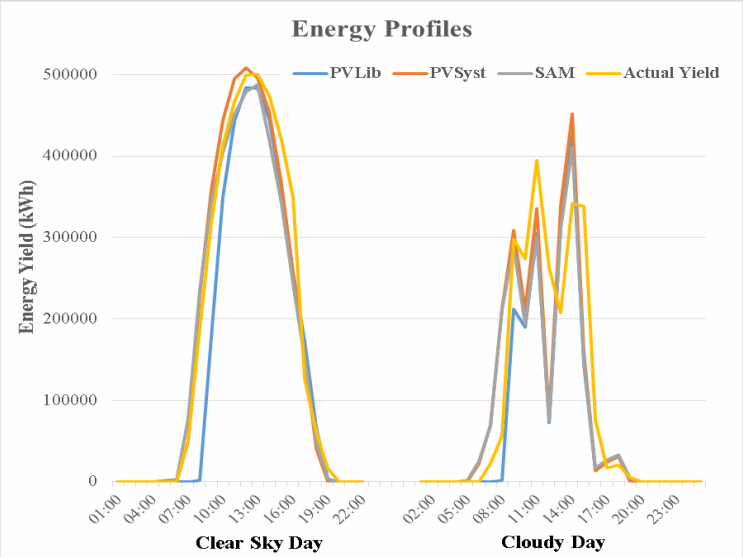

Figure 3.6: Clear sky and cloudy day energy profiles

using inbuilt system loss models.

3.4.2.10 Conclusions

Analysis of the software packages revealed that each software package has its own merits that makes it more suitable than the others for certain simulations, and demerits that serve as disadvantages in certain instances. In terms of accuracy and robustness, PVSyst seemed to outperform the rest, closely followed by SAM. In terms of modelling flexibility, PVLib and SAM did well, while PVSyst was held back by its rigid form. In terms of other general characteristics and functionalities, it seemed SAM would be the most suitable, of the three software packages evaluated in this paper, for the next section of work involving optimisation strategy formulation and implementation. SAM proved to be a fairly accurate, complete, easy to install and user-friendly solar PV simulation tool that also comes with the perks of modelling flexibility and a wide range of reporting and analysis options which could potentially come in handy.

3.4.3 Iterative optimisation approach

One way of determining design parameters for optimally designing a PV system is by iterating through all possible values and then choosing the one value that best satisfies the design objective(s). When there are more alternative system configurations to choose from, it might also be worthwhile to compare the performances of the options with each other simultaneously. Parametric analysis enables the system designer to quantitatively and qualitatively compare different PV systems with each other simultaneously. In this example, we used an iterative approach to determine the optimal tilt angle that would yield the highest amount of energy per year, month and season. The results were then compared to those of the rule-of-thumb, ROT, recommendation (tilt = latitude) as well as the yield from single and dual axis tracking systems using parametric analysis. NREL SAM's scripting ability and parametric analysis features were implemented towards this end.

3.4.3.1 SAM scripting and parametric analysis

SAM has an in-built scripting language known as LK. It is a powerful, yet simple, scripting language that is designed to be compact, fast and easy to embed in other applications. It is

quite similar to Visual Basic for Applications (VBA) in Microsoft Excel and works on Windows and OSX platforms alike [77]. In SAM, particularly, it helps extend the inbuilt functionality of the program and enables users to automate redundant tasks and large numbers of simulations. Some of the features of the LK scripting language include:

- ability to use user-written functions,
- conditional statements (if, else, etc...) and loops (while, for, etc...) just like any other programming language,
- ability to implement data structures such as hash tables, arrays (single and multidimensional), and
- a built-in library of functions for simple input and output tasks as well as more complex subroutines such as regressions, sampling, plotting and accessing web services.

SAM's parametric analysis enables PV system designers to assign more than one value to input variables and assess their influence on the output results and it can even take the place of the iterative approach in some cases. Parametric analyses in SAM produce tables and graphs that can also be exported to third-party platforms for further investigation and presentation.

3.4.3.2 Procedure

The following procedure was used in this investigation to optimise energy production for our test site by calculating optimal tilt angles for different periods in the year and comparing the different system setups with each other:

1. Use SAM script to iterate through possible tilt angles, θ_T, to find the optimum tilt angle, $\theta_{T,opt}$, that gives the highest total annual energy yield.
2. Use iterative SAM script to find the optimum tilt angles, $\theta_{Tm,opt}$, that maximise the total energy yield for each month.
3. Derive the seasons' optimum tilt angles, $\theta_{Ts,opt}$, from the averages of the tilt angles of the three months that constitute that particular season according to the South African seasons given in Table 3.4 obtained from [78].
4. Derive the biannual optimum tilt angles, $\theta_{Tb,opt}$, by averaging the optimum tilt angles in the 6 months between the two equinoxes, in March and September. For the biannual tilt method, summer tilt, therefore, is an average of the October to March period, while the winter tilt is the average for the period starting in April and ending in September. This method of calculating the biannual tilt led to projection of a higher energy yield than the rule-of-thumb approximation for the biannual tilt which stipulates that the optimum tilt angle should be 15° more than the latitude for the six winter months and 15° less than the latitude for the six summer months [58].
5. Compare all the above-mentioned methods' monthly yields with that of the $\theta_{T,opt} = Latitude$ and the tracking systems. The different systems were simulated and their total monthly and annual energy yields were compared all at once using SAM's parametric analysis.

Figure 3.7 shows the algorithm for the iterative process that was implemented in SAM LK to loop through the possible tilt angles, 0 to 90 degrees, to optimise the systems for maximum energy yield.

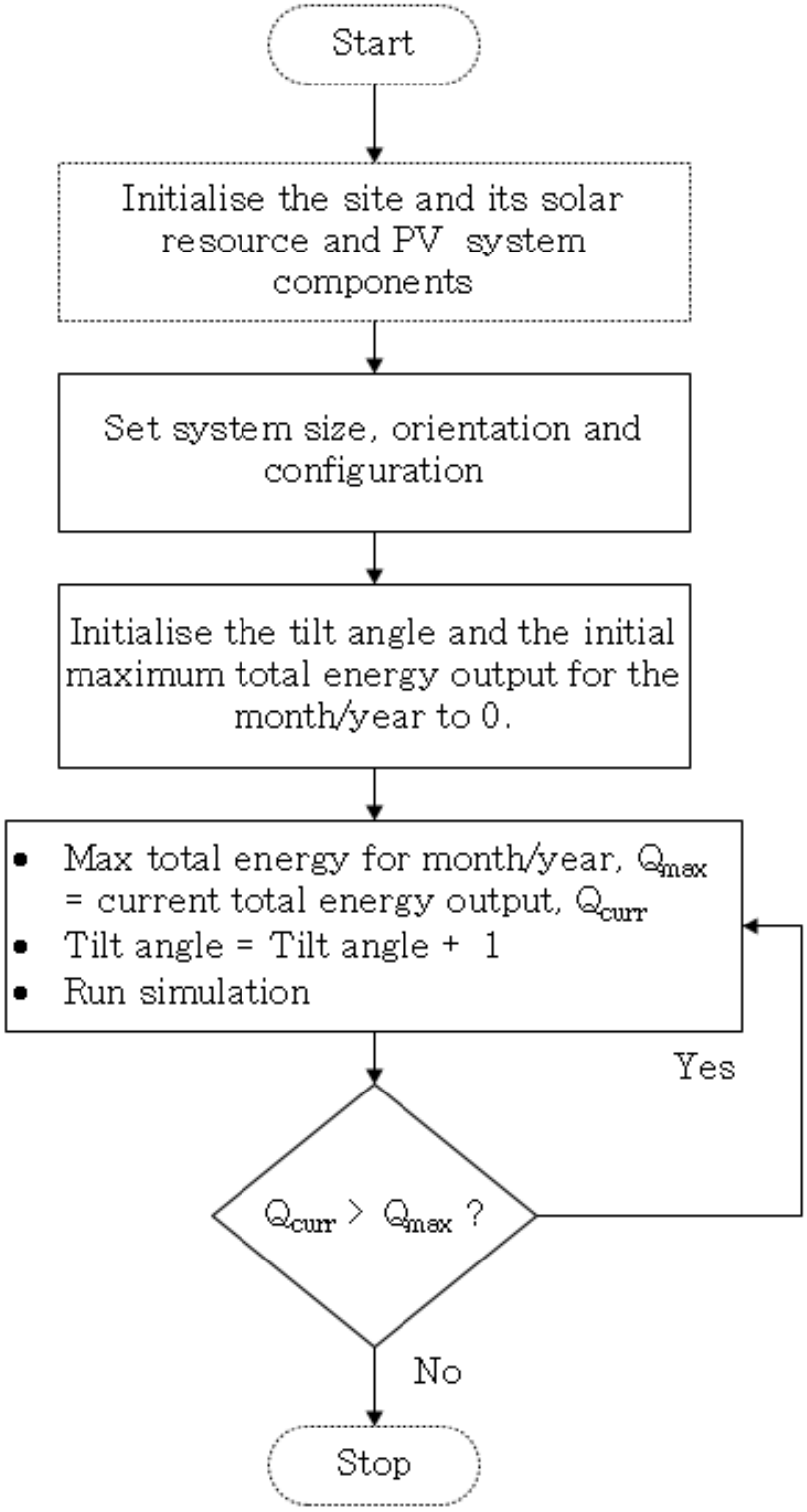

Figure 3.7: Algorithm for iterative tilt angle optimisation

Table 3.5 summarises the monthly, seasonal and biannual tilt angles as calculated for our test site. In all the comparisons, the same model and number of PV modules and inverters were used. Only the tilt methods and mounting methods were varied, accordingly.

Table 3.4: Table of season calendar dates

S. Hemisphere	Dates	N. Hemisphere
Autumn	1 March - 31 May	Spring
Winter	1 June - 31 August	Summer
Spring	1 September - 30 November	Autumn
Summer	1 December - 28/29 February	Winter

Table 3.5: Table with the calculated monthly, seasonal and biannual tilt angles

Tilt angles				
Month	Optimal tilt angle	Seasonal Tilt	Biannual	Annual
January	0	3	8	32
February	8	3	8	32
March	26	44	8	32
April	52	44	52	32
May	54	44	52	32
June	63	58	52	32
July	56	58	52	32
August	52	58	52	32
September	34	16	52	32
October	15	16	8	32
November	0	16	8	32
December	0	3	8	32

3.4.3.3 Results

Figures 3.8 and 3.9 show the results of the parametric analysis of various tilting and mounting methods. The plot shown in Figure 3.8 shows the monthly variation of system yield for various tilting and mounting methods. Energy production seems fairly consistent for most of the methods save for the two tracking systems which show significant drops in energy in winter; the single-axis tracker dropping more significantly than the dual-axis tracking system. Figure 3.9 shows the comparison of annual energy yield for various tilting and mounting methods. The percentage difference between each mounting or tilting method's yield with that of an optimally tilted fixed system is shown on top of each bar. The results show that adjusting the tilt angle of the fixed tilt systems periodically can boost energy production. This is not only valuable in optimising annual energy production, but also optimising energy production for specific months or seasons. The rule of thumb was also proven to be fairly accurate as its energy production was within 0.1% of the actual optimal energy yield produced at at tilt angle of 32°.

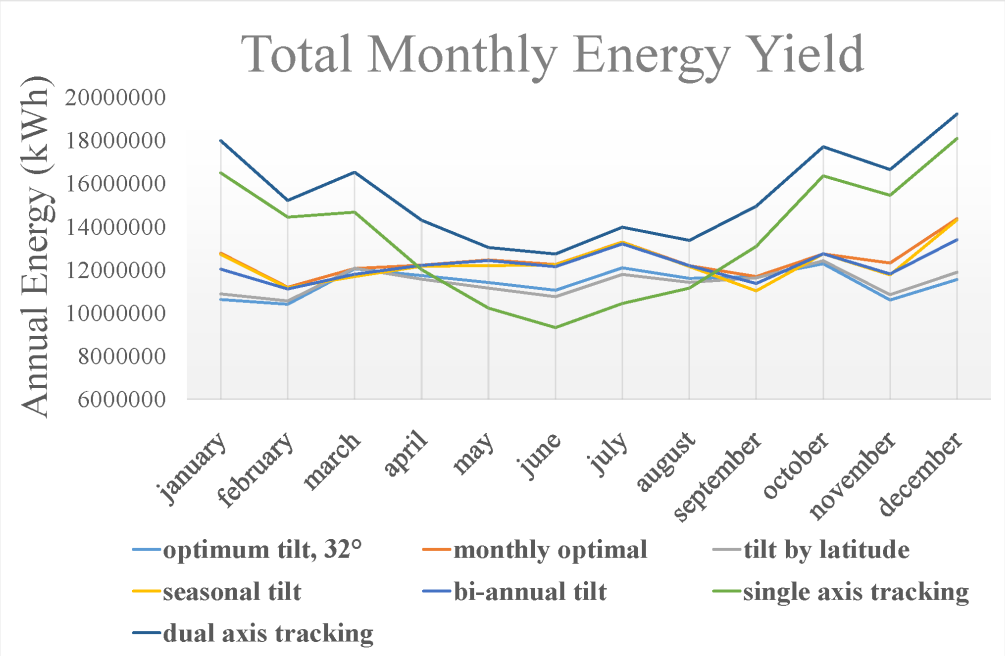

Figure 3.8: Monthly Energy Yield comparison of various tilting and mounting methods

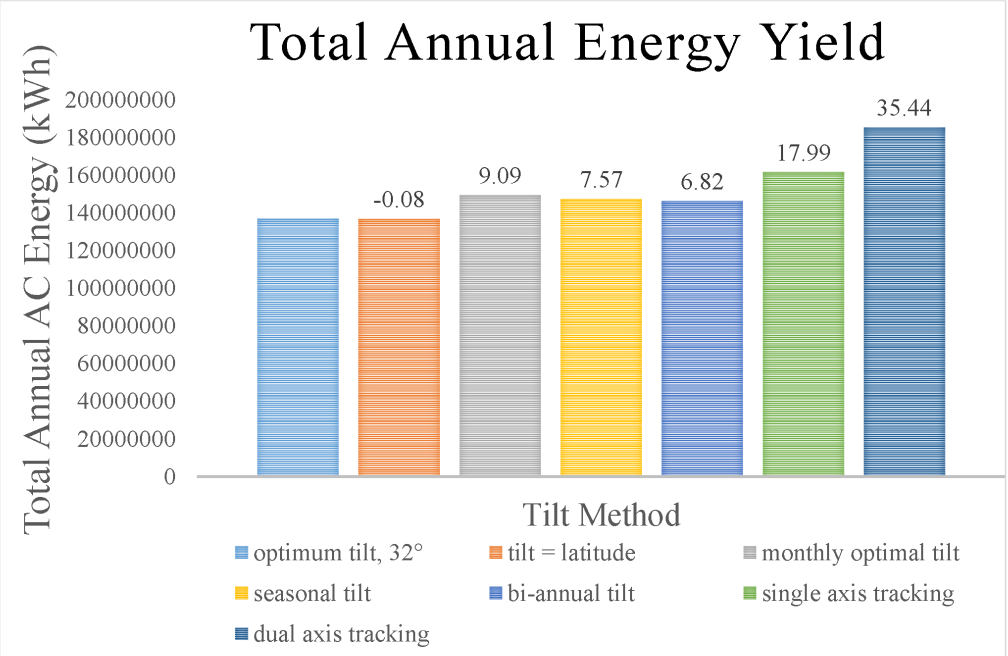

Figure 3.9: Total Energy Yield Comparison for the various tilt and mounting methods

3.4.3.4 Conclusion

The parametric analysis helped us quantify the differences in the yield of the various mounting methods. Tracking systems generally performed significantly better than any of the other

systems, but the adjustable tilt systems offer a less expensive way to drive system performance so they might be worth considering depending on how practical that might be in the particular site's case. The seasonal, monthly and biannual tilt methods showed great potential in boosting energy production and would be interesting compromises between fixed tilt and single-axis tracking systems. The iterative approach was very useful in determining the optimal tilt angles and automation of the process by means of scripting helped circumvent the monotony that is usually part of iterative processes. The main challenge with this method is the fact that it is extremely tedious to go through each and every one of the possible design variables, especially if there are other parameters that also need to be designed for. Evolutionary programming methods and their ingenious iterative approaches, as will be discussed in the Optimisation Strategy Chapter, would prove useful in this regard.

3.4.4 Multi-objective optimisation

It is not uncommon for the PV system design process to involve multiple design parameters and multiple design objectives. When this happens, there might be need to find a reasonable compromise so that the final PV system does not optimise one objective or parameter over the other. This is usually where multi-objective optimisation comes in handy. One such design scenario occurs when PV system designers are designing for optimal tilt and row spacing. These two design variables tend to be antagonistic because optimally designing one tends to compromise the other, especially in a constrained design space, as explored in the following design scenario investigation.

In the case of fixed tilt systems on space-constrained sites, PV system designers would typically want to design the system for maximum power density, so as to fit in as many solar panels as they can in the available area. In designing for maximum power density, rows of modules are placed closer together and the tilt is lowered to reduce inter-row shading. This results in a higher peak capacity but the modules will be less productive individually.

In cost-constrained projects, however, system designers would probably rather design for maximum panel energy yield to ensure that the system gives the best value for money in module performance since module costs alone make up a substantial portion of the system costs compared to any other component in the PV system [79]. To get the maximum energy yield from each module, the designer will have to design for an optimum tilt and space the modules far apart to avoid shading. While this is good for energy production as it maximises the amount of irradiation reaching each panel's surface and reduces shading, this design decision reduces the number of modules that can fit into a unit area.

A multi-objective optimisation for tilt and row spacing, to find a compromise between the two design considerations, was performed in Helioscope using shading analysis. Helioscope was not part of the initial PV system tool investigation as given in Section 3.4.2, but it was found suitable for this particular investigation.

3.4.4.1 About Helioscope

Named after the instrument that is used to observe the sun and sunspots, Helioscope is a PV system design tool from Folsom Labs that incorporates system layout and performance modelling to simplify the solar PV system design process [31]. It is a cloud-based software program designed to be easier and cheaper to use than other commercially available design tools such as PVsyst. Helioscope uses the same underlying algorithms as PVsyst, also comes with

an extensive component library and has global weather coverage and enables users to design PV systems with relative ease, without requiring them to know too many engineering-level intricacies [80]. Simulation results from Helioscope were evaluated by BEW Engineering [81] and they proved to be fairly consistent with PVsyst results [80].

Helioscope, however, can only handle PV systems of up to 5 MW in capacity so it was necessary for us to scale down the size of our test-case to an appropriate level. Scaling down in no way compromises our investigations because the main goal was not to calculate shading losses precisely but rather identify their trends within the context of our test-case's design parameters and constraints. Helioscope's robust shade and sketch-up integration made it ideal for the pitch-tilt multi-objective optimisation investigation even though SAM and PVsyst could have also been implemented with a bit of extra effort. Compared to PVSyst, defining a shading scene in Helioscope is much easier and straightforward. With SAM, the optimisation would tend to lean more towards the optimisation of the ground cover ratio, since SAM uses GCR in its shading computations rather than directly using the pitch [54], instead of the intended pitch-tilt multi-objective optimisation even though the ultimate effect would be the same.

3.4.4.2 Procedure

A multi-objective optimisation was performed over an area 174661.7m^2 in size with a baseline system design set as 30° tilt, north-facing azimuth and an inter-row spacing of 4.14m based on a scaled down version of the test-case design specification. The simulation was repeated for 20° and 40° tilt angles and the inter-row spacing was varied from 1.14m to 7.14m in one-metre increments. The assumptions in this case are:

- that the configuration of the PV modules is set according to the recommendation of the module manufacturer in the portrait configuration,
- the azimuth is at its optimum at 0°, facing the true north direction, and
- no other obstacles are in the vicinity of the solar array to cause shading so all shading losses in this case can be attributed to inter-row shading.

Specific Yield, defined by the equation:

$$Yield_{specific} = \frac{AnnualEnergy_{total}(kWh)}{InstalledCapacity_{total}(kWp)}, \tag{3.2}$$

is essential in this analysis because as we vary the row-spacing and tilt angles, the number of PV modules that can fit into the space provided also changes and this, in turn, affects the nameplate capacity of each modelled system. Specific Yield, therefore, allows us to compare the overall performance of each of the 21 systems on a standardised scale.

3.4.4.3 Results

Figures 3.10 and 3.11 show the results of the shading losses and the specific yield as the tilt angles and inter-row spacing were varied. From the figures, it can be deduced that the lower tilt angle, 20°, showed fairly consistent performance for the most part, regardless of the inter-row spacing. The sensitivity of the system's performance also seemed to increase as the tilt angle was increased and this is mostly evident in the gradient of the 20°, 30° and 40° line graphs in the sub-'2.14m inter-row spacing' region. It was also noted that specific yield increases as the inter-row spacing increases until a certain distance beyond which increasing the row spacing will not do much to improve the system performance. This distance is just over 4.14 m. There

is also evidence of a minimum row spacing below which the system performance will start decreasing drastically and this is around 2.14 m for the three tilt angles. A row distance below 2.14 m would generally prove more taxing where module performance is concerned, while a row distance above 5.14 m would be wasteful in land utilisation so for system designers, the 2.14 m to 5.14 m row distance region would be an area of key interest.

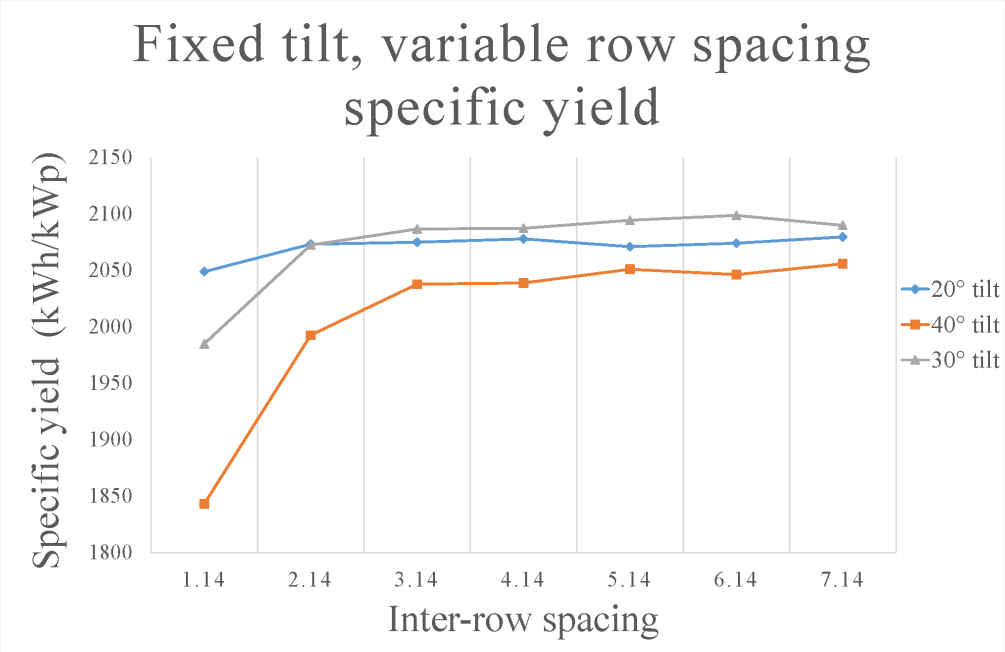

Figure 3.10: Graph of variation of system performance with inter-row spacing

Figure 3.11 also shows a similar trend and confirms that the closer module rows are placed to each other, the more they make shade on each other and the less productive the system performance will be.

3.4.4.4 Conclusion

Multi-objective optimisation could be useful to determine reasonable compromises in the PV system design process. The approach, however, could suffer if the number of variables or objectives increase as it is already a rigorous process with two design variables and objectives, judging by this design example. Optimisation methods that take into account multiple design objectives and multiple variables can be quite useful in this regard. This is noted and implemented in the optimisation strategy chapter.

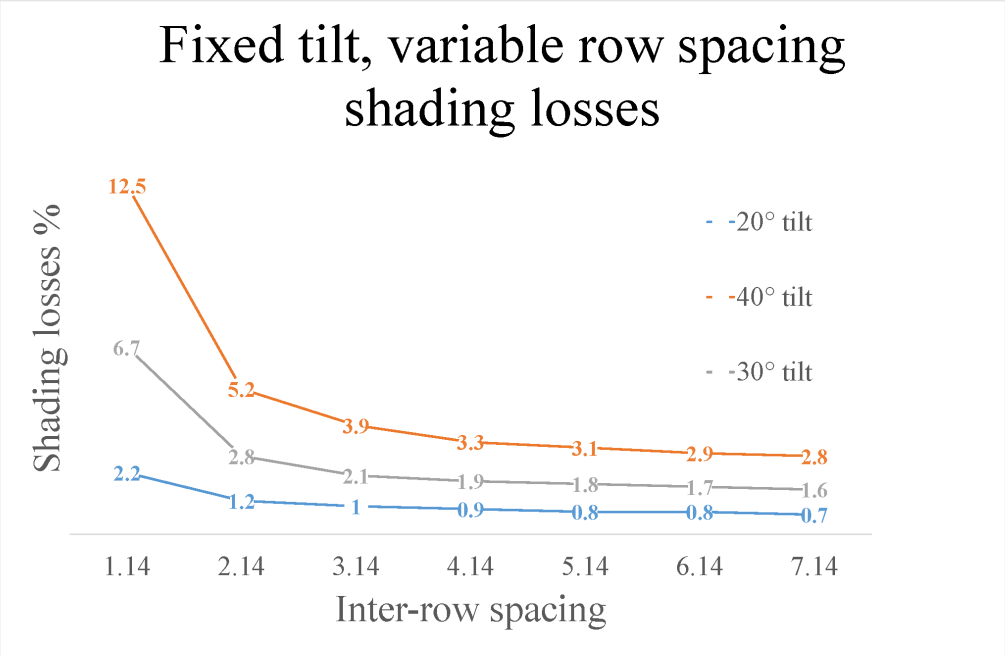

Figure 3.11: Graph showing variation of shading losses with inter-row spacing

3.4.5 Other non-conventional design alternatives

As mentioned in [26], recent trends and changes in the solar PV industry have warranted a revisit to design methods to determine what changes need to be made for adaptation purposes. Methods that do not adhere to the traditional design conventions, such as the rule-of-thumb, are becoming a popular way of optimising system performance in various aspects and also helping designers bypass certain design constraints. One such example is the east-west orientation method.

The east-west orientation is a racking style where consecutive PV module rows are oriented facing the east and west directions in an alternating fashion as shown in Figure 3.12. The

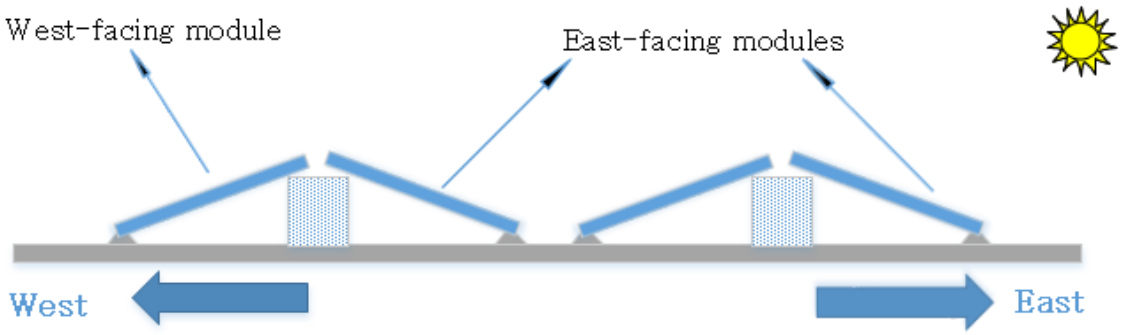

Figure 3.12: A pictoral representation of the east-west orientation.

east-west orientation is based on an understanding of the apparent motion of the sun due to

the earth's rotation as it rises from the east and sets in the west as shown in Figure 3.13. As such, in this orientation the east-facing modules produce more energy in the morning while the west-facing modules cater for the afternoon. Even though the east-west orientation usually results in a lower peak, the set up enables modules to capture peak power production for longer durations and during the earlier and later hours of the day. It also allows modules to be fitted closer to each other since it results in minimal shading. The system will consequently have a higher power density since more PV modules will be able to fit in per unit area.

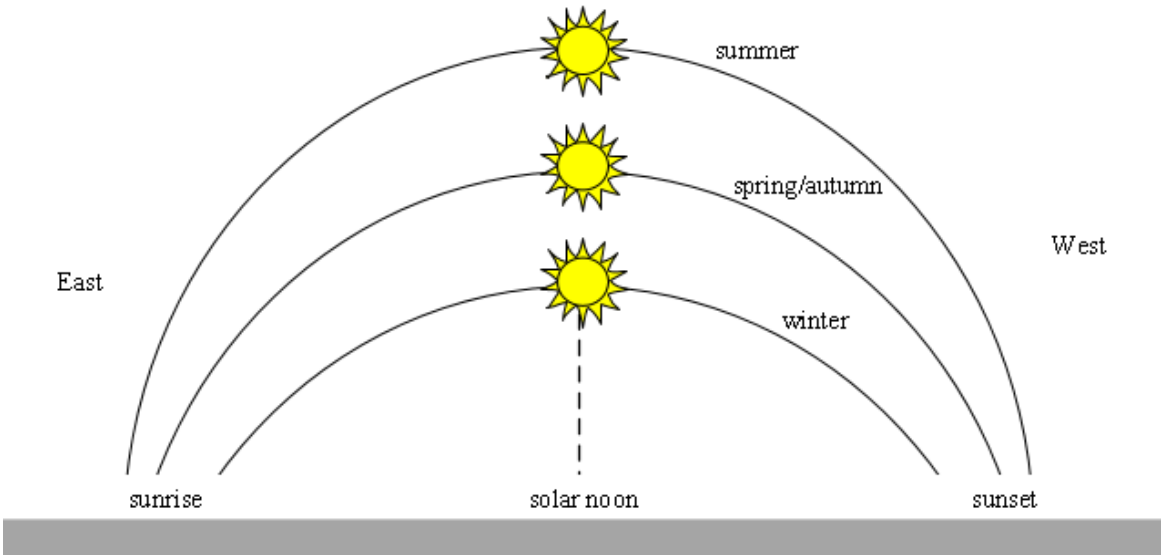

Figure 3.13: Depiction of the apparent path of the sun as the day and year passes.

In addition to improved power density and reduced shading, east-west orientation also has a variety of other advantages [82]. These advantages include:

- improved aerodynamics since the panels will be back to back at a low tilt. This results in less drag and less air-scoop unlike in North or South facing systems where the setups are vulnerable to southerly or northerly winds.
- more efficient use of inverter capacity because of the ability to use over-paneling as a consequence of a lower peak output.
- lower costs due to less maintenance and more efficient use of components such as mounting material.
- more consistent energy supply during the day and potential use in matching facilities' demand curves especially in regions where Feed-In Tariffs (FITs) are in place.

3.4.5.1 Procedure

A comparison of North-facing and East-West orientation was conducted to simulate the potential benefits of the east-west orientation using tilt angles of 20°, 30° and 40° for a space-constrained piece of land measuring $174661.7m^2$ on the test-case site. The pitch in each scenario was determined such that it was the shortest possible distance that resulted in 0% inter-row shading losses and the goal was to fit as many PV modules as possible in the given area. Using the same tilt angle at each iteration, energy yield, plant performance and installed capacities for the two orientations were simulated in Helioscope and compared.

3.4.5.2 Results

Figures 3.14, 3.15 and 3.16 show the summary of results. Figure 3.14 shows how the east-west orientation can be used to improve installed capacity on a space-constrained piece of land since it results in very little inter-row shading. Figure 3.15 shows how the poor individual module performance can be compensated for by the increased installed capacity to boost the total annual energy yield of a system in an east-west orientation in a space constrained design space. In projects with high fixed costs, designers will also be able to boost the system's energy production capacity per unit area without too much of a negative impact on overall project costs.

The low specific yield for the east-west orientation shown in Figure 3.16 is due to the fact that module layout will not be optimally designed to produce the highest amount of energy at solar noon, when GHI is supposed to be at its highest, and at any particular time before and after solar noon, only half of the modules will be optimally oriented for maximum energy yield. This results in a relative under-performance of the east-west systems, compared to systems oriented facing towards the equator.

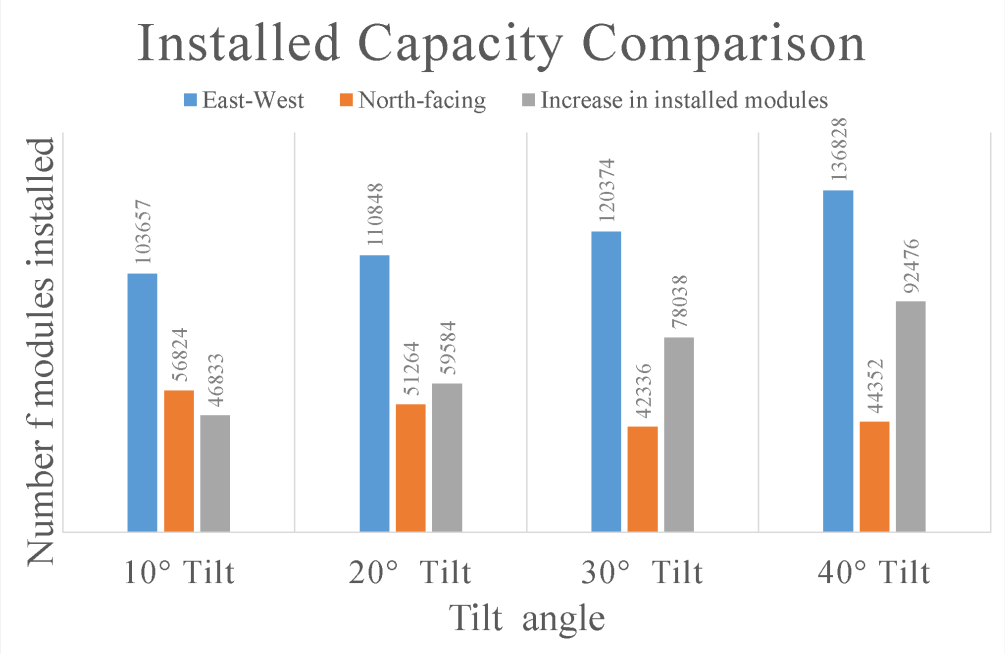

Figure 3.14: Comparison of installation capacity showing the increase in the number of PV modules that can fit into the site due to the east-west orientation.

3.4.5.3 Conclusion

The east-west orientation method was particularly interesting as it goes against convention, but proved to be potentially useful in overcoming issues that come with many space-constrained locations and projects with high fixed costs. For a small sacrificial drop in system performance, system designers will be able to fit more PV modules per unit area using the east-west orientation and get more energy yield, compared to the north-facing orientation. In addition to that, the

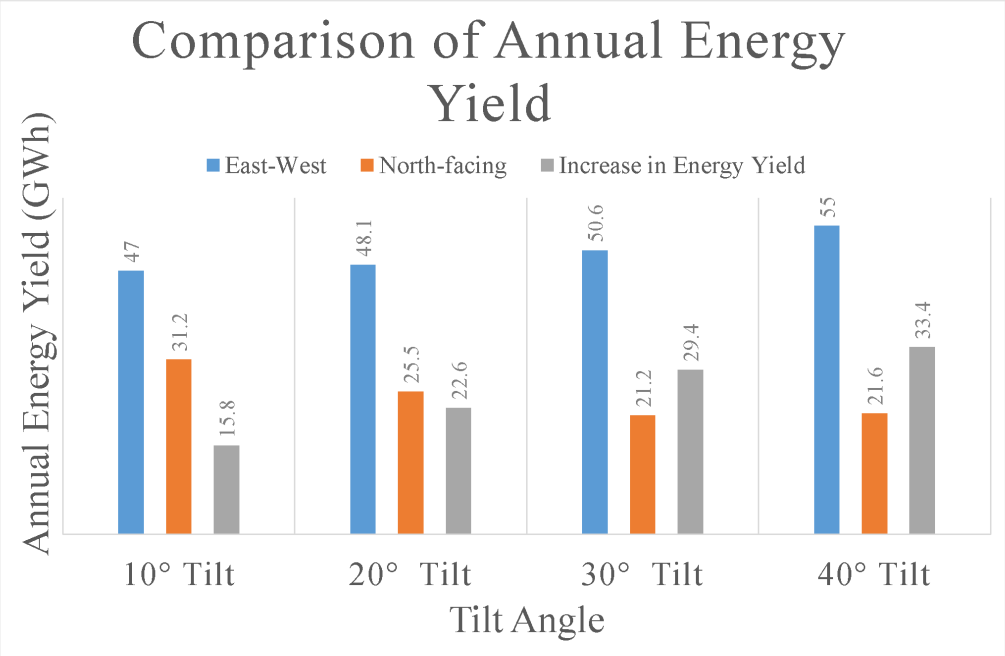

Figure 3.15: Comparison of energy output of the PV systems indicating the increases in the energy production due to the east-west orientation.

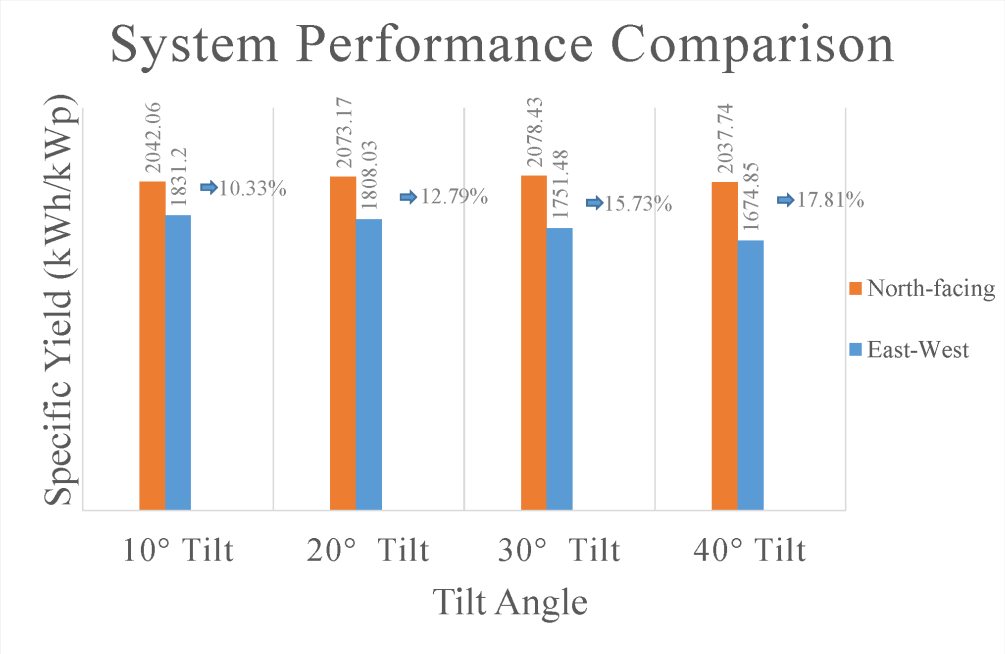

Figure 3.16: Comparison of the system performances showing a reduction the percentage drop in production due to the east-west orientation.

east-west orientation method harnesses intrinsic value in several other plant design aspects and ties in together with what was pointed out earlier in Section 3.2, that the focus of PV system design is starting to take more interest in the balance of system aspects as well as other PV system performance indicators to optimise PV system designs. We concluded that it would be worthwhile to devise a plant layout strategy that would take into account several design objectives simultaneously. Multi-objective optimisation methods that are discussed in the Optimisation Strategies Chapter will enable us to achieve this goal.

3.5 Summary

In this chapter, various elements that go into plant design optimisation were reviewed. The process involved investigating the tools and strategies currently being implemented by some PV system designers to find their purposes and strengths and to identify areas that could use some improvement. Some of the key insights from this preliminary plant design and optimisation process are:

- Every design tool is made with a particular goal in mind and this sets PV system design tools apart from each other. It is important for PV system designers to knowledgeably select design tools that will enable them to perform their modelling and analysis thoroughly and accurately.
- Iterative optimisation approaches, as investigated in this study, are very helpful in the optimisation process but with increased dimensionality in design objectives and variables, it might get more cumbersome to implement them. This could be solved by using evolutionary programming methods which make use of algorithms that can navigate complicated iterations.
- In cases involving several, sometimes antagonistic, variables and objectives, multi-objective optimisation could be implemented to circumvent the challenges of having to prioritise one objective over the other(s). Optimisation methods that perform operations on multiple variables and/or multiple objectives could be helpful in this regard.
- Nonconventional design optimisation processes also play an important role in overcoming certain design constraints and challenges. They also are better adapted to the current trends in the PV industry. The east-west orientation method used in the design example brought multi-objective optimisation into the picture as a way to make the design process more holistic to intentionally develop systems that excel in satisfying several design objectives simultaneously.

All these conclusions were then used to formulate an optimisation framework for utility scale PV systems that combines the accurate PV system design modelling in reputable, bankable design tools and a more comprehensive approach to PV system layout design.

Chapter 4

Optimisation Strategies

4.1 Introduction

The main objective of this project is to investigate strategies to optimise PV plant design layout. In PV system layout design, optimisation is the process of improving the PV system's orientation and setup to better achieve the desired design goal. For design layout optimisation, this process involves selecting design parameters such as module tilt and azimuth angle and the ground cover ratio (GCR) to optimise energy yield, plant performance and/or cost of energy production for the desired project site. The main elements needed for the successful design layout optimisation are:

- PV system modelling tools that are capable of accurately estimating the response of the plant design objectives to variations in the design parameters,
- Clearly defined site conditions and constraints for the plant being designed, and
- An effective method to go through the possible solutions to select the best option.

In this chapter, these elements are explored and made use of in the development of an optimisation framework for PV system layout using evolutionary programming techniques.

4.2 Evolutionary Algorithms (EAs) in the design of grid-connected PV systems

Evolutionary Algorithms (EAs) are a part of evolutionary computation which is a metaheuristic (higher-level) optimisation procedure. EAs use techniques adopted from nature and biological evolution to find solutions for complex problems and have been used widely in several science and engineering fields to date. These methods include Ant Colony, Particle Swarm Optimization (PSO) and Genetic Algorithms (GAs) [83] and [84]. In the renewable energy industry, and more specifically in solar PV, this new generation approach to system design is being used in several ways to replace and sometimes consolidate the traditional design approach which often follows rigorous procedures such as iteration and linear programming. Some of the areas in which EAs have been used extensively include PV-wind hybrid system designs and methods for Maximum Power Point Tracking (MPPT). Sinha and Chandel did a substantial review of recent trends in optimisation techniques implemented in solar PV-wind hybrid systems in [85]. The major outcomes from this review indicate that EA methods are not only improving over time but are also proving to be useful, especially towards tackling the involute problems often encountered in the renewable energy research sector.

Several sources also show the implementation of optimisation algorithms in Maximum Power Point Tracking (MPPT). Sreedhar and Jagadeesh, briefly describe and review several of these optimisation techniques and find that the biologically inspired algorithms generally perform better than the other methods they were compared to such as the Constant Voltage Tracking (CVT) method, the Perturbation and Observation (P&O) method and the curve-fitting method in [86].

Authors such as Kornelakis et al [87], [88] and [89], Weinstock and Appelbaum [90] and Gallardo [91] have some of the best work in the optimisation of layout design and sizing of grid-connected PV systems using EA techniques which is more relevant to the main focus of this thesis. Weinstock and Appelbaum present a single objective-multivariable solar field design of fixed tilt solar panels. Kornelakis et al present methodology to optimise system design and evaluate project economic viability for grid-connected PV systems on an island in Greece. The PVGCS modelling uses mathematical equations to facilitate the design process by optimising various device-type combinations and then selecting the one which is the most economically profitable. Gallardo builds up on work related to that done by Weinstock and Appelbaum to successfully design a general methodology for designing PV systems based on ecodesign principles. The work by Gallardo is very elaborate and the only drawbacks to it are, like the author states, the lack of an approach that allows the integration of the optimisation algorithm with commercially available PV system simulation tools and, to a reasonable extent, the computational expense as evidenced by the time the simulations took to run using Gallardo's methodology. The focus of Gallardo's research also is more towards optimisation for more eco-friendly PV system designs, as opposed to the focus of this thesis which is optimisation of the PV plant designs for better performance and energy production.

4.3 Optimisation Methodology

4.3.1 Simulation Software

Three software packages were evaluated for the purpose of optimisation and SAM was selected as the final option. From the initial evaluation, SAM's capabilities presented three big opportunities for its use in optimisation processes, namely:

(a) The parametric analysis functionality which could enable us to perform iterative optimisation processes in SAM with relative ease

(b) The ability of SAM to interface with other software programs which meant that optimisation algorithms could be implemented on a different platform to provide optimal parameters that could be integrated with SAM simulations

(c) SAM's scripting ability which means that code could be written to automate some processes or to formulate algorithms that could be used for optimisation in SAM.

For the purposes of this optimisation strategy, the second option was chosen to take advantage of the Graphical User Interface (GUI) in SAM to facilitate the initial plant design set up and then exporting the setup to MATLAB for integration with the optimisation toolbox. Using SAM's GUI, the respective weather file of the desired location is loaded and the inverter and module models are selected from the components databases in the SAM software libraries. The system sizing is performed by specifying the desired array size and DC to AC ratio, followed by the configuration and orientation of the modules and inverters. Through SAM's sizing algorithm, the system configuration at reference conditions is automatically generated, based

on the module and inverter models' electrical properties. Shading, irradiance, DC, AC and transformer losses to be taken into account in the simulations as well as the parameters for the financial modelling are also set up. Figure 4.1 shows the flowchart that summarises the SAM simulation setup process. After completion of the setup, the corresponding code is generated in MATLAB format in preparation for the next stage of the optimisation which will be facilitated by the MATLAB Optimisation Toolbox.

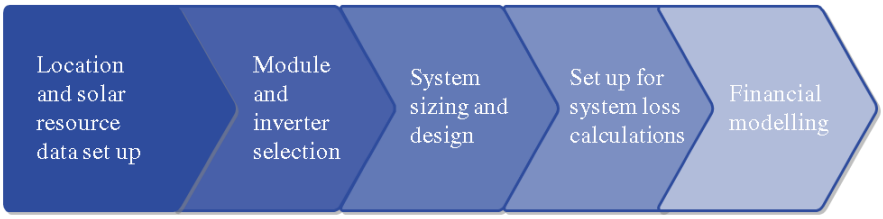

Figure 4.1: SAM simulation process flow

4.3.2 Module Technology

The approach used in comparing the module technologies was to keep the system design parameters constant as far as possible in a similar way to the current method. The datasheets of the modules are given in Appendices A, B and C.

4.3.3 Optimisation Toolbox

The MATLAB Optimisation Toolbox provides various routines that can be used to determine parameters that minimise or maximise objectives or to solve equations. This is facilitated by solvers (subroutines) that can be used to perform constrained or unconstrained optimisation on a wide variety of problems including, discrete, continuous and large-scale problems. The optimisation problem is set up using three main constituents namely:

- objective function
- constraints
- function

4.3.3.1 Objective Function

An objective function is a method that shows the relationship between a design variable and the outcome that is meant to be optimised. The user creates an objective function, denoted symbolically by f(x), which is a measure of the performance of a system as the variable 'x' is varied. 'x' can, therefore, be viewed as a column vector of design variables which can affect the performance of the system. Conventionally, optimisation in the toolbox entails minimization of the objective function, therefore, in the event that maximisation is preferred, the optimisation procedure is simply the minimisation of the negative of the objective function, -f(x). In our optimisation problem cases the objective function is built from the MATLAB code generated from the SAM simulation setup and the plant layout parameters make up the design variable column vector.

4.3.3.2 Constraints

Constraints are limitations in the design space which in PV system design procedures are hugely influenced by the design goals themselves, the simulation software restriction or from site-specific limitations. Where applicable, the user defines a set of constraints in the problem setup to restrict the solution space according to these limitations. Constraints are generally classified as one of the following types:

- Linear inequalities of the form A*x $\leq$ b, where A is a matrix and b is a vector
- Linear equalities of the form A_{eq}*x = b_{eq}, specified by matrix A_{eq} and the vector b_{eq}
- Lower and upper bounds on the variables, specified as vectors
- Nonlinear constraint functions that define the nonlinear constraints

4.3.3.3 Function

The user also needs to choose an appropriate solver for the particular optimisation problem. There are four main subdivisions for the optimisation algorithms in the toolbox depending on the type of problems that need to be solved:

- Linear or nonlinear problems
- Constrained or unconstrained problems,
- Single or multi-variable problems
- Single or multi-objective problems

The PV system layout optimisation problem using SAM software falls under nonlinear constrained optimisation and our test cases looked into multivariable problems of both single and multi-objective natures.

4.4 Single Objective Optimisation

The optimisation toolbox provides three main single-objective optimisation functions. These are:

- fminbnd - to find a minimum of a single-variable function over a fixed interval
- fmincon - to find a minimum of a constrained nonlinear multivariable function
- fseminf - to find a minimum of a semi-infinitely constrained nonlinear multivariable function

Our optimisation problem cases do not involve semi-infinite constraints so the only options were the fminbnd and fmincon functions. The fminbnd is only limited to cases where a single variable is being evaluated and this restricts its usefulness in our optimisation problems. The fmincon function was then selected because it offers more functionality with its ability to evaluate multiple variables simultaneously.

4.4.1 Algorithm

fmincon has five algorithm options namely:

- Interior point,
- Trust region reflective,
- Sequential quadratic programming (SQP) and
- Active-set.

According to the MATLAB optimisation toolbox documentation, it is recommended that the user attempts to implement the interior point algorithm first before turning to the other options. The interior point algorithm is a large scale algorithm, capable of handling not only large, sparse problems but small dense problems as well.

The original problem is denoted by

$$\min_x f(x), \tag{4.1}$$

subject to h(x)= 0 and g(x)$\leq$ 0,
where h(x) represents equality constraints and g(x) represents inequality constraints. To solve the original problem, it is approximated using the barrier function as

$$\min_{x,s} f_\mu(x,s) = \min_{x,s} f(x,s) - \mu \sum_i ln(s_i), \tag{4.2}$$

subject to h(x)= 0 and g(x)+ s = 0 for each $\mu > 0$.
The approximate problem represents the original problem as a sequence of equality constrained problems which are easier to solve than the original inequality constrained problem. The step attempts to solve he resulting Karush-Kuhn-Tucker (KKT) equations from the approximate problem using a linear approximation. The KKT conditions are similar to the condition that the gradient must be zero at a minimum, only that they are modified to hold for constrained problems. To solve the approximate problem the algorithm implements Newton's method for minimization. If the Newton (direct) step fails, the algorithm tries to implement a conjugate gradient step which uses a trust region. A trust region is a neighbourhood N around the point x where the behaviour of the function f(x) can be reasonably reflected by a simpler function q. The trust-region subproblem is denoted by:

$$\min_s \{q(s), s \in N)\} \tag{4.3}$$

To run the optimisation, the user supplies the objective function, the constraints and a preferred starting point for the solver. In addition to that, it is imperative that the approximation of derivatives by the solver is done using central differences and not forward differences. This way the algorithm takes twice as many function evaluations but yields more accurate results.

4.5 Multi-objective Optimisation

In many real-life situations and processes, optimisation problems are often multi-objective in nature, and the design process for PV plant layouts is not exempt from that. In several situations it may not be adequate to represent plant design optimisation as a single-objective optimisation so multi-objective optimisation will have to be implemented. There are often instances when several factors such as techno-economic and sometimes environmental design

objectives need to be taken into account simultaneously during the layout design stage. This increases the problem's dimensionality and as a result, it is very rare to find a single optimal solution for that particular problem, especially if two or more of the design objectives are antagonistic. Multi-objective Optimisation (MOO) methods can therefore be implemented in such scenarios to find some reasonable compromises in the achievement of design objectives. MOO procedures enable the optimisation of multiple design variables for several, often antagonistic, design objectives simultaneously in a constrained design space using mathematical programming techniques. The generic mathematical formulation of a multi-objective optimisation problem is to find a design vector:

$$\overrightarrow{X} = [x(1), x(2), \ldots, x(n)]^T, \tag{4.4}$$

subject to m inequality constraints:

$$g_i(\overrightarrow{X}) \leq 0 \qquad i = 1, 2, \ldots, m$$

and p equality constraints:

$$h_i(\overrightarrow{X}) = 0 \qquad i = 1, 2, \ldots, p$$

to optimise the vector function:

$$f(\overrightarrow{X}) = [f_1(\overrightarrow{X}), f_2(\overrightarrow{X}), \ldots, f_q(\overrightarrow{X})]^T.$$

As stated before, it is very rare in such problem cases to find a single $\overrightarrow{X^*}$ such that

$$f_i(\overrightarrow{X^*}) \leq f_i(\overrightarrow{X}) \qquad \forall \overrightarrow{X} \in F, \qquad i = 1, 2, \ldots, q,$$

where F is the feasible region that satisfies the constraints.

The reasonable trade-offs among different design objectives that MOO procedures find in such scenarios are a type of optimum solutions known as Pareto optimum solutions. Named after Vilfredo Pareto who formulated it, a Pareto optimal is a point $\overrightarrow{X^*} \in F$ that for every $\overrightarrow{X} \in F$ is either

$$f_i(\overrightarrow{X^*}) = f_i(\overrightarrow{X}) \qquad i = 1, 2, \ldots, q$$

or at least

$$f_i(\overrightarrow{X^*}) < f_i(\overrightarrow{X}).$$

In layman's terms, a solution vector $\overrightarrow{X^*}$ is a Pareto optimal if there are no other solutions better than it with respect to all design objectives. $\overrightarrow{X^*}$ needs to be the best solution in at least one objective to be accepted according to the Pareto optimality criterion. For that reason, $\overrightarrow{X^*}$ is regarded as a non-dominated solution, and a set of these non-dominated (Pareto optimal) solutions form a surface known as a Pareto front [88] and [92]. Figure 4.2 shows an illustration of this in a design space, **F** (the shaded area) for a bi-objective optimisation problem. The boundary, in red, between P_1 and P_2 shows the Pareto front and points x_1 and x_3 are non-dominated and hence Pareto optimal solutions, but x_2 is not.

The Pareto front illustrates the nature of the trade-offs that need to be made in order to find good, non-dominated solutions. Multi-Criteria Decision Making methods can then be implemented to select the best solution from the Pareto front, based on the designer's preferences or weighting on the various design objectives.

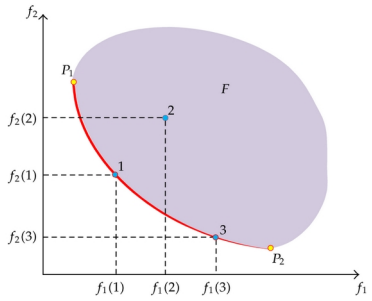

Figure 4.2: Illustration of a Pareto optimal solution set from a 2 dimensional performance space

In the following sections, a multivariable-multiobjective optimisation approach to plant design layout is presented. Subsection 4.5.1 is dedicated to the algorithm implemented in the MOO while subsection 4.5.2 pays particular attention to the multi-criteria decision making process and subsection 5.3.3 addresses the formulation of the MOO problem.

4.5.1 Algorithm

As can be established from section 4.2 there are various evolutionary or stochastic methods that can be implemented to solve constrained and unconstrained optimisation problems of a non-linear nature. These methods, e.g Genetic algorithms, Neural Network Particle Swarm Optimisation and Differential Evolution, are especially suitable where the mathematical properties of the problem such as derivability and continuity are difficult to establish. The method selected for our multi-objective optimisation cases is based on genetic algorithms (GA). GAs are based on the Darwinian theory of evolution and the principle of the survival of the fittest. This process is what is used to refine a population of possible solutions in search and optimisation problems until a working solution or set of solutions is found.

4.5.1.1 Biological Background

The theory of evolution states that in any population, there are distinguishing traits among individuals that can make certain individuals better adapted to survive and reproduce than others. These traits, if heritable, can be passed on to offspring and new generations of better-suited individuals survive while the weaker ones become extinct. The traits are contained in material called deoxyribonucleic acid (DNA) and each cell of a living organism contains strings of DNA known as chromosomes. Each chromosome contains a set of genes or blocks of DNA which, during the process of reproduction, are recombined to form new chromosomes and in turn new individuals.

Similarly, in genetic algorithms, there is a set of possible solutions in the design space known as a population. Each population is made up of individuals, which are the GA equivalence of chromosomes. Fit individuals from the current population are then selected, recombined and sometimes mutated to form new individuals. This process is repeated until the best individual or set of individuals is found.

4.5.1.2 Simple Genetic Algorithm

A simplified version of a genetic algorithm goes through the following steps:

1. Generate an initial population,

2. Assign fitness value (a measure of how close an individual is to the desired solution) to all individuals,
3. Select individuals from the current generation for reproduction,
4. Produce new offspring by means of mutation and/or recombination,
5. Compute new fitness for all individuals and get rid of all unfit individuals,
6. Use stopping criteria to check if the best solution or solution set has been found. if not, repeat steps 3 to 6.

Figure 4.3 is a flow chart of the process as described above.

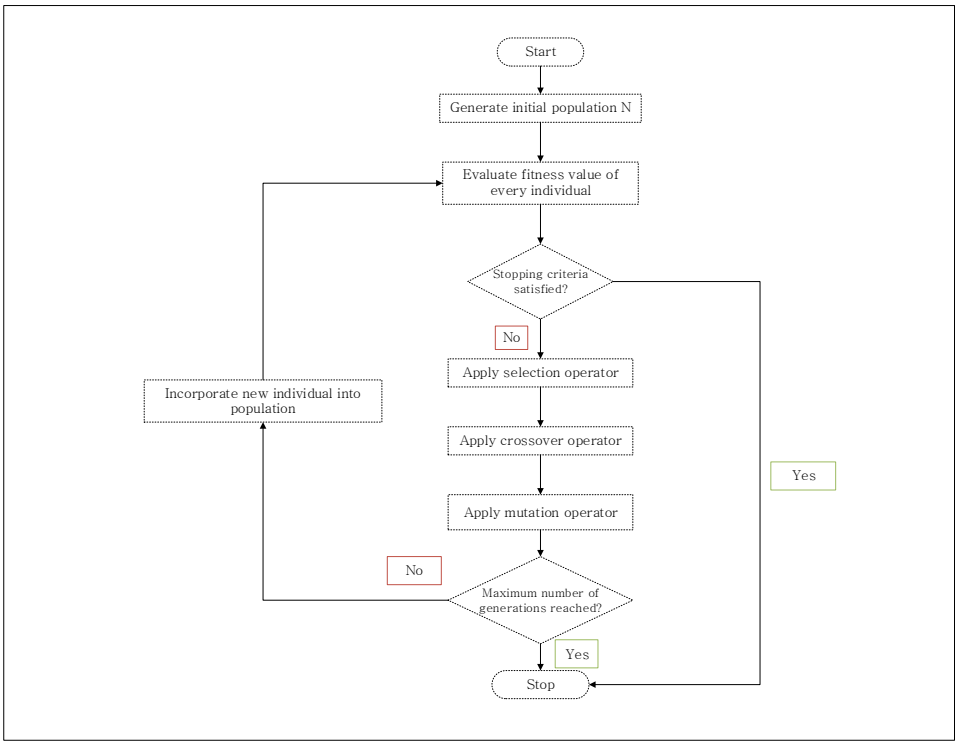

Figure 4.3: Genetic algorithm flow chart

4.5.1.3 Genetic Algorithm Operators

There are three basic operators that are implemented on current generations of GA populations to produce new populations. These are selection, crossover and mutation.

Selection By this operation, a number of individuals is randomly chosen out of the current generation and then the ones with the highest fitness values are selected out of them. The better an individual's fitness is, the more likely that individual is to be chosen. GAs usually have several methods to perform this selection operation. Some of the commonly used ones are:

- Roulette wheel selection
- Rank selection
- Tournament selection
- Steady state selection.

The multi-objective genetic algorithm in the MATLAB optimisation toolbox uses tournament selection in which two random individuals are chosen from the current generation and the fittest of the two is picked to be a parent in the next population generation. Figure 4.4 shows an example of a tournament selection in which n(=2) chromosomes are chosen from the current generation and the chromosome with the highest fitness value out of the 2 is selected to be a parent in the process of creating the next generation.

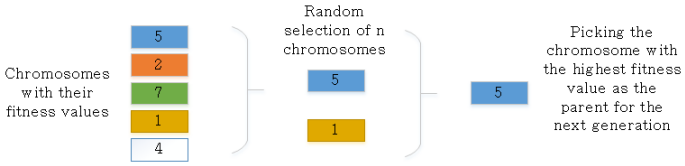

Figure 4.4: Illustration of the tournament selection operation

Crossover The crossover genetic operator is used to vary the programming of chromosomes from one generation to another. In this process, a new individual is created by the combination of different elements from the parents selected from the previous generation. Figure 4.5 shows examples of the crossover operation using two methods but there are several other crossover techniques such as uniform and half-uniform crossover and three parent crossover, that one can also make use of.

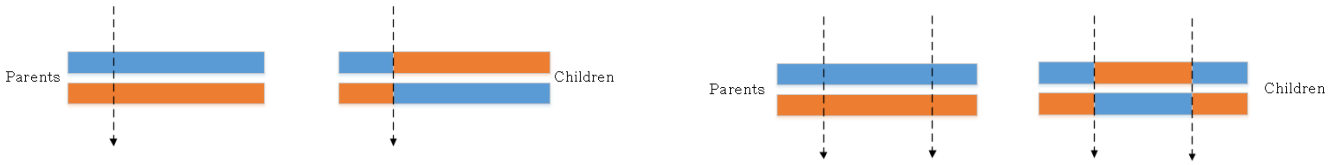

(a) Single-point crossover (b) Two-point crossover

Figure 4.5: An illustration of the crossover operation

Mutation This genetic operator is mainly used to preserve and maintain diversity in the population, from one generation to another. If there is no diversity in the population, the evolution of the individuals will slow down and eventually stop at local minima whilst the algorithm is meant to find global minima. Mutation is often realised by altering one or more gene values in a chromosome to differentiate it from its initial state, often aided by a predefined mutation probability. The key is to keep the probability low such that the search does not end up being a primitive random search. An easy way to illustrate mutation is by using a bit string:

$$10100011 \Rightarrow 10100010$$

In this example, the child, on the right hand side of the arrow, is produced by the mutation of the last bit of the parent, on the left hand side of the arrow, and the bit that is mutated is known as the mutant gene. Bit string mutation is but one example of several mutation techniques that can be applied to GAs. Other methods include flip bit, uniform, non-uniform, gaussian and shrink mutation.

4.5.2 Multiple Criteria Decision Making (MCDM)

MCDM is a part of operations research that deals with multiple, conflicting criteria in decision making. This is almost inevitable when it comes to multi-objective optimisation as there might be solutions which are the best in at least one dimension but not a great solution in other dimensions. A simple illustration of such a scenario is the performance space shown in Figure 4.6. Solution A is better with respect to objective F_1 but worse with respect to F_2, while solution B is better with regards to objective F_2 but worse with respect to F_1. If the Pareto criterion were to be applied to this performance space, the Pareto front would be made up of solutions A and B and it would not be easy to select the best solution of the biobjective problem out of the two. With increased dimensionality and complexity of relationships between the objectives, there is also likely to be an increase in the number of non-dominated solutions in the Pareto Set. Deciding on the best option out of all the provided solutions would therefore definitely take a different turn. Methods such as prioritisation and weighting of some of the objectives over others would therefore be helpful, and that is what MCDM is about.

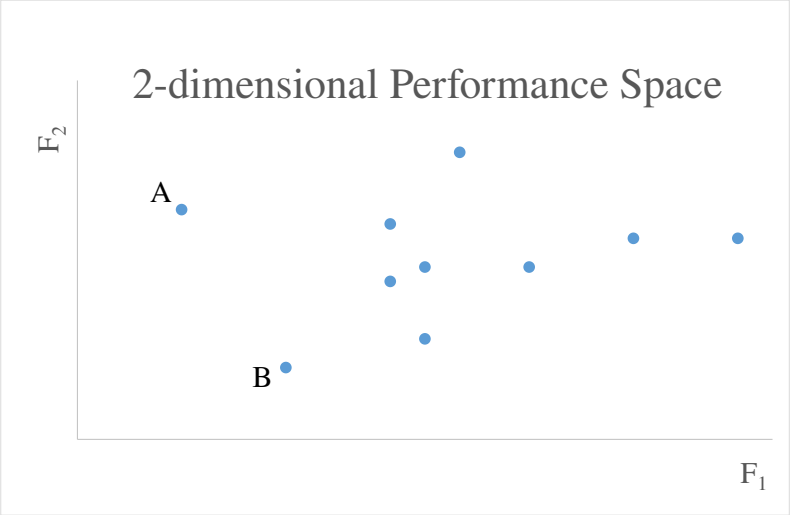

Figure 4.6: 2-dimensional performance space from a bi-objective optimisation problem

There are several approaches to MCDM. The list includes the Simple Additive Weighting (SAW), the TOPSIS method, Analytical Hierarchical Processes (AHP) and Goal Programming. One of the most popular of these methods is TOPSIS which stands for Technique for Order Preference by Similarity to Ideal Solution. The TOPSIS method is ideal for identifying the solution that is the most attractive over all dimensions and it is applicable even if the dimensions have incommensurable units [93]. Some of the common implementations of TOPSIS in multiobjective optimisation include the multi-objective ecodesign of PVGCS in [94], chemical engineering applications in [95] and the multi-objective optimisation for multicontaminant industrial water network design in [96].

4.5.2.1 TOPSIS

The TOPSIS method selects the solution based on proximity to two artificial solutions that it hypothesises:

- Positive Ideal Solution (PIS) - which constitutes the best attributes in all the dimensions, and
- Negative Ideal Solution (NIS)- which has the worst level of all the attributes across all the dimensions.

The following steps show the stages of the TOPSIS method and how they are implemented:
Step 1: Construction of the decision matrix.
In this step, a matrix of m alternatives by n criteria is created.

		Criteria			
		C_1	C_2	...	C_n
Alternatives	A_1	x_{11}	x_{12}	...	x_{1n}
	A_2	x_{21}	x_{22}	...	x_{2n}
	⋮				
	A_m	x_{m1}	x_{m2}	...	x_{mn}

Table 4.1: Decision matrix

Step 2: Creation of normalised decision matrix N.
Each objective or criteria might come in its own unit of measurement which is different from the next one and this makes comparisons across criteria very difficult. These are what are referred to as incommensurable units. The purpose of this step is therefore to transform every value in the decision matrix into a normalised, non-dimensional value between 0 and 1 so that the different criteria can be compared. There are several ways to perform the normalisation procedure and Milani et al [97] and Celen [98], amongst other authors, have done studies into them. Celen's comparative studies to analyse normalisation procedures conclude that the vector normalisation procedure in Equation 4.5 generates the most consistent results. [98]. This is the method that was selected as it is one of the most commonly used. The normalisation equation is given as:

$$N = [z_{ij}]_{m*n}, \quad z_{ij} = \frac{x'_{ij}}{\sqrt{\sum_{i=1}^{m}(x'_{ij})^2}}, \quad j = 1, \ldots, n \ \textit{and} \ i = 1, \ldots, m. \tag{4.5}$$

$x'_{ij} = x_{ij}$ for all benefit attributes and $x'_{ij} = \frac{1}{x_{ij}}$ for all cost attributes.
The term benefit attributes refers to the criteria where the higher the value, the better is whereas cost attributes are criteria where less is better.

Step 3: Creation of weighted matrix V.
Weights of importance are assigned to each criteria, relative to others, and a weighted matrix,V, is created by multiplying elements in the normalised matrix N by the corresponding criterion weight:

$$V = [v_{ij}]_{m*n} = [w_j] * [z_{ij}]_{m*n} \quad j = 1, \ldots, n \ \textit{and} \ i = 1, \ldots, m. \tag{4.6}$$

where w_j is the weight of the j-th criterion,$\sum_{j=1}^{n} w_j$.

Step 4: Determination of the positive and negative ideal solutions (PIS and NIS).

$$A^+ = \{v_1^+, \ldots, v_n^+\} \ \ where \ \ v_j^+ = \{(\max_i(v_{ij}) \ if \ j \in J)\}, (\min_i(v_{ij}) \ if \ j \in J')\} \tag{4.7}$$

$$A^- = \{v_1^-, \ldots, v_n^-\} \ \ where \ \ v_j^- = \{(\min_i(v_{ij}) \ if \ j \in J)\}, (\max_i(v_{ij}) \ if \ j \in J')\} \tag{4.8}$$

where J is the index set of benefit attributes and J' is the index set of cost attributes.

Step 5: Calculation of the Euclidean distance.

The measure of the separation of each alternative from the PIS and NIS is determined using the euclidean distance. The respective distances from the PIS and NIS are calculated as:

$$d_i^+ = \sqrt{\sum_{j=1}^{n}(v_{ij} - v_j^+)^2}, \quad i = 1, \ldots, m. \tag{4.9}$$

$$d_i^- = \sqrt{\sum_{j=1}^{n}(v_{ij} - v_j^-)^2}, \quad i = 1, \ldots, m. \tag{4.10}$$

Step 6: Determination of the relative closeness (closeness coefficient) to the ideal solution.

The relative closeness of each alternative to the ideal solution is calculated as:

$$c_i^+ = \frac{d_i^-}{d_i^+ + d_i^-}, \quad i = 1, \ldots, m. \tag{4.11}$$

where $0 \leq c_i^+ \leq 1$.

The higher the value the value of c_i^+ the higher the rank of that alternative and the more favourable it is. This is essentially one way of saying that the ideal solution is the one solution that is sufficiently close to the PIS, while sufficiently distant from the NIS.

4.6 Conclusion

In this chapter, the optimisation strategy was broken down and each vital step was explained in more detail to shed some light as to its importance in the optimisation process and what each step entails. It was noted that evolutionary computing could be quite useful in the optimisation of the PV system design process given the number of design objectives that need to be evaluated simultaneously. The optimisation procedure also ideally ought to take into account the complex relationships of various design objectives in response to changes in the design variables, while ensuring that the process adheres to constraints in the design space, something that several functions in the MATLAB optimisation toolbox are capable of. Based on the problem cases under investigation, the appropriate optimisation algorithms in the MATLAB Toolbox were selected and implemented in conjunction with a reliable PV system simulation software program, SAM, to perform multivariable-single- and multi-objective optimisation of the system design while concurrently reducing the redundancy in some of the modelling steps and improving the speed, accuracy and precision of the design variable selection. An extra step was introduced in the multiobjective optimisation case to assist with the selection of the best solution from the non-dominated solution set returned by the genetic algorithm. The step uses the TOPSIS method to perform the multi-criteria decision making (MCDM) process. This MCDM procedure was preferred as it is fairly easy to implement and successfully navigates its way around the challenges of incommensurable units and increased dimensionality presented by the multiple design objectives in the problem cases.

Chapter 5

Results and Analyses

5.1 Introduction

In this chapter, the proposed methodology for multivariable optimisation is evaluated by means of some design examples. First, two single-objective problems are investigated to find the optimal layouts of the PV modules, characterised by a combination of the tilt angle, azimuth angle and ground cover ratio and sometimes the rotational limit, that result in maximum annual energy output (Q_{out}), maximum performance ratio of the plant and minimum system losses. A detailed outline of each problem's formulation as well as its optimisation results are given and three evaluations are given for each problem, to cater for the three PV module technologies in our investigation.

In a similar fashion, two multi-objective optimisation cases are also investigated. The optimisation is achieved by means of a multi-objective genetic algorithm and each genetic algorithm run returns a set of layouts that are best at optimising one or more objectives in one way or another. The different layouts are then ranked from the best to the worst using a multicriteria decision making (MCDM) method known as TOPSIS, which stands for Technique for Order of Preference by Similarity to Ideal Solution. Using the TOPSIS method, the layouts by each module technology are compared to each other and ranked, and the same is done for the best layout of each module technology to find out which technology yields the best results.

Another design example is formulated to illustrate how multiple objectives can be taken into consideration simultaneously, but with different weights to resemble precedence of certain design objectives over others. This is because multi-objective design problems rarely have equally important design goals. Some objectives are usually more important than others, and weighting can help take that into account.

The structure of the chapter is as follows: single-objective optimisation is covered in Section 5.2 and multi-objective optimisation problems are covered in Section 5.3. Section 5.4 will then summarise the findings of the optimisation framework investigated in this chapter.

5.2 Single objective optimisation

5.2.1 Solver Options

The execution of the fmincon function required additional options to be selected. The purpose of these options is to facilitate the convergence of simulation runs towards optimal solutions

and can be summarised as follows:

- The initial starting point of the iterations was set to be: $\theta_T = 0°$, $\phi_C = 0°$ and a $GCR_{inv} = 1.1111$
- The 'approximated derivatives' option was set such that the function would search for central differences in successive iterations as opposed to forward differences for better accuracy. The penalty for the central differences option was that it would be relatively slower than the forward differences option, but with the central differences option the average simulation run was seven seconds which is fast enough and, in fact, significantly faster than other normal iterative methods.
- The stopping criteria were set as summarised in Table 5.1

Table 5.1: fmincon stopping criteria

Criteria	Value
Maximum number of iterations	1000
Maximum function evaluations	3000
X tolerance	10^{-10}
Unbounded threshold	10^{-20}
Function tolerance	10^{-4}
Constraint tolerance	10^{-3}

5.2.2 Case 1: Fixed Tilt System

5.2.2.1 Problem formulation

In this particular case, the objective was to find the optimal design layout vector $\overrightarrow{X}$ to maximise annual energy fed into the grid, maximise the performance ratio and minimise system losses of a fixed tilt PV system on a site in the Northern Cape Province of South Africa. The objective functions, therefore, were:

1. Maximise total annual energy yield, $Q_{out,max}$: $f_1(\overrightarrow{X})$
2. Maximise performance ratio, PR_{max}: $f_2(\overrightarrow{X})$
3. Minimise system losses (DC + AC losses), System Losses$_{min}$: $f_3(\overrightarrow{X})$

and they were executed separately using the fmincon solver in MATLAB.

The design variables, module tilt angle, module azimuth angle and ground cover ratio (GCR), were passed to the optimisation tool in the form of a vector. As a general rule, as described in the fundamental background chapter, the optimal tilt and azimuth angles ought to be selected to facilitate maximum energy capture by the PV modules while the optimal GCR

needs to be selected to prevent reductions in energy capture due to shading or wastage of land area available for the PV plant set-up. The design vector of the fixed tilt problem case was:

$$\vec{X} = \begin{Bmatrix} \theta_T \\ \phi_C \\ GCR_{inv} \end{Bmatrix} = \begin{Bmatrix} x(1) \\ x(2) \\ x(3) \end{Bmatrix}, \tag{5.1}$$

where,
θ_T = module surface tilt angle
ϕ_C = module surface azimuth angle
GCR_{inv} = the inverse of the GCR.
$x(3)$ is set to be the inverse of the GCR value and not the GCR so that it fits perfectly with the inequality formulation which is of the form $A * x \leq b$ as described in the Optimisation Strategy Chapter.

Constraints
The constraints of the problem were:

- Linear inequalities
  This constraint arose from the restriction in the land area available for the PV system layout design. The test case is an actual plant which occupies 105 hectares so the maximum land area available for the design layout was set to equal that. In SAM, land area is calculated as:

$$\begin{aligned} LandArea &= \frac{TMA}{GCR} * 0.0002471 \\ &= TMA * GCR_{inv} * 0.0002471 \\ &= TMA * 0.0002471 * GCR_{inv} \end{aligned} \tag{5.2}$$

  where:
  TMA is the total module area and the constant, 0.0002471, converts square meters to acres in equation 5.2 since computation of system costs in SAM is done by using the cost of land in dollars per acre. Consequently, the maximum available land area constraint also needed to be converted and set to 260 acres. The A matrix in the formulation of the land area inequality has three elements:

  - A[0] = 0, for the tilt angle,
  - A[1] = 0, for surface azimuth and
  - A[2] = TMA*0.0002471.

  The TMA varies from one PV module model to another so the A[2] values are derived as follows:

- Lower and upper bounds
  The upper and lower bounds of the design variables were set to put some practicality limits to the design space. According to SAM the θ_T must be a value between 0° and 90° and the ϕ_C must be an angle between 0° and 360° so the constraints were set as shown in Table 5.4. The GCR must be a value between 0.01 and 0.99 according to SAM but we decided on a range a range starting from 0.1 to 0.9 since most practical setups actually estimate the ideal range of GCR to be from 0.3 to 0.7 in most fixed tilt case [99]. The values of these side constraints were all the same for the different PV module technologies and are as shown in Table 5.4.

Table 5.2: Inequality constraint parameters

Module Technology	Module Area(m^2)	Number of Modules	TMA (m^2)	A[2]
MonoSi	1.852	245988	455569.8	112.6
PolySi	2.126	237932	505843.4	124.995
Thin Film	0.72	667610	480679.2	118.6

Table 5.3: Inequality constraint parameters

Module Technology	A			b
	A[0]	A[1]	A[2]	
MonoSi	0	0	112.6	260
PolySi	0	0	124.995	260
Thin Film	0	0	118.6	260

Table 5.4: Lower and upper bounds of solar PV system design variables

Bounds	θ_T	ϕ_C	GCR_{inv}
Lower	0	0	1.111
Upper	89	359	10

5.2.2.2 Results

The fmincon constrained minimisation function was applied as described in Subsubsection 5.2.2.1 for each of the three PV module technologies. The entire design space was evaluated in about seven seconds, on average, in each of the individual single objective optimisation runs and the three optimal layouts, one for each module technology, were compiled and tabulated as shown in Table 5.5. The results show the layouts that lead to the maximisation of the total annual energy production in each of the three PV module technologies' cases. Analysis of the performance of the different technologies showed that Thin Film modules performed the best, followed by the mono-crystalline silicon modules and then polycrystalline modules in the given design example.

Table 5.5: Fixed-tilt total annual energy output, Q_{out}, optimisation results

Module Technology	Design Parameters			$Q_{out}(kWh)$
	θ_T	ϕ_C	GCR_{inv}	
MonoSi	28.693	1.26	2.309	$1.55 \cdot 10^8$
PolySi	27.97	0.298	2.08	$1.51 \cdot 10^8$
Thin Film	30.523	0.099	2.192	$1.58 \cdot 10^8$

The same process of constrained minimisation was performed to find orientations that would lead to maximised performance ratios (PR) for the three PV module technologies being investigated. Each simulation run was also seven seconds long, on average, and the results of each PV module technology's constrained minimisation were compiled and documented as shown in Table 5.6. The results show the design parameters that would result in a module layout optimised for maximum PR in each module technology's case and compares the final maximised PR values of these technologies against each other. From the results, it can be concluded that the Thin Film modules led to the highest PR, followed by monocrystalline and then lastly polycrystalline modules. In all cases, the orientations resulting in maximised PR were characterised by low tilt and azimuth angles and relatively high ground cover ratios of approximately 50% of the installation area.

Table 5.6: Optimisation results for maximum PR in MonoSi, PolySi and Thin Film PV module technologies

Module Technology	Design Parameters			PR
	θ_T	ϕ_C	GCR_{inv}	
MonoSi	0.99	0.99	2.101	0.839
PolySi	1.081	1.081	2.071	0.83
Thin Film	0.99	0.99	2.101	0.8457

The constrained minimisation procedure was performed to find orientations that would lead to the minimisation of system losses in the same fixed tilt PV system and again, simulation runs were performed for the three PV module technologies being investigated. The average simulation run for each technology was approximately seven seconds and the results were compiled and documented as shown in Table 5.7. The results show the design parameters that would result in a module layout optimised for minimum system losses in each module technology's case and compares the final minimised system loss values of these technologies against each other. From the results, it can be concluded that the Thin Film modules led to the lowest total system losses, followed by monocrystalline and then lastly polycrystalline modules. In all cases the orientations resulting in minimised system losses were characterised by low tilt and azimuth angles and relatively high ground cover ratios of approximately 50% of the installation area.

Table 5.7: Optimisation results for minimum system losses in MonoSi, PolySi and Thin Film PV module technologies

Module Technology	Design Parameters			System Losses (%)
	θ_T	ϕ_C	GCR_{inv}	
MonoSi	1.872	6.848	2.101	13.31
PolySi	0.303	1.168	1.841	15.465
Thin Film	0.99	0.99	2.101	12.57

The optimal layouts for total energy output, performance ratio and system losses were compared in terms their satisfaction of each of the objectives investigated in Case 1. The results were also compared to simulation results generated by mounting polySi modules according to the test site's tilt angle, azimuth angle and GCR. These comparisons were drawn only using polySi modules because that is the technology currently in use at the test site. The idea was to illustrate how close or far off the existing plant layout, as well as the layouts optimised for the other two objectives were, from the actual optimised values and graphs of these comparisons are given in Figure 5.1(a-d). As can be deduced from the graphs, there is definitely room for improvement in the existing plant layout's case to get to the optimal values of the three design objectives. Furthermore, the results show that optimising the design layout for one of the objectives does not necessarily optimise the layout to satisfy the other two objectives. To simultaneously satisfy the different objectives, multi-objective optimisation techniques would need to be implemented and this is discussed in Section 5.3.

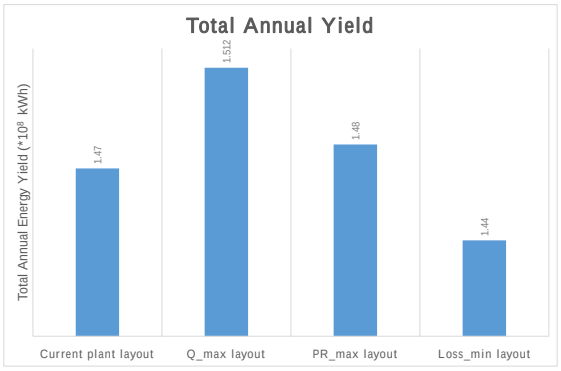

(a) Total Annual Energy Output comparison

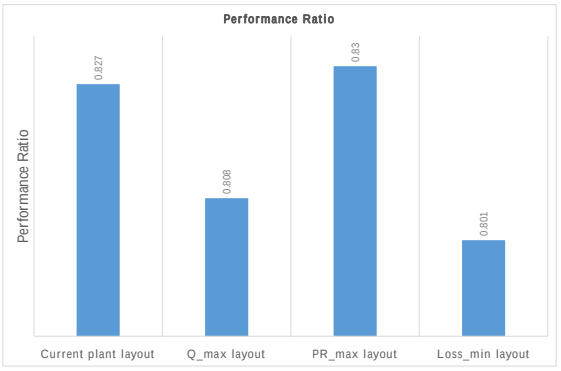

(b) Performance Ratio comparison

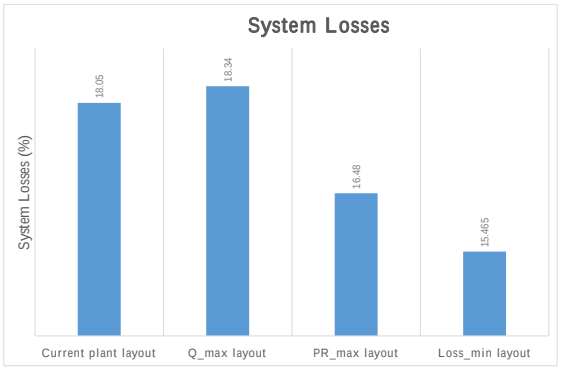

(c) System Losses comparison

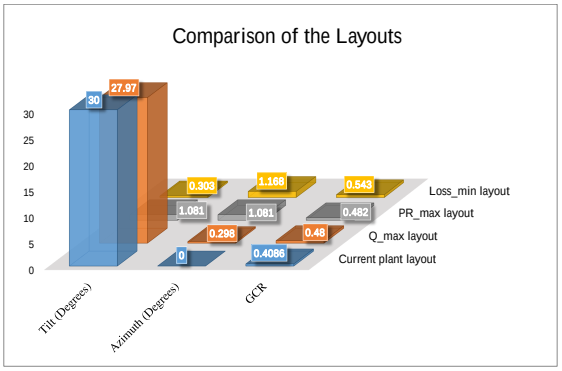

(d) Layouts under investigation

Figure 5.1: Comparison of the performance of PolySi module technologies with respect to each objective for the fixed tilt case, Case 1

5.2.3 Case 2: Single Axis Tracking System

5.2.3.1 Problem formulation

In this particular case, the objective was to find the optimal design layout vector $\vec{X}$ to maximise annual energy fed into the grid, maximise PR and minimise system losses for a single-axis

tracking PV system on a site in the Northern Cape Province of South Africa. The objective functions for single axis tracking systems were the same as in the fixed tilt case: The objective functions, therefore, were:

1. Maximise total annual energy yield, $Q_{out,max}$: $f_1(\overrightarrow{X})$
2. Maximise performance ratio, PR_{max}: $f_2(\overrightarrow{X})$
3. Minimise system losses (DC + AC losses), System Losses$_{min}$: $f_3(\overrightarrow{X})$

and they were executed separately using the fmincon solver.

The design parameters vector, however, was made up of the module tilt angle, the module azimuth angle, the tracker rotation limit and ground cover ratio (GCR). The tracker rotation limit gives the maximum or minimum allowable rotation angle for the one-axis tracker systems in SAM. A value of θ_{Rot} degrees is such that the tracker is allowed to rotate θ_{Rot} degrees about the center line in both directions from the horizontal [5]. The design vector of the single-axis tracking problem case was:

$$\overrightarrow{X} = \begin{Bmatrix} \theta_T \\ \phi_C \\ \theta_{Rot} \\ GCR_{inv} \end{Bmatrix} = \begin{Bmatrix} x(1) \\ x(2) \\ x(3) \\ x(4) \end{Bmatrix}, \tag{5.3}$$

where,
θ_T = module surface tilt angle
ϕ_C = module surface azimuth angle
θ_{Rot} = tracker rotation limit
GCR_{inv} = the inverse of the GCR.

Constraints

The constraints of the problem were set up as follows:

- Linear inequalities
  The test case was adopted from the size of an actual 75 MWp single-axis tracker plant which occupies 225 hectares so the maximum land area available for the design layout was set to 556 acres.

Table 5.8: Inequality constraint parameters

Module Technology	A				b
	A[0]	A[1]	A[2]	A[3]	
MonoSi	0	0	0	112.6	556
PolySi	0	0	0	124.995	556
Thin Film	0	0	0	118.6	556

- Lower and upper bounds
  The upper and lower bounds of the design variables were set up the same way as in the fixed tilt case (see Table 5.4). The upper and lower bounds of the tracker rotation limit were set to 5° and 85° as they are the minimum and maximum allowable values, respectively. Table 5.9 shows a summary of the upper and lower bounds for the one-axis tracker problem.

Table 5.9: Lower and upper bounds on solar PV system design variables

Bounds	θ_T	ϕ_C	θ_{Rot}	GCR_{inv}
Lower	0	0	5	1.111
Upper	89	359	85	10

5.2.3.2 Results

Constrained minimisation was performed on the tracking systems to determine the technology and module layout that would lead to a maximised energy production on the 75 MWp test-plant. Table 5.10 shows the simulation results, with monocrystalline technology leads to the highest energy output, followed by Thin Film technology and lastly polycrystalline modules, in the same design space.

Table 5.10: Single-axis tracking total annual energy output, Q_{out}, optimisation results

Module Technology	Design Parameters				$Q_{out}(kWh)$
	θ_T	ϕ_C	θ_{Rot}	GCR_{inv}	
MonoSi	36.04	355.5	40.1	4.675	$2.03 \cdot 10^8$
PolySi	26.5	10.66	43.06	3.706	$1.99 \cdot 10^8$
Thin Film	33.7	2.48	63.4	4.68	$2.09 \cdot 10^8$

Results of design parameters for a maximised PR for each module technology were compiled and tabulated as given in Table 5.11. The results also show that for systems with the same nameplate capacities, monocrystalline technology had the highest PR, followed by Thin Film technology and then polycrystalline modules would have the worst.

Table 5.11: Single-axis tracking performance ratio, PR, optimisation results

Module Technology	Design Parameters				PR
	θ_T	ϕ_C	θ_{Rot}	GCR_{inv}	
MonoSi	88.33	87.5	113.45	1.69	0.877
PolySi	88.7	88.9	16.8	2.01	0.845
Thin Film	87.3	4.05	61.03	4.92	0.86

Constrained optimisation to determine orientations which would result in minimum system losses was performed. The results generated from the optimisation were compiled and documented as shown in Table 5.12. From the results, it can be deduced that the Thin Film technology would result in the lowest system losses, followed by monocrystalline and lastly the polycrystalline technology.

Table 5.12: Single-axis tracking performance ratio, PR, optimisation results

Module Technology	Design Parameters				System Losses (%)
	θ_T	ϕ_C	θ_{Rot}	GCR_{inv}	
MonoSi	1.081	1.081	6.176	2.116	15.88
PolySi	2.12	6.491	12.826	3.54	16.79
Thin Film	2.443	2.183	7.488	1.363	14.128

5.3 Multi-objective optimisation

The purpose of this optimisation was to find the optimal design layout vector, $\overrightarrow{X}$, to optimise three plant performance indicators simultaneously for both a fixed tilt PV system and a single axis tracking system using a site in the Northern Cape Province of South Africa as a test site. In the formulation of multi-objective optimisation problems, certain aspects, namely the objective function and the solver options of the algorithm, remained unchanged for the different cases investigated and were given as in Subsection 5.3.1. The rest of the features of the problems, which differed from one case to the other, are then given within the corresponding case's problem formulation in the subsequent subsections.

5.3.1 Solver Options

The execution of the multi-objective optimisation genetic algorithm needed additional options to be selected. The purpose of these options is to facilitate the convergence of simulation runs towards optimal solutions and can be summarised as:

- The initial population was created using the 'Feasible population' function which creates a random population which satisfies the bounds and the linear constraints provided by the user.
- The selection operator used the 'Tournament' function. This function selects two random individuals from the current generation and chooses the best individual out of the two to be a parent.
- The reproduction operator used a crossover fraction of 0.8 to create children at each new generation. As such, 80% of each successive generation was created from crossover.
- Mutation was responsible for the creation of the remaining 20% of the children at each new generation and was facilitated by the 'Adaptive feasible' function. This function randomly generates adaptive directions for progression based on the last successful or unsuccessful generation.

- The Pareto front population fraction is kept at 0.35 to keep the most fit population down and maintain diversity in the population and is facilitated by the in-built 'distancecrowding' function. Population diversity, as described in earlier sections, is crucial to the fruitful exploration of a GA to ensure that the population converges but does not do so prematurely.
- The stopping criteria were set as summarised in Table 5.13

Table 5.13: MOGA stopping criteria

Criteria	Value
Maximum number of generations	1000
Time limit	∞
Fitness limit	-∞
Stall time limit	∞
Stall generations	100
Function tolerance	10^{-4}
Constraint tolerance	10^{-3}

5.3.2 Choice of design objectives

The multi-objective framework was formulated in such a way that it could be used for the simultaneous optimisation of several, and sometimes antagonistic, plant performance indicators with the hopes of expanding the focus of the design procedure to look at more than one objective at a time. Unfortunately, at the time the work was done there was not enough for the levelised cost of energy (LCOE) to be included as one of the design objectives as cost-breakdown information for a practical financial model that exemplifies current industry trends and practices was not available. This was mainly because the solar market in Africa is still fairly small so confidentiality is extremely important in such matters, as projects can be easily identifiable. As a result data on cost breakdowns are hardly readily availed by solar developers in the country [100]. In the end, a design example featuring land use, performance ratio and energy output as design objectives was used to present the framework.

5.3.3 Case 1 - Fixed Tilt, Equal Weights

5.3.3.1 Objective Function Formulation

The fixed tilt multi-objective problem was characterised by three objective functions which were:

1. Maximise total annual energy yield, Q_{out}: $f_1(\overrightarrow{X})$
2. Minimise land area usage, *Land*: $f_2(\overrightarrow{X})$
3. Maximise performance ratio, PR: $f_3(\overrightarrow{X})$

The resulting design objective vector was:

$$F(\overrightarrow{X}) = \begin{Bmatrix} Q_{out} \\ Landarea \\ PR \end{Bmatrix} = \begin{Bmatrix} f_1(\overrightarrow{X}) \\ f_2(\overrightarrow{X}) \\ f_3(\overrightarrow{X}) \end{Bmatrix}, \tag{5.4}$$

5.3.3.2 Problem Formulation

Design parameters

The design parameters vector was the same as the one for the single-objective optimisation problem case, given in Subsubsection 5.2.2.1 for fixed tilt systems. The design vector is characterised by the three design parameters as:

$$\overrightarrow{X} = \begin{Bmatrix} \theta_T \\ \phi_C \\ GCR_{inv} \end{Bmatrix} = \begin{Bmatrix} x(1) \\ x(2) \\ x(3) \end{Bmatrix}, \tag{5.5}$$

where,
θ_T = module surface tilt angle
ϕ_C = module surface azimuth angle
GCR_{inv} = the inverse of the GCR.

TOPSIS Parameters

The application of the TOPSIS method requires that each design objective be assigned the correct criteria sign and a weight, λ. The criteria sign range is a positive unit (+1), if the design objective is to be maximised, and a negative unit (-1) if the design objective is to be minimised. The initial investigation assumed equal weighting of a unit for each objective. Table 5.14 summarises the criteria and weights for this particular investigation's TOPSIS implementation.

Table 5.14: Criteria and weights for the TOPSIS method

	Q_{out}	Land area usage	PR
Criteria sign	+1	-1	+1
Weight	1	1	1

Constraints

The corresponding bounded constraints were formulated the same way as described in Subsubsection 5.2.2.1 and are summarised in Table **??**. The linear inequality constraint as applied to the single-objective problems was not used in the multi-objective cases because land usage was to be used as a design objective instead.

Table 5.15: Lower and upper bounds of solar PV system design variables

Bounds	θ_T	ϕ_C	GCR_{inv}
Lower	0	0	1.111
Upper	89	359	10

5.3.3.3 Results

As described in the optimisation strategy chapter, the multi-objective optimisation for fixed tilt systems was executed by means of a multi-objective genetic algorithm (MOGA). The antagonism in the various objectives being designed for meant that no single layout could lead to the optimisation of all the objectives at once so a Pareto front was generated. The Pareto front represented several alternative ways of laying out the arrays in each module technology's case in a way that would be beneficial to the achievement of one or more of the three design objectives. Each layout in the solution set was defined by the tilt angle, azimuth angle and the ground cover ratio, GCR, (given as an inverse, GCR_{inv} for the purpose of the simulations, refer to Subsubection 5.2.2.1) and shows the corresponding influence the parameters have on the three design objectives.

The TOPSIS method was then used to find an acceptable compromise in the layouts such that the selection of the final layout would be based on each alternative's proximity to the ideal solution and distance from the non-ideal solution. The solutions were ranked from the best using the relative closeness coefficient as described in the TOPSIS nethod outline in the Optimisation Strategy Chapter. It is worth mentioning again that in this evaluation, as indicated in the problem formulation, the importance of all objectives was assumed to be the same so all the objectives were weighted equally. Tables 5.16, 5.17 and 5.18 show the Pareto fronts of the monocrystalline, polycrystalline and thin film module technologies, respectively.

An additional step was then taken to select the best performing layouts from each module technology's Pareto front and pit them against each other to determine the best performing module technology in this design scenario. Table 5.19 shows the resulting ranking of the three different technologies after they were put through the TOPSIS method. The Thin Film technology performed the best out of the three, followed by the monocrystalline technology and then lastly the polycrystalline technology.

Table 5.16: Fixed Tilt MonoSi Pareto front

θ_T	ϕ_C	GCR_{inv}	$Q_{out,year}$ (kWh)	Land area used	PR	Closenesss Coeff	Rank
0,537667	1,833885	1,1111	1,37E+08	125,078	0,828987	0,996688	1
0,11285	1,833885	1,1111	1,37E+08	125,078	0,829139	0,996595	2
5,836793	0,33445	1,173611	1,41E+08	132,1149	0,815404	0,992478	3
39,03782	4,211961	2,175078	1,52E+08	244,8513	0,818444	0,88021	4
2,409527	87,42346	3,286091	1,37E+08	369,9195	0,829873	0,755103	5
21,96655	25,43673	4,042909	1,52E+08	455,1155	0,830035	0,669924	6
27,80457	341,3956	4,391459	1,54E+08	494,3522	0,826861	0,630687	7
7,930363	100,9917	4,419519	1,35E+08	497,511	0,831378	0,627498	8
53,8891	36,7796	6,278051	1,4E+08	706,7283	0,836357	0,418276	9
44,47812	25,1907	6,897904	1,49E+08	776,506	0,833371	0,348525	10
58,30252	53,38639	7,530551	1,3E+08	847,7239	0,836904	0,277252	11
77,46206	43,17247	7,829544	1,13E+08	881,3819	0,844139	0,243555	12
64,1818	17,19639	7,947074	1,34E+08	894,6124	0,837465	0,230379	13
63,17443	60,14977	8,248634	1,23E+08	928,5594	0,838721	0,196395	14
71,35178	53,80541	8,98052	1,18E+08	1010,949	0,842703	0,113989	15
82,01798	47,62673	9,945921	1,07E+08	1119,625	0,847102	0,005277	16
81,90861	47,63308	9,992796	1,07E+08	1124,902	0,847163	3,2E-05	17

Table 5.17: Fixed Tilt PolySi Pareto front

θ_T	ϕ_C	GCR_{inv}	$Q_{out,year}$ (kWh)	Land area used	PR	Closenesss Coeff	Rank
0,537741	1,833397	1,1111	1,36E+08	138,8807	0,818096	0,992065	1
28,29722	3,860474	1,244104	1,36E+08	155,5054	0,725212	0,983087	2
24,75675	5,836019	1,516114	1,46E+08	189,5051	0,784854	0,954327	3
28,30241	2,231479	2,197376	1,52E+08	274,6587	0,813254	0,87783	4
39,20124	38,6273	4,006285	1,45E+08	500,7612	0,81696	0,674376	5
64,68456	5,674133	4,46337	1,32E+08	557,894	0,820813	0,62286	6
23,42938	53,17622	4,744507	1,44E+08	593,0344	0,820625	0,59136	7
56,02497	0,932095	5,393802	1,42E+08	674,1924	0,821583	0,518347	8
71,89996	21,94978	5,908869	1,22E+08	738,5726	0,825497	0,460228	9
83,05503	47,52825	6,949164	1,03E+08	868,6031	0,826391	0,34309	10
78,54437	49,37105	7,37889	1,08E+08	922,3163	0,82862	0,294813	11
48,30448	45,19499	7,546371	1,39E+08	943,2504	0,824498	0,27644	12
80,34592	55,92698	8,137169	1,05E+08	1017,096	0,830328	0,20952	13
74,8226	45,1918	8,792787	1,15E+08	1099,045	0,831131	0,13594	14
31,86059	0,047765	9,982456	1,54E+08	1247,746	0,821109	0,023654	15
84,76675	58,83206	9,938267	98740368	1242,223	0,832901	0,00695	16
79,96354	57,64601	9,999997	1,05E+08	1249,939	0,833491	0,002761	17
79,96354	57,64606	9,999993	1,05E+08	1249,938	0,833491	0,002761	18

Table 5.18: Fixed Tilt Thin Film Pareto Front

θ_T	ϕ_C	GCR_{inv}	$Q_{out,year}$ (kWh)	Land area used	PR	Closenesss Coeff	Rank
27,325	0,084147	1,111208	1,53E+08	121,2701	0,815541	0,996733	1
0,537667	1,833885	1,1111	1,4E+08	121,2583	0,845734	0,989613	2
20,21536	44,58465	1,620504	1,48E+08	176,8513	0,834797	0,942366	3
2,780583	42,33594	1,616985	1,42E+08	176,4673	0,846024	0,942297	4
39,36899	6,912212	2,097899	1,56E+08	228,9512	0,842332	0,888934	5
28,89885	1,69588	3,153415	1,58E+08	344,1434	0,843911	0,770195	6
80,70094	38,51896	3,707639	1,11E+08	404,6277	0,855992	0,706633	7
54,37466	42,24433	4,011111	1,4E+08	437,7468	0,849752	0,673438	8
87,21361	72,61783	4,601405	93928168	502,1676	0,857782	0,605728	9
83,2639	44,81732	5,70721	1,08E+08	622,8481	0,864582	0,481912	10
41,3404	45,04646	6,33199	1,47E+08	691,0324	0,848151	0,412783	11
65,59724	32,29402	7,053186	1,33E+08	769,7391	0,859228	0,331358	12
31,39818	0,024528	7,874206	1,58E+08	859,34	0,844238	0,241043	13
66,38543	58,35785	8,472173	1,24E+08	924,5983	0,862137	0,172015	14
78,81813	73,67347	8,922294	1,04E+08	973,7215	0,867816	0,120456	15
88,59699	92,18474	9,238952	83788152	1008,279	0,871105	0,084248	16
88,82833	72,52951	9,987533	93686824	1089,975	0,872834	0,005719	17
88,95333	72,52951	9,987533	93541896	1089,975	0,872853	0,005636	18

Table 5.19: Fixed Tilt Ranking of the best configurations from the 3 different technologies

Technology	θ_T	ϕ_C	GCR_{inv}	$Q_{out,year}$ (kWh)	Land area	PR	Closenesss Coeff	Rank
MonoSi	0,537667	1,833885	1,1111	1,37E+08	125,078	0,828987	0,53475	2
PolySi	0,537741	1,833397	1,1111	1,36E+08	138,8807	0,818096	0,000269	3
Thin Film	27,325	0,084147	1,111208	1,53E+08	121,2701	0,815541	0,998583	1

5.3.4 Case 2 - Single Axis Tracking, Equal Weights

5.3.4.1 Problem Formulation

5.3.4.2 Objective Function Formulation

The single axis tracking multi-objective problem was characterised by three objective functions which were:

1. Maximise total annual energy yield, Q_{out}: $f_1(\overrightarrow{X})$
2. Minimise land area usage , $Landarea$: $f_2(\overrightarrow{X})$
3. Maximise performance ratio, PR: $f_3(\overrightarrow{X})$

This is because the tracking systems make use of backtracking and this deals with the PV system's self-shading loss problems.

The resulting design objective vector was:

$$F(\overrightarrow{X}) = \begin{Bmatrix} Q_{out} \\ Landarea \\ PR \end{Bmatrix} = \begin{Bmatrix} f_1(\overrightarrow{X}) \\ f_2(\overrightarrow{X}) \\ f_3(\overrightarrow{X}) \end{Bmatrix}, \tag{5.6}$$

Design parameters

The design parameters vector was the same as that of the tracking case given in Subsubsection 5.2.3.1. The design parameters vector was, therefore:

$$\overrightarrow{X} = \begin{Bmatrix} \theta_T \\ \phi_C \\ \theta_{Rot} \\ GCR_{inv} \end{Bmatrix} = \begin{Bmatrix} x(1) \\ x(2) \\ x(3) \\ x(4) \end{Bmatrix}, \tag{5.7}$$

where,
θ_T = module surface tilt angle
ϕ_C = module surface azimuth angle
θ_{Rot} = tracker rotation limit
GCR_{inv} = the inverse of the GCR.

TOPSIS parameters

Table 5.20 summarises the criteria and weights for this particular problem's TOPSIS implementation:

Table 5.20: Criteria and weights for the TOPSIS method

	Q_{out}	Land area	PR
Criteria sign	+1	-1	+1
Weight	1	1	1

Table 5.21: Lower and upper bounds of solar PV system design variables

Bounds	θ_T	ϕ_C	θ_{Rot}	GCR_{inv}
Lower	0	0	5	1.111
Upper	89	359	85	10

Constraints
The constraints of the problem were set up as shown in Table 5.21:

5.3.4.3 Results

Pareto fronts generated from the multi-objective optimisation of single axis tracking systems are shown in Tables 5.22, **??** and 5.24. The bold values in each column represent the best case scenario for each design objective. After the TOPSIS method was applied, the various layouts were ranked according to their closeness to the ideal solution, as shown in the 'Rank' column. The best and the worst layouts in the Pareto front were highlighted green and red, respectively.

An additional step was also taken to select the best performing layouts from each module technology's Pareto front and pit them against each other to determine the best performing module technology in this design scenario. Table 5.25 shows the resulting ranking of the three different technologies after they were put through the TOPSIS method. The Thin Film technology was by far the best out of the three, followed by the monocrystalline technology and then lastly the polycrystalline technology.

Table 5.22: MonoSi Pareto Front - Tracking

θ_T	ϕ_C	θ_{Rot}	GCR_{inv}	$Q_{out,year}(kWh)$	Land area used	PR	Closeness Coeff	Rank
1,100167	2,583885	5	1,1111	1,44E+08	125,078	0,829645	0,965658	1
76,44965	80,87462	16,84505	1,33134	1,09E+08	149,8707	0,851926	0,942216	2
79,25495	116,2148	19,12457	1,195229	79550760	134,5485	0,842703	0,93326	3
28,21867	16,61694	52,01599	1,775623	1,87E+08	199,8842	0,815622	0,924355	4
85,03451	65,35196	46,85173	1,742779	1,22E+08	196,1869	0,849249	0,915677	5
78,9039	86,68032	27,5212	2,339926	1,1E+08	263,4086	0,851245	0,853183	6
23,29035	5,411698	27,67661	3,070497	1,91E+08	345,6498	0,82684	0,779856	7
69,19155	58,57939	53,54066	3,409069	1,54E+08	383,7633	0,844432	0,740398	8
75,91149	43,82272	58,70844	3,924963	1,62E+08	441,8382	0,850968	0,683138	9
84,63264	49,4144	52,94807	4,232635	1,44E+08	476,4732	0,854779	0,647951	10
31,92984	15,76828	39,62676	4,917822	1,98E+08	553,6055	0,823243	0,573172	11
68,66479	35,03547	53,1935	5,6165	1,74E+08	632,2567	0,846011	0,494249	12
81,99318	49,83343	75,61133	6,397774	1,64E+08	720,2057	0,857117	0,406504	13
27,13342	8,136346	68,6656	7,178502	2,1E+08	808,0933	0,823059	0,322523	14
34,71267	18,85969	53,59603	9,061377	2,04E+08	1020,051	0,82365	0,122316	15
30,85514	8,161073	69,24016	9,997416	2,11E+08	1125,422	0,823229	0,065612	16
30,93809	8,160811	69,305	9,999602	2,11E+08	1125,668	0,823233	0,065595	17
88,44413	24,04567	80,99968	9,896312	1,73E+08	1114,041	0,862403	0,049112	18

Table 5.23: Evaluation of PolySi modules in a fixed tilt with different weights

θ_T	ϕ_C	GCR_{inv}	$Q_{out,year}$ (kWh)	Land area used	PR	CC1	Rank 1	CC2	Rank 2
0,537741	1,833397	1,1111	1,36E+08	138,8807	0,818096	0,992065	1	0,984262	1
28,29722	3,860474	1,244104	1,36E+08	155,5054	0,725212	0,983087	2	0,978318	2
24,75675	5,836019	1,516114	1,46E+08	189,5051	0,784854	0,954327	3	0,954003	3
28,30241	2,231479	2,197376	1,52E+08	274,6587	0,813254	0,87783	4	0,877938	4
39,20124	38,6273	4,006285	1,45E+08	500,7612	0,81696	0,674376	5	0,674627	5
64,68456	5,674133	4,46337	1,32E+08	557,894	0,820813	0,62286	6	0,62283	6
23,42938	53,17622	4,744507	1,44E+08	593,0344	0,820625	0,59136	7	0,591711	7
56,02497	0,932095	5,393802	1,42E+08	674,1924	0,821583	0,518347	8	0,518798	8
71,89996	21,94978	5,908869	1,22E+08	738,5726	0,825497	0,460228	9	0,460157	9
83,05503	47,52825	6,949164	1,03E+08	868,6031	0,826391	0,34309	10	0,342707	10
78,54437	49,37105	7,37889	1,08E+08	922,3163	0,82862	0,294813	11	0,294631	11
48,30448	45,19499	7,546371	1,39E+08	943,2504	0,824498	0,27644	12	0,277653	12
80,34592	55,92698	8,137169	1,05E+08	1017,096	0,830328	0,20952	13	0,209374	13
74,8226	45,1918	8,792787	1,15E+08	1099,045	0,831131	0,13594	14	0,136323	14
31,86059	0,047765	9,982456	1,54E+08	1247,746	0,821109	0,023654	15	0,046102	15
84,76675	58,83206	9,938267	98740368	1242,223	0,832901	0,00695	16	0,006944	16
79,96354	57,64601	9,999997	1,05E+08	1249,939	0,833491	0,002761	17	0,005475	17
79,96354	57,64606	9,999993	1,05E+08	1249,938	0,833491	0,002761	18	0,005475	18

Table 5.24: Thin Film Pareto Front - Tracking

θ_T	ϕ_C	θ_{Rot}	GCR_{inv}	$Q_{out,year}(kWh)$	Land area used	PR	Closeness Coeff	Rank
0,537667	5,021385	5,000244	1,1111	1,46E+08	121,2583	0,845125	0,958096	1
74,74597	34,015	11,92926	1,245089	1,32E+08	135,881	0,863666	0,94689	2
27,561	13,805	50,78984	1,747066	1,89E+08	190,6635	0,82315	0,927085	3
86,37965	116,8384	24,08482	1,142483	74407160	124,6833	0,863696	0,916301	4
86,27028	116,6958	23,94029	1,11221	73763328	121,3794	0,863213	0,916266	5
76,80504	48,04264	39,97448	1,888153	1,44E+08	206,0608	0,862856	0,902674	6
82,92486	91,30166	32,3949	2,104921	1,05E+08	229,7175	0,868975	0,87016	7
86,80354	78,94392	45,61889	2,342562	1,15E+08	255,6521	0,86932	0,849455	8
84,02272	95,73228	12,76826	2,323053	94695968	253,523	0,872356	0,846258	9
88,08156	76,71907	56,06746	2,659097	1,22E+08	290,1966	0,869536	0,817827	10
2,77192	10,48428	7,444234	3,933046	1,57E+08	429,2273	0,848502	0,681767	11
19,58151	18,14759	19,35673	4,431561	1,84E+08	483,6319	0,840679	0,627664	12
4,899029	5,558087	55,75197	5,438474	2E+08	593,52	0,839135	0,516313	13
58,50853	16,70521	43,65259	6,036098	1,92E+08	658,7407	0,850272	0,449517	14
29,43773	8,679419	76,01778	9,999433	2,13E+08	1091,274	0,830289	0,083727	15
31,15916	10,51302	75,44469	9,999677	2,13E+08	1091,3	0,830501	0,083485	16
5,499363	9,631891	78,33934	9,8723	2,05E+08	1077,399	0,83897	0,081053	17
88,72978	28,26615	82,06904	9,978879	1,75E+08	1089,03	0,878846	0,062304	18

Table 5.25: Ranking of the best configurations from the 3 different technologies under investigation after applying TOPSIS.

Technology	θ_T	ϕ_C	θ_{Rot}	GCR_{inv}	$Q_{out,year}(kWh)$	Land area	PR	Closeness Coeff	Rank
MonoSi	1,44E+08	125,078	0,829645	1,100167	2,583885	5	1,1111	0,168518	3
PolySi	1,74E+08	166,2364	0,80861	28,57031	13,67791	39,9932	1,329956	0,674982	2
Thin Film	1,46E+08	121,2583	0,845125	0,537667	5,021385	5,000244	1,1111	0,872967	1

5.3.5 Case 3 - Fixed Tilt, Different Weights

5.3.5.1 Problem formulation

In many design scenarios design objectives hardly have the same level of importance. This can be factored in by changing the 'weight' of each objective in the application of the TOPSIS method according to the particular PV project's focus. The greater the weight of the objective is, relative to the others, the more important it is in that particular design scenario. To illustrate this, a fixed tilt problem was conceptualised where:

- the main goal was to design a 75 MWp plant for a maximised annual energy yield so $Q_{out,year}$ was assigned a unit weight,
- second to this goal was achieving a maximised performance ratio and minimising Land area use so PR and Land area objectives were assigned weights of 0.5 each.

While the rest of the problem formulation remained the same as the one given in Case 1 of the multi-objective optimisation problems (Subsubsection 5.3.3.2), the weights were different and were as summarised in Table 5.26.

Objective	Q_{out}	Land area	PR
Criteria sign	+1	-1	+1
Weight	1	0.5	0.5

Table 5.26: Criteria and weights for the TOPSIS method

5.3.5.2 Results

The closeness coefficient (CC) of the layouts in the Pareto front and ranks of each alternative layout were compared between the initial case, where equal weights were used, and the new case where the different weights were implemented. This was done for all three PV module technologies and the results were recorded and tabulated as shown in Tables 5.27, 5.28 and 5.29.

As can be observed from the results, the weights have a bearing on how close an alternative layout can be regarded to be to the ideal solution. The results in this example now favoured layouts leading to higher energy production, more than those leading to minimised land use or maximised PR which is what was expected. While the ranks in all three technologies remained the same, the closeness coefficient of each of their alternative layouts was evidently affected.

Table 5.27: Evaluation of MonoSi modules in a fixed tilt system with different weights.

θ_T	ϕ_C	GCR_{inv}	$Q_{out,year}$ (kWh)	Land area used	PR	CC1	Rank 1	CC2	Rank 2
0,537667	1,833885	1,1111	1,37E+08	125,078	0,828987	0,996688	1	0,993397	1
0,11285	1,833885	1,1111	1,37E+08	125,078	0,829139	0,996595	2	0,993212	2
5,836793	0,33445	1,173611	1,41E+08	132,1149	0,815404	0,992478	3	0,991187	3
39,03782	4,211961	2,175078	1,52E+08	244,8513	0,818444	0,88021	4	0,880225	4
2,409527	87,42346	3,286091	1,37E+08	369,9195	0,829873	0,755103	5	0,755067	5
21,96655	25,43673	4,042909	1,52E+08	455,1155	0,830035	0,669924	6	0,669983	6
27,80457	341,3956	4,391459	1,54E+08	494,3522	0,826861	0,630687	7	0,630765	7
7,930363	100,9917	4,419519	1,35E+08	497,511	0,831378	0,627498	8	0,627488	8
53,8891	36,7796	6,278051	1,4E+08	706,7283	0,836357	0,418276	9	0,418361	9
44,47812	25,1907	6,897904	1,49E+08	776,506	0,833371	0,348525	10	0,348728	10
58,30252	53,38639	7,530551	1,3E+08	847,7239	0,836904	0,277252	11	0,277328	11
77,46206	43,17247	7,829544	1,13E+08	881,3819	0,844139	0,243555	12	0,243532	12
64,1818	17,19639	7,947074	1,34E+08	894,6124	0,837465	0,230379	13	0,230525	13
63,17443	60,14977	8,248634	1,23E+08	928,5594	0,838721	0,196395	14	0,19645	14
71,35178	53,80541	8,98052	1,18E+08	1010,949	0,842703	0,113989	15	0,114037	15
82,01798	47,62673	9,945921	1,07E+08	1119,625	0,847102	0,005277	16	0,005277	16
81,90861	47,63308	9,992796	1,07E+08	1124,902	0,847163	3,2E-05	17	6,21E-05	17

Table 5.28: Evaluation of PolySi modules in a fixed tilt with different weights

θ_T	ϕ_C	GCR_{inv}	$Q_{out,year}$ (kWh)	Land area used	PR	Closenesss Coeff	Rank		
0,537741	1,833397	1,1111	1,36E+08	138,8807	0,818096	0,992065	1	0,984262	1
28,29722	3,860474	1,244104	1,36E+08	155,5054	0,725212	0,983087	2	0,978318	2
24,75675	5,836019	1,516114	1,46E+08	189,5051	0,784854	0,954327	3	0,954003	3
28,30241	2,231479	2,197376	1,52E+08	274,6587	0,813254	0,87783	4	0,877938	4
39,20124	38,6273	4,006285	1,45E+08	500,7612	0,81696	0,674376	5	0,674627	5
64,68456	5,674133	4,46337	1,32E+08	557,894	0,820813	0,62286	6	0,62283	6
23,42938	53,17622	4,744507	1,44E+08	593,0344	0,820625	0,59136	7	0,591711	7
56,02497	0,932095	5,393802	1,42E+08	674,1924	0,821583	0,518347	8	0,518798	8
71,89996	21,94978	5,908869	1,22E+08	738,5726	0,825497	0,460228	9	0,460157	9
83,05503	47,52825	6,949164	1,03E+08	868,6031	0,826391	0,34309	10	0,342707	10
78,54437	49,37105	7,37889	1,08E+08	922,3163	0,82862	0,294813	11	0,294631	11
48,30448	45,19499	7,546371	1,39E+08	943,2504	0,824498	0,27644	12	0,277653	12
80,34592	55,92698	8,137169	1,05E+08	1017,096	0,830328	0,20952	13	0,209374	13
74,8226	45,1918	8,792787	1,15E+08	1099,045	0,831131	0,13594	14	0,136323	14
31,86059	0,047765	9,982456	1,54E+08	1247,746	0,821109	0,023654	15	0,046102	15
84,76675	58,83206	9,938267	98740368	1242,223	0,832901	0,00695	16	0,006944	16
79,96354	57,64601	9,999997	1,05E+08	1249,939	0,833491	0,002761	17	0,005475	17
79,96354	57,64606	9,999993	1,05E+08	1249,938	0,833491	0,002761	18	0,005475	18

Table 5.29: Evaluation of Thin Film modules in a fixed tilt system with different weights

θ_T	ϕ_C	GCR_{inv}	$Q_{out,year}$ (kWh)	Land area used	PR	CC1	Rank 1	CC2	Rank 2
27,325	0,084147	1,111208	1,53E+08	121,2701	0,815541	0,996733	1	0,993503	1
0,537667	1,833885	1,1111	1,4E+08	121,2583	0,845734	0,989613	2	0,979472	2
20,21536	44,58465	1,620504	1,48E+08	176,8513	0,834797	0,942366	3	0,941639	3
2,780583	42,33594	1,616985	1,42E+08	176,4673	0,846024	0,942297	4	0,940234	4
39,36899	6,912212	2,097899	1,56E+08	228,9512	0,842332	0,888934	5	0,889245	5
28,89885	1,69588	3,153415	1,58E+08	344,1434	0,843911	0,770195	6	0,771021	6
80,70094	38,51896	3,707639	1,11E+08	404,6277	0,855992	0,706633	7	0,704131	7
54,37466	42,24433	4,011111	1,4E+08	437,7468	0,849752	0,673438	8	0,673878	8
87,21361	72,61783	4,601405	93928168	502,1676	0,857782	0,605728	9	0,602593	9
83,2639	44,81732	5,70721	1,08E+08	622,8481	0,864582	0,481912	10	0,48102	10
41,3404	45,04646	6,33199	1,47E+08	691,0324	0,848151	0,412783	11	0,415614	11
65,59724	32,29402	7,053186	1,33E+08	769,7391	0,859228	0,331358	12	0,33367	12
31,39818	0,024528	7,874206	1,58E+08	859,34	0,844238	0,241043	13	0,249519	13
66,38543	58,35785	8,472173	1,24E+08	924,5983	0,862137	0,172015	14	0,175808	14
78,81813	73,67347	8,922294	1,04E+08	973,7215	0,867816	0,120456	15	0,121779	15
88,59699	92,18474	9,238952	83788152	1008,279	0,871105	0,084248	16	0,083991	16
88,82833	72,52951	9,987533	93686824	1089,975	0,872834	0,005719	17	0,011349	17
88,95333	72,52951	9,987533	93541896	1089,975	0,872853	0,005636	18	0,011185	18

5.3.6 Case 4 - Single Axis Tracking, Different Weights

5.3.6.1 Problem Formulation

The single axis tracking multi-objective problem was also subjected to prioritised weights as in Case 3 following the same conceptual design in which:

- the main goal was to design a 75 MWp plant for a maximised annual energy yield so $Q_{out,year}$ was assigned a unit weight,
- second to this goal was achieving a maximised performance ratio and minimising Land area use so PR and Land area objectives were assigned weights of 0.5 each.

The corresponding weights were, therefore, as summarised in Table 5.30.

Objective	Q_{out}	Land area	PR
Criteria sign	+1	-1	+1
Weight	1	0.5	0.5

Table 5.30: Criteria and weights for the TOPSIS method

5.3.6.2 Results

The TOPSIS method was implemented and the resulting rankings and closeness coeeficient (CC) were tabulated and compared to those from the equally-weighted single axis tracking multi-objective problem given in Subsubsection 5.2.3.1. The results for the monocrystalline, polycrystalline and thin film technology modules were as shown in Tables 5.31, 5.32 and 5.33.

5.4 Conclusions

The optimisation framework presented in this chapter was successfully integrated with a reputable PV system design tool. This enabled the framework to utilise functionalities in both the optimisation toolbox and the design tool to quickly, easily and accurately model PV system performance. The toolbox provided several ways of optimising the design process, of which two were fully explored in this chapter to tackle the design of a PV module layout in a design space defined by multiple variables which ought to be taken into account simultaneously. SAM, with its inbuilt subroutines and predefined variables enabled the evaluation of several plant performance parameters with relative ease and this can be extended to touch on other parameters, system layouts such as can be defined by splitting the PV system into up to four different subarrays, and use of other time periods, such as specific hours of the day or particular months or seasons of the year, not covered in this chapter. The framework is therefore adaptable to several other design objectives and design variables to best suit the design goals within the confines of SAM's capabilities.

The fmincon solver's interior-point algorithm and the multi-objective genetic algorithm (MOGA), implemented in the optimisation process, enabled multiple design parameters to be taken into account simultaneously, within the confines of predefined constraints in the design space. This proved to be less cumbersome and faster than the original trial method that the design engineers currently use and the iterative approach that was investigated in the Preliminary

Table 5.31: Evaluation of layouts of MonoSi modules in a single-axis tracking system with objectives with different weights.

θ_T	ϕ_C	θ_{Rot}	GCR_{inv}	$Q_{out,year}$ (kWh)	Land area	PR	CC1	Rank 1	CC2	Rank 2
1,1001671	2,583885	5	1,1111	1,44E+08	125,078	0,829645	0,965658	1	0,933707	1
76,449654	80,87462	16,84505	1,33134	1,09E+08	149,8707	0,851926	0,942216	2	0,897307	3
79,254946	116,2148	19,12457	1,195229	79550760	134,5485	0,842703	0,93326	3	0,875607	5
28,218669	16,61694	52,01599	1,775623	1,87E+08	199,8842	0,815622	0,924355	4	0,92182	2
85,034514	65,35196	46,85173	1,742779	1,22E+08	196,1869	0,849249	0,915677	5	0,886648	4
78,903904	86,68032	27,5212	2,339926	1,1E+08	263,4086	0,851245	0,853183	6	0,831237	6
23,290351	5,411698	27,67661	3,070497	1,91E+08	345,6498	0,82684	0,779856	7	0,780735	7
69,191546	58,57939	53,54066	3,409069	1,54E+08	383,7633	0,844432	0,740398	8	0,737278	8
75,911485	43,82272	58,70844	3,924963	1,62E+08	441,8382	0,850968	0,683138	9	0,682291	9
84,632635	49,4144	52,94807	4,232635	1,44E+08	476,4732	0,854779	0,647951	10	0,645429	10
31,929841	15,76828	39,62676	4,917822	1,98E+08	553,6055	0,823243	0,573172	11	0,5774	11
68,664793	35,03547	53,1935	5,6165	1,74E+08	632,2567	0,846011	0,494249	12	0,497555	12
81,993183	49,83343	75,61133	6,397774	1,64E+08	720,2057	0,857117	0,406504	13	0,410247	13
27,133417	8,136346	68,6656	7,178502	2,1E+08	808,0933	0,823059	0,322523	14	0,336836	14
34,71267	18,85969	53,59603	9,061377	2,04E+08	1020,051	0,82365	0,122316	15	0,159303	15
30,855144	8,161073	69,24016	9,997416	2,11E+08	1125,422	0,823229	0,065612	16	0,123143	16
30,938086	8,160811	69,305	9,999602	2,11E+08	1125,668	0,823233	0,065595	17	0,123114	17
88,444133	24,04567	80,99968	9,896312	1,73E+08	1114,041	0,862403	0,049112	18	0,091905	18

Table 5.32: Evaluation of PolySi modules in a single-axis tracking system with different weights.

θ_T	ϕ_C	θ_{Rot}	GCR_{inv}	$Q_{out,year}$ (kWh)	Land area	PR	CC1	Rank 1	CC2	Rank 2
28,570315	13,67791	39,9932	1,329956	1,74E+08	166,2364	0,80861	0,965564	1	0,946927	1
3,2896077	1,783148	5,000185	1,1111	1,45E+08	138,8807	0,819371	0,956801	2	0,917419	2
44,987454	33,35379	13,947	1,619432	1,62E+08	202,4191	0,821706	0,934466	3	0,915226	3
79,102403	62,10481	14,54495	1,798239	1,15E+08	224,7689	0,84172	0,900802	4	0,85797	6
84,442914	108,9202	10,00559	1,638795	79648472	204,8394	0,840845	0,896294	5	0,83059	7
84,480742	109,003	10,009	1,705936	79666936	213,2316	0,840649	0,891873	6	0,827653	8
75,139569	54,54231	36,10246	2,006985	1,36E+08	250,8608	0,835562	0,888359	7	0,862516	5
6,8373735	11,05188	47,65152	2,310485	1,84E+08	288,7966	0,816101	0,864462	8	0,862721	4
83,714473	102,1834	29,12561	3,739012	96562984	467,3538	0,842458	0,697101	9	0,677483	9
83,859626	98,90498	23,54674	4,177602	95736920	522,1748	0,842989	0,649122	10	0,63288	10
9,0977445	2,464374	12,61781	4,525765	1,67E+08	565,6931	0,824323	0,616312	11	0,61767	11
73,922883	45,96376	5,810664	5,519751	1,23E+08	689,9352	0,839829	0,502603	12	0,498508	12
61,47455	44,09715	61,74716	8,135417	1,79E+08	1016,878	0,832304	0,218638	13	0,24186	13
60,966014	22,36667	62,96374	9,200731	1,93E+08	1150,035	0,832924	0,116878	14	0,168001	14
42,128701	28,718	63,16714	9,503582	2E+08	1187,89	0,819638	0,096911	15	0,15867	15
27,624343	10,68017	69,11961	9,999757	2,09E+08	1249,909	0,816451	0,083595	16	0,154291	16
64,797783	23,1929	66,01007	9,999854	1,91E+08	1249,921	0,836621	0,072844	17	0,135769	17
86,659078	24,84075	80,46224	9,957074	1,73E+08	1244,573	0,850025	0,061835	18	0,116156	18

Table 5.33: Evaluation of Thin Film modules in a single axis tracking with different weights.

θ_T	ϕ_C	θ_{Rot}	GCR_{inv}	$Q_{out,year}$ (kWh)	Land area	PR	CC1	Rank 1	CC2	Rank 2
0,5376671	5,021385	5,000244	1,1111	1,46E+08	121,2583	0,845125	0,958096	1	0,919812	2
74,745975	34,015	11,92926	1,245089	1,32E+08	135,881	0,863666	0,94689	2	0,901908	3
27,561	13,805	50,78984	1,747066	1,89E+08	190,6635	0,82315	0,927085	3	0,923264	1
86,379654	116,8384	24,08482	1,142483	74407160	124,6833	0,863696	0,916301	4	0,845605	5
86,270279	116,6958	23,94029	1,11221	73763328	121,3794	0,863213	0,916266	5	0,845471	6
76,805043	48,04264	39,97448	1,888153	1,44E+08	206,0608	0,862856	0,902674	6	0,879149	4
82,924864	91,30166	32,3949	2,104921	1,05E+08	229,7175	0,868975	0,87016	7	0,830795	7
86,803536	78,94392	45,61889	2,342562	1,15E+08	255,6521	0,86932	0,849455	8	0,820321	8
84,022722	95,73228	12,76826	2,323053	94695968	253,523	0,872356	0,846258	9	0,806966	9
88,081556	76,71907	56,06746	2,659097	1,22E+08	290,1966	0,869536	0,817827	10	0,796881	10
2,7719204	10,48428	7,444234	3,933046	1,57E+08	429,2273	0,848502	0,681767	11	0,67959	11
19,581509	18,14759	19,35673	4,431561	1,84E+08	483,6319	0,840679	0,627664	12	0,631228	12
4,8990292	5,558087	55,75197	5,438474	2E+08	593,52	0,839135	0,516313	13	0,525322	13
58,508529	16,70521	43,65259	6,036098	1,92E+08	658,7407	0,850272	0,449517	14	0,459727	14
29,437727	8,679419	76,01778	9,999433	2,13E+08	1091,274	0,830289	0,083727	15	0,154516	15
31,159163	10,51302	75,44469	9,999677	2,13E+08	1091,3	0,830501	0,083485	16	0,154105	16
5,4993627	9,631891	78,33934	9,8723	2,05E+08	1077,399	0,83897	0,081053	17	0,148638	17
88,729784	28,26615	82,06904	9,978879	1,75E+08	1089,03	0,878846	0,062304	18	0,117153	18

Design Chapter. The MOGA was also able to design for multiple objectives at the same time, which was a better way of designing PV systems to simultaneously optimally satisfy various, sometimes antagonistic, design objectives as it takes into account more plant performance indicators.

The MOGA, when handling antagonistic design objectives, tends to yield multiple alternative PV system layouts as options to optimally design for one objective or the other. To select the best option out of these alternatives, a multi-criteria decision making (MCDM) tool known as TOPSIS is implemented. TOPSIS, which stands for Technique for Order of Preference by Similarity to Ideal Solution, enables all alternative options to be evaluated and ranked according to how closely they resemble the ideal solution. This method was successfully implemented to choose the best layout and the best module technology for each design scenario. The weights can be used to remodel the ideal solution and its makeup such that more emphasis is placed on design objectives that are deemed more important than others in that particular design scenario. This is a better design approximation, compared to designing a system with a single design objective in mind, which results in the oversimplification of the design process especially in cases where more than one design objective needs to be achieved and the objectives are potentially antagonistic. This is also better than performing a multi-objective design with all objectives weighted equally because that is seldom the case in reality.

Chapter 6

Conclusions

In this chapter, conclusions drawn from the other chapters of this thesis are summarised. This is then followed by a section containing recommendations in relation to the work presented in this project.

6.1 Conclusions

6.1.1 Introduction

In this opening chapter, a general context around the need for renewable energy sources was given. Emphasis was, however, placed on solar energy and the state of the solar industry was evaluated in the worldwide as well as the South African context. Thereafter, the research problem of the lack of an efficient, integrated and hollistic approach to PV system design optimisation was noted and investigated. The project's objectives were then laid out such that frameworks for design optimisation could be formulated to:

- replace or complement the current, sometimes arduous, plant design procedures,
- be easily adaptable to various design scenarios since not all projects are ever the same, especially in terms of constraints and design objectives,
- provide a faster and more well-rounded approach to the design process by simultaneously designing for multiple parameters and/or multiple objectives,
- yield accurate and bankable PV system designs by integrating powerful optimisation algorithms with reliable PV system design tools.

6.1.2 Theoretical Background

In this chapter, the fundamentals behind solar PV systems were presented. This covered conditions favourable for solar PV projects, a breakdown of the PV system, system performance parameters, the basics of PV system design and the role of simulation software in the design and evaluation process. The purpose of this chapter was to highlight the key elements that make up the PV system and its design procedure as a form of background for the design optimisation procedures implemented in the thesis.

6.1.3 Preliminary Design

In this chapter, various elements that go into plant design optimisation were reviewed. The process involved investigating the tools and strategies currently being implemented by some

PV system designers to find out their purposes and strengths and to identify areas that could do with some improvement. Some of the key insights from this preliminary plant design and optimisation process were:

- The vital role system design tools play in the design process and the importance of selecting tools that enable developers to perform system modeling thoroughly and accurately.
- The need for optimisation frameworks capable of handling multiple iterations and the simultaneous optimisation of several design variables and objectives.
- How some nonconventional design optimisation processes also play an important role in overcoming certain design constraints and challenges and shed more insight with regards to the complex relationship of several design variables and objectives.

These key deductions were then used to formulate optimisation frameworks for the design of utility scale PV systems.

6.1.4 Optimisation Strategies

In this chapter, the optimisation strategy was broken down and each vital step was explained in more detail to shed some light as to its importance in the optimisation process and what each step entails. It was noted that evolutionary computing could be quite useful in the optimisation of the PV system design process given the number of design objectives that needed to be evaluated simultaneously. The optimisation procedure was modelled to take into account the complex relationships of various design objectives in response to changes in the design variables while ensuring that the process adhered to constraints in the design space. Based on the problem cases under investigation, the appropriate optimisation algorithms in the MATLAB Toolbox were selected and implemented in conjunction with a reliable PV system simulation software program, SAM, to perform single- and multi-objective optimisation of the system design. A multi-criteria decision making (MCDM) procedure was implemented to assist with the selection of optimal layouts according to their satisfaction of the design objectives in the multi-objective optimisation cases.

6.1.5 Results and Analysis

The optimisation frameworks presented in this chapter were successfully integrated with a reputable PV system design tool. This enabled the frameworks to utilise functionalities in both the optimisation toolbox and the design tool to quickly, easily and accurately model PV system performance. The toolbox provided several ways of optimising the design process, of which two were fully explored in this chapter to tackle the design of a PV module layout in a design space defined by multiple variables which ought to be taken into account simultaneously. SAM, with its inbuilt subroutines and predefined variables enables the evaluation of several plant performance parameters with relative ease and this can be extended to the design of several other performance parameters, system layouts and timeframes, making the frameworks discussed in this chapter adaptable.

The fmincon solver's interior-point algorithm and the multiobjective genetic algorithm (MOGA), implemented in the optimisation process, enabled multiple design parameters to be taken into account simultaneously, within the confines of predefined constraints in the design space. This proved to be less cumbersome and much faster than the method that the design engineers currently use as mentioned in the problem statement. The MOGA was also able to design

for multiple objectives at the same time, which was a better way of designing PV systems to simultaneously optimally satisfy various, sometimes antagonistic, design objectives as it takes into account several plant performance indicators at the same time.

The MOGA, when handling antagonistic design objectives, tends to yield multiple alternative PV system layouts in its Pareto optimal solution set. To select the best option out of these alternatives, a multi-criteria decision making (MCDM) tool known as TOPSIS is implemented. TOPSIS, which stands for Technique for Order of Preference by Similarity to Ideal Solution, enables all alternative options to be evaluated and ranked according to how closely they resemble the ideal solution. This method was successfully implemented to choose the best layout and the best module technology for each design scenario. The TOPSIS weights were used to remodel the ideal solution and its makeup such that more emphasis was placed on design objectives that are deemed more important than others in that particular design scenario.

6.2 Recommendations

Strong evidence has recently emerged pointing to the possibility of significant amounts of savings in the PV system design if certain practices in the balance of system (BoS) design process are also improved. One such example is the cost-saving wiring method known as the leapfrog method as shown in Figure 6.1. According to the author of 'Cost-saving PV source-circuit wiring method' [8], the leapfrog method leads to material cost savings of up to $20 000 on a 5 MW PV system with 72-cell modules. BoS optimisation could, therefore, be worth investigating and adding to the overall plant design optimisation.

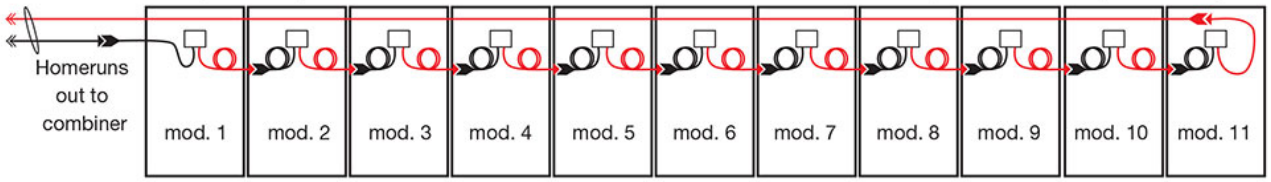

(a) Daisy chain wiring

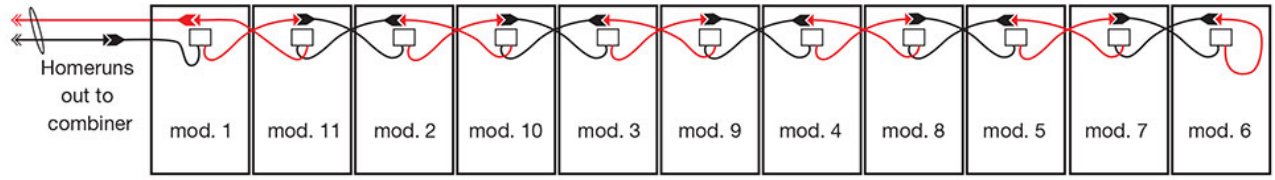

(b) Leapfrog wiring

Figure 6.1: Illustration of source circuits connected using the daisy chain and leapfrog wiring methods. Figures adopted from [8]

A drawback that is common in the application of multiobjective genetic algorithms (MOGA) is that an increase in the dimensions or objectives of the problem leads to a larger computational burden and, in turn, affects how quickly the optimisation process can be executed. Multivariate reduction techniques such as principal component analysis (PCA) can then be used in such cases to reduce some of the redundant objectives and consequently the computational burden of multi-objective optimisation procedures.

Alternative implementations of the optimisation frameworks can be achieved by means of other design tools, optimisation toolboxes and evolutionary programming techniques. For instance, a SAM simulation setup can be exported to python form and integrated with a python-based optimisation toolbox such as the distributed evolutionary algorithms in python (DEAP) to execute the frameworks presented in this thesis. This is but one of many other ways in which evolutionary programming techniques can be harnessed in order to improve the PV system design process. The given alternative toolboxes and software, and many others, can be taken into consideration for future work, depending on designers' preferences, proficiency and various other factors.

Appendices

Appendix A

Canadian Solar PV Module Datasheet

CanadianSolar

MAXPOWER
CS6X-310|315|320|325P

The high quality and reliability of Canadian Solar's modules is ensured by 15 years of experience in module manufacturing, well-engineered module design, stringent BOM quality testing, an automated manufacturing process and 100% EL testing.

KEY FEATURES

- Excellent module efficiency of up to 16.94 %
- Outstanding low irradiance performance: 96.0 %
- No.1 PTC — High PTC rating of up to 91.97%
- IP67 — IP67 junction box for long-term weather endurance
- Heavy snow load up to 5400 Pa, wind load up to 2400 Pa

25 years linear power output warranty

10 years product warranty on materials and workmanship

MANAGEMENT SYSTEM CERTIFICATES*

ISO 9001:2008 / Quality management system
ISO/TS 16949:2009 / The automotive industry quality management system
ISO 14001:2004 / Standards for environmental management system
OHSAS 18001:2007 / International standards for occupational health & safety

PRODUCT CERTIFICATES*

IEC 61215 / IEC 61730: TÜV-Rheinland / VDE / KEMCO / MCS / CE / CEC AU / INMETRO
UL 1703 / IEC 61215 performance: CEC listed (US)
UL 1703: CSA / IEC 61701 ED2: VDE / IEC 62716: VDE / IEC 60068-2-68: SGS
Take-e-way / UNI 9177 Reaction to Fire: Class 1

* As there are different certification requirements in different markets, please contact your local Canadian Solar sales representative for the specific certificates applicable to the products in the region in which the products are to be used.

CANADIAN SOLAR INC. is committed to providing high quality solar products, solar system solutions and services to customers around the world. As a leading PV project developer and manufacturer of solar modules with over 15 GW deployed around the world since 2001, Canadian Solar Inc. (NASDAQ: CSIQ) is one of the most bankable solar companies worldwide.

CANADIAN SOLAR INC.
545 Speedvale Avenue West, Guelph, Ontario N1K 1E6, Canada, www.canadiansolar.com, support@canadiansolar.com

ENGINEERING DRAWING (mm)

Rear View

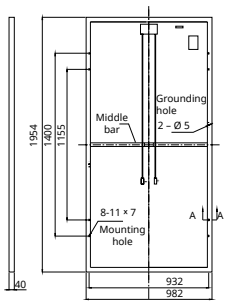

Frame Cross Section A-A

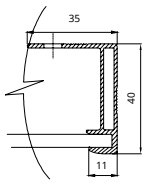

Mounting Hole

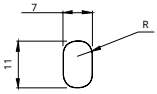

CS6X-320P / I-V CURVES

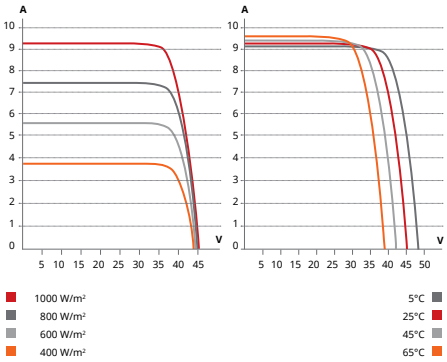

ELECTRICAL DATA | STC*

CS6X	310P	315P	320P	325P
Nominal Max. Power (Pmax)	310 W	315 W	320 W	325 W
Opt. Operating Voltage (Vmp)	36.4 V	36.6 V	36.8 V	37.0 V
Opt. Operating Current (Imp)	8.52 A	8.61 A	8.69 A	8.78 A
Open Circuit Voltage (Voc)	44.9 V	45.1 V	45.3 V	45.5 V
Short Circuit Current (Isc)	9.08 A	9.18 A	9.26 A	9.34 A
Module Efficiency	16.16%	16.42%	16.68%	16.94%
Operating Temperature	-40°C ~ +85°C			
Max. System Voltage	1000 V (IEC) or 1000 V (UL)			
Module Fire Performance	TYPE 1 (UL 1703) or CLASS C (IEC 61730)			
Max. Series Fuse Rating	15 A			
Application Classification	Class A			
Power Tolerance	0 ~ + 5 W			

* Under Standard Test Conditions (STC) of irradiance of 1000 W/m², spectrum AM 1.5 and cell temperature of 25°C.

MECHANICAL DATA

Specification	Data
Cell Type	Poly-crystalline, 6 inch
Cell Arrangement	72 (6×12)
Dimensions	1954×982×40 mm (76.9×38.7×1.57 in)
Weight	22 kg (48.5 lbs)
Front Cover	3.2 mm tempered glass
Frame Material	Anodized aluminium alloy
J-Box	IP67, 3 diodes
Cable	4 mm² (IEC) or 4 mm² & 12 AWG 1000V (UL), 1150 mm
Connector	T4-1000V or PV2 series
Per Pallet	26 pieces, 620 kg (1366.9 lbs)
Per Container (40' HQ)	624 pieces

ELECTRICAL DATA | NOCT*

CS6X	310P	315P	320P	325P
Nominal Max. Power (Pmax)	225 W	228 W	232 W	236 W
Opt. Operating Voltage (Vmp)	33.2 V	33.4 V	33.6 V	33.7 V
Opt. Operating Current (Imp)	6.77 A	6.84 A	6.91 A	6.98 A
Open Circuit Voltage (Voc)	41.3 V	41.5 V	41.6 V	41.8 V
Short Circuit Current (Isc)	7.36 A	7.44 A	7.50 A	7.57 A

* Under Nominal Operating Cell Temperature (NOCT), irradiance of 800 W/m², spectrum AM 1.5, ambient temperature 20°C, wind speed 1 m/s.

TEMPERATURE CHARACTERISTICS

Specification	Data
Temp. Coefficient (Pmax)	-0.41 % / °C
Temp. Coefficient (Voc)	-0.31 % / °C
Temp. Coefficient (Isc)	0.053 % / °C
Nominal Operating Cell Temperature	45±2 °C

PERFORMANCE AT LOW IRRADIANCE

Outstanding performance at low irradiance, average relative efficiency of 96.0 % from an irradiance of 1000 W/m² to 200 W/m² (AM 1.5, 25°C).

PARTNER SECTION

The specification and key features described in this datasheet may deviate slightly and are not guaranteed. Due to on-going innovation, research and product enhancement, Canadian Solar Inc. reserves the right to make any adjustment to the information described herein at any time without notice. Please always obtain the most recent version of the datasheet which shall be duly incorporated into the binding contract made by the parties governing all transactions related to the purchase and sale of the products described herein.

Caution: For professional use only. The installation and handling of PV modules requires professional skills and should only be performed by qualified professionals. Please read the safety and installation instructions before using the modules.

Scan this QR-code to discover solar projects built with this module

Appendix B

Kyocera PV Module Datasheet

HIGH EFFICIENCY MULTICRYSTAL PHOTOVOLTAIC MODULE

KYOCERA

KD 300-80 P Series

KD315GX-LPB KD320GX-LPB

CUTTING EDGE TECHNOLOGY

As a pioneer with over 35 years in the solar energy industry, Kyocera demonstrates leadership in the development of solar energy products. Kyocera's *Kaizen* Philosophy, commitment to continuous improvement, is shown by repeatedly achieving world record cell efficiencies.

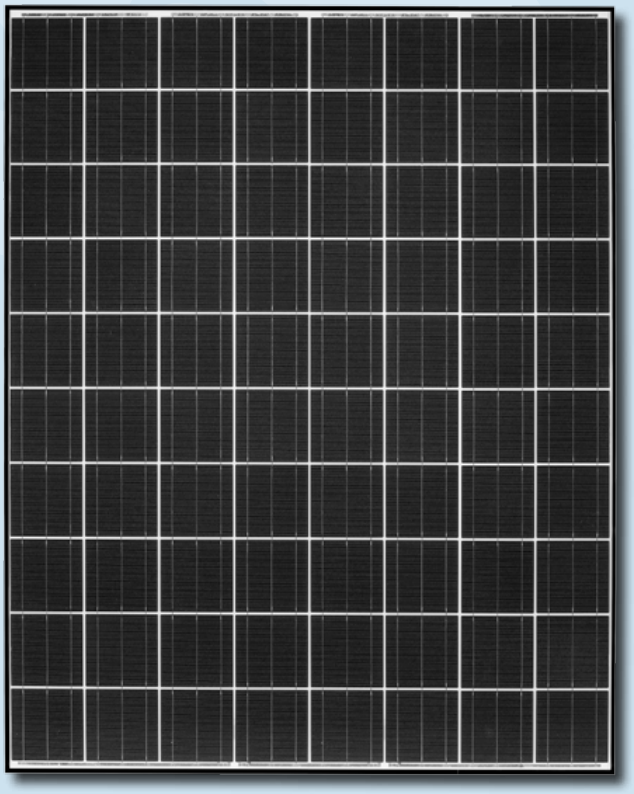

QUALITY BUILT IN

- UV stabilized, aesthetically pleasing black anodized frame
- Supported by major mounting structure manufacturers
- Easily accessible grounding points on all four corners for fast installation
- Proven junction box technology with 12 AWG PV wire to work with transformerless inverters
- Quality locking MC4 plug-in connectors to provide safe and quick connections

RELIABLE

- Proven superior field performance
- Tight power tolerance
- Only module manufacturer to pass rigorous long-term testing performed by TÜV Rheinland

QUALIFICATIONS AND CERTIFICATIONS

TÜV c UL us bsi. JET

NEC 2008 Compliant, UL 1703, and ISO 14001
UL1703 Certified and Registered, UL Fire Safety Class C, CEC, FSEC

SOLAR by KYOCERA

ELECTRICAL SPECIFICATIONS

Standard Test Conditions (STC)
*STC = 1000 W/M² irradiance, 25°C module temperature, AM 1.5 spectrum**

	KD315GX-LPB	KD320GX-LPB	
P_{mp}	315	320	W
V_{mp}	39.8	40.1	V
I_{mp}	7.92	7.99	A
V_{oc}	49.2	49.5	V
I_{sc}	8.50	8.60	A
$P_{tolerance}$	+5/-3	+5/-3	%

Nominal Operating Cell Temperature Conditions (NOCT)
*NOCT = 800 W/M² irradiance, 20°C ambient temperature, AM 1.5 spectrum**

T_{NOCT}	45	45	°C
P_{max}	226	230	W
V_{mp}	35.8	36.1	V
I_{mp}	6.34	6.40	A
V_{oc}	45.0	45.3	V
I_{sc}	6.88	6.96	A
PTC	276.4	280.9	W

Temperature Coefficients

P_{max}	-0.46	-0.45	%/°C
V_{mp}	-0.52	-0.51	%/°C
I_{mp}	0.0064	0.0065	%/°C
V_{oc}	-0.36	-0.36	%/°C
I_{sc}	0.061	0.060	%/°C
Operating Temp	-40 to +90	-40 to +90	%/°C

System Design

Series Fuse Rating	15 A
Maximum DC System Voltage (UL)	600 V
Hailstone Impact	1in (25mm) @ 51mph (23m/s)

* Subject to simulator measurement uncertainty of +/- 3%.
KYOCERA reserves the right to modify these specifications without notice.

NEC 2008 COMPLIANT
UL 1703 LISTED

MODULE CHARACTERISTICS

Dimensions: *length/width/height*	**65.43in/51.97in/1.8in (1662mm/1320mm/46mm)**
Weight:	**60.6lbs (27.5kg)**

PACKAGING SPECIFICATIONS

Modules per pallet:	**20**
Pallets per 53' container:	**22**
Pallet box dimensions: *length/width/height*	**66in/53in/47in (1675mm/1330mm/1190mm)**
Pallet box weight:	**1323 lbs (600kg)**

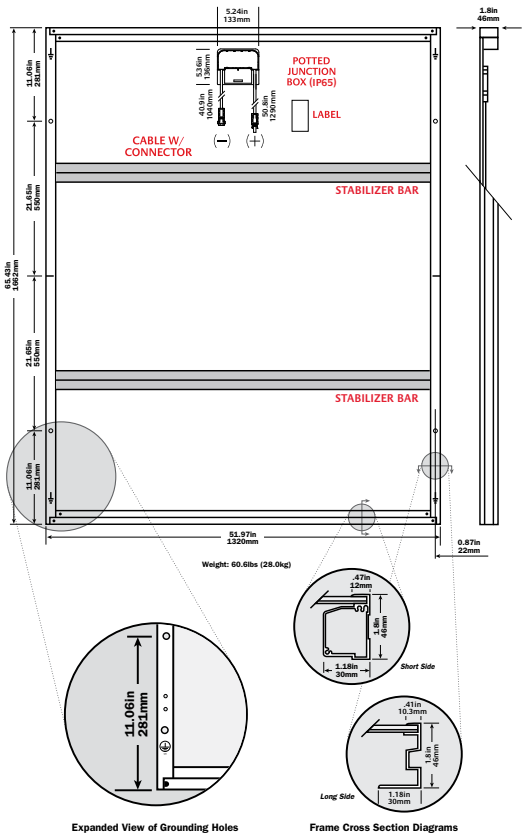

WARNING: Read the instruction manual in its entirety prior to handling, installing & operating Kyocera Solar modules.

Legend
MOUNTING HOLES .35in (9mm) DRAINAGE HOLES GROUND SYMBOL .35in (9mm)

040513

OUR VALUED PARTNER

KYOCERA Solar, Inc. 800-223-9580 800-523-2329 fax www.kyocerasolar.com

Appendix C

First Solar PV Module Datasheet

First Solar Series 4™ PV Module

ADVANCED THIN FILM SOLAR TECHNOLOGY

117.5 WATT MODULE EFFICIENCY OF 16.3%

INDUSTRY BENCHMARK SOLAR MODULES

As a global leader in PV energy, First Solar's advanced thin film solar modules have set the industry benchmark with over 10 gigawatts (GW) installed worldwide and a proven performance advantage over conventional crystalline silicon solar modules. Generating more energy than competing modules with the same power rating, First Solar's Series 4™ and Series 4A™ PV Modules deliver superior performance and reliability to our customers.

PROVEN ENERGY YIELD ADVANTAGE

- Generates more energy than conventional crystalline silicon solar modules with the same power
- Superior temperature coefficient resulting in greater energy yield in typical field operating temperatures
- Superior spectral response resulting in a proven energy yield advantage in humid environments
- Anti-reflective coated glass (Series 4A™) enhances energy production

ADVANCED PERFORMANCE & RELIABILITY

- Long-term power-output warranted for 25 years
- Compatible with advanced 1500V plant architectures
- Highly predictable energy in all climates and applications
- Independently certified for reliable performance in high temperature, high humidity, extreme desert and coastal environments based on accelerated life and stress tests

CERTIFICATIONS & TESTS

- PID-Free, Thresher Test, Long-Term Sequential Test, and ATLAS 25+[1]
- IEC 61646 1500V, IEC 61730 1500V, CE
- IEC 61701 Salt Mist Corrosion, IEC 60068-2-68 Dust and Sand Resistance
- ISO 9001:2008 and ISO 14001:2004
- UL 1703 and ULC 1703 Listed Class B Fire Rating (Class A Spread of Flame)
- CSI Eligible (CA-USA), FSEC (FL-USA), MCS (UK), CEC Listed (Australia), JET (Japan)[2], SII (Israel), InMetro (Brazil)[2]

MODULE WARRANTY[3]

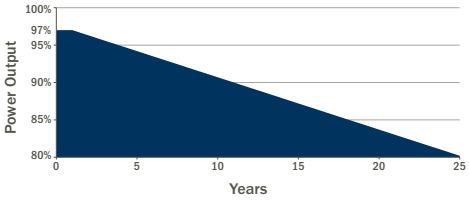

- 25-Year Linear Performance Warranty[4]
- 10-Year Limited Product Warranty

First Solar, Inc. | firstsolar.com | info@firstsolar.com

PD-5-401-04-2 | December 2015

FIRST SOLAR SERIES 4™ PV MODULE

MECHANICAL DESCRIPTION	
Length	1200mm
Width	600mm
Weight	12kg
Thickness	6.8mm
Area	0.72m²
Leadwire	2.5mm², 610mm
Connectors	MC4[9]
Bypass Diode	None
Cell Type	Thin-film CdTe semiconductor, up to 216 cells
Frame Material	None
Front Glass	3.2mm heat strengthened Series 4A™ includes anti-reflective coating
Back Glass	3.2mm tempered
Encapsulation	Laminate material with edge seal
Load Rating	2400Pa[10]

MODULE NUMBERS AND RATINGS AT STC[5,6]							
NOMINAL VALUES		FS-4105-2 FS-4105A-2	FS-4107-2 FS-4107A-2	FS-4110-2 FS-4110A-2	FS-4112-2 FS-4112A-2	FS-4115-2 FS-4115A-2	FS-4117-2 FS-4117A-2
Nominal Power (± 5%)	P_{MPP} (W)	105.0	107.5	110.0	112.5	115.0	117.5
Voltage at P_{MAX}	V_{MPP} (V)	67.8	68.6	69.4	70.2	70.5	71.2
Current at P_{MAX}	I_{MPP} (A)	1.55	1.57	1.59	1.60	1.63	1.65
Open Circuit Voltage	V_{OC} (V)	86.0	86.6	87.2	87.7	87.8	88.2
Short Circuit Current	I_{SC} (A)	1.74	1.75	1.75	1.75	1.78	1.79
Module Efficiency	%	14.6	14.9	15.3	15.6	16.0	16.3
Maximum System Voltage	V_{SYS} (V)	1500 [7]					
Limiting Reverse Current	I_R (A)	4.0					
Maximum Series Fuse	I_{CF} (A)	4.0					
MODULE NUMBERS AND RATINGS AT 800W/m², NOCT[8] 45°C, AM 1.5 [6]							
Nominal Power (± 5%)	P_{MPP} (W)	78.3	80.1	82.0	83.9	85.8	87.6
Voltage at P_{MAX}	V_{MPP} (V)	62.6	63.1	64.1	65.0	65.5	65.9
Current at P_{MAX}	I_{MPP} (A)	1.25	1.27	1.28	1.29	1.31	1.33
Open Circuit Voltage	V_{OC} (V)	81.0	81.6	82.1	82.6	82.7	83.1
Short Circuit Current	I_{SC} (A)	1.40	1.41	1.41	1.41	1.44	1.44
TEMPERATURE CHARACTERISTICS							
Module Operating Temperature Range	(°C)	-40 to +85					
Temperature Coefficient of P_{MPP}	T_K (P_{MPP})	-0.34%/°C					
Temperature Coefficient of V_{OC}	T_K (V_{OC})	-0.29%/°C					
Temperature Coefficient of I_{SC}	T_K (I_{SC})	+0.04%/°C					

SUPERIOR TEMPERATURE COEFFICIENT

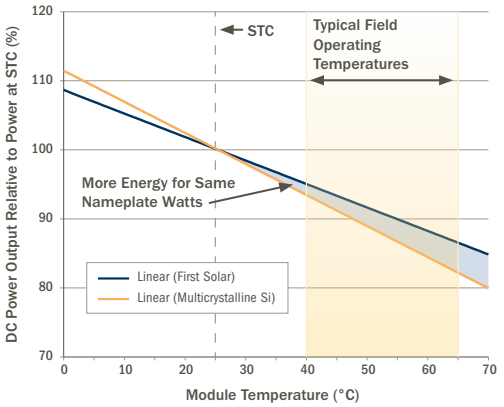

MECHANICAL DRAWING

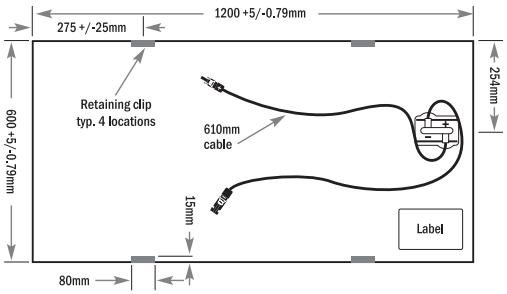

END-OF-LIFE RECYCLING

- Recycling services available through First Solar's industry-leading recycling program or customer-selected third party.

1 Device package meets ATLAS 25+.
2 Testing Certifications/Listings pending.
3 Limited power output and product warranties subject to warranty terms and conditions.
4 Ensures 97% rated power in first year, -0.7%/year through year 25.
5 Standard Test Conditions (STC) 1000W/m², AM 1.5, 25°C
6 All ratings ±10%, unless specified otherwise. Specifications are subject to change.
7 Application Class A for 1000V (class II), Application Class B for 1500V (class 0)
8 Nominal Operating Cell Temperature: Module operation temperature at 800W/m² irradiance, 20°C air temperature, 1m/s wind speed.
9 Multi-Contact MC4 (PV-KST4/PV-KBT4)
10 Higher load ratings can be met with additional clips or wider clips, subject to testing

List of References

[1] W. Moomaw, P. Burgherr, G. Heath, M. Lenzen, J. Nyboer, and A. Verbruggen, "Annex II: Methodology," *IPCC Special Report on Renewable Energy Sources and Climate Change Mitigation*, vol. 16, no. 10, p. NP, 2014. [Online]. Available: http://www.ncbi.nlm.nih.gov/pubmed/25180255

[2] N. M. Haegel, R. Margolis, T. Buonassisi, D. Feldman, A. Froitzheim, R. Garabedian, M. Green, S. Glunz, H.-M. Henning, B. Holder, I. Kaizuka, B. Kroposki, K. Matsubara, S. Niki, K. Sakurai, R. A. Schindler, W. Tumas, E. R. Weber, G. Wilson, M. Woodhouse, and S. Kurtz, "Terawatt-scale photovoltaics: Trajectories and challenges," *Science*, vol. 356, no. 6334, pp. 141–143, 2017. [Online]. Available: http://www.sciencemag.org/lookup/doi/10.1126/science.aal1288

[3] Solargis, "Free download of global and regional solar resource maps / Overview | Solargis." [Online]. Available: http://solargis.com/products/maps-and-gis-data/free/overview/

[4] Earthworks Magazine, "South Africa's renewable energy projects - Earthworks magazine South Africa." [Online]. Available: http://earthworksmagazine.co.za/south-africas-renewable-energy-projects/

[5] NREL SAM U.S. Department of Energy Office of Energy Efficiency and Renewable Energy, "System Advisor Model (SAM)." [Online]. Available: https://sam.nrel.gov/

[6] G. M. Masters, *Wind Power Systems, in Renewable and Efficient Electric Power Systems*, 2nd ed. Wiley, John & Sons, 2004.

[7] Earthworks, "South Africa's renewable energy projects - Earthworks magazine South Africa." [Online]. Available: http://earthworksmagazine.co.za/south-africas-renewable-energy-projects/

[8] C. Colp, "Cost-saving PV source-circuit wiring method," *7.3*, 2014.

[9] J. Skye, "Why Is Renewable Energy Needed?" [Online]. Available: http://greenliving.lovetoknow.com/Why_Do_We_Need_Renewable_Energy

[10] B. Goss, "Design process optimisation of solar photovoltaic systems," Ph.D. dissertation.

[11] BBC, "BBC Bitesize - Higher Geography - Reasons for increase in demand for energy - Revision 1." [Online]. Available: http://www.bbc.co.uk/education/guides/zpmmmp3/revision/1

[12] C. Philibert, "Three Reasons Why Renewable Energy Is So Important To The Power Industry | Power Conversion." [Online]. Available: https://www.gepowerconversion.com/inspire/three-reasons-why-renewable-energy-so-important-po

[13] UCSUSA, "Benefits of Renewable Energy Use | Union of Concerned Scientists." [Online]. Available: http://www.ucsusa.org/clean-energy/renewable-energy/public-benefits-of-renewable-power#.WWy

[14] INTERNATIONAL ENERGY AGENCY, "Snapshot of Global Photovoltaic Markets," pp. 1–16, 2016.

[15] Energy Trend, "PV Price Quotes." [Online]. Available: http://pv.energytrend.com/pricequotes.html

[16] S. Ringbeck and J. Sutterlueti, "BoS costs: status and optimization to reach industrialgrid parity," *Prog. Photovolt: Res. Appl.*, vol. 27, no. February 2013, pp. 659–676, 2012. [Online]. Available: http://dx.doi.org/10.1002/pip.1160

[17] Department of Energy, *State of Renewable Energy in Souh Africa*, 2015, vol. 14, no. 3. [Online]. Available: http://www.tandfonline.com/doi/abs/10.1080/21550085.2011.605855

[18] L.-A. Steenkamp, "Powering up: A look at section 12B allowance for renewable energy machinery - The SA Institute of Tax Professionals." [Online]. Available: http://www.thesait.org.za/news/269950/Powering-up-A-look-at-section-12B-allowance-for-renewab

[19] Green Energy Solutions, "Updated SARS Tax Incentive for Solar Power!" [Online]. Available: http://www.greenenergysolutions.co.za/updated-sars-tax-incentive-for-solar-power/

[20] City Power Johannesburg, "CITY OF JOHANNESBURG TARIFFS." [Online]. Available: https://www.citypower.co.za/customers/Pages/Tariff-Info.aspx

[21] Electricity Services Department and Environmental Resource Management Department of the City of Cape Town, "Safe and Legal Installations of Rooftop Photovoltaic Systems," pp. 2–3, 2016. [Online]. Available: http://resource.capetown.gov.za/documentcentre/Documents/Procedures, guidelines and regulations/Safe and Legal PV installations March 2016.pdf

[22] eThikwini Municipality, "eThikwini MunicipalityTariffs." [Online]. Available: http://www.durban.gov.za/City_Services/electricity/Tariffs/Pages/default.aspx

[23] Green Business Guide, "Reverse metering in the Nelson Mandela Bay Metro - The Green Business GuideThe Green Business Guide." [Online]. Available: http://www.greenbusinessguide.co.za/reverse-metering-in-the-nelson-mandela-bay-metro/

[24] SAURAN, "SAURAN network - Southern African Universities Radiometric Network." [Online]. Available: http://www.sauran.net/Page/About

[25] A. Nakumuryango and R. Inglesi-Lotz, "South Africa's performance on renewable energy and its relative position against the OECD countries and the rest of Africa," *Renewable and Sustainable Energy Reviews*, vol. 56, pp. 999–1007, 2016. [Online]. Available: http://dx.doi.org/10.1016/j.rser.2015.12.013

[26] P. Grana,Paul; Gibbs, "The 3 Best Ways to Optimize a Commercial PV System." [Online]. Available: https://www.greentechmedia.com/articles/read/The-3-Best-Ways-to-Optimize-a-Commercial-PV-S

[27] K. Joyce, "Optimizing PV Plant Design to Achieve a Low Levelized Cost of Energy by," pp. 1–8. [Online]. Available: http://bv.com/docs/reports-studies/optimizing-pv-plant-design-to-achieve-a-low-levelized-cost-of-e

[28] Merriam-Webster, "Dictionary and Thesaurus | Merriam-Webster," 2015. [Online]. Available: http://www.merriam-webster.com/

[29] R. Terlinden, T. Fricke, A. Linke, and C. Rost, "Redefining Bankability in Utility-Scale PV | Sunny. The SMA Corporate Blog." [Online]. Available: https://en.sma-sunny.com/en/redefining-bankability-in-utility-scale-pv/

[30] G. Algermissen, "Bankability: What it Means and Why it is Important for Your Solar Project," 2015. [Online]. Available: https://blog.pickmysolar.com/solar-bankability-what-it-means-and-why-it-is-important

[31] Folsom Labs, "Optimizing a Solar Array's Tilt and Module Spacing | AltEnergyMag." [Online]. Available: http://www.altenergymag.com/content.php?post_type=2372

[32] I. Woofenden, "ENERGY BASICS: PV System Types | Home Power Magazine." [Online]. Available: https://www.homepower.com/articles/solar-electricity/equipment-products/energy-basics-pv-syste

[33] Solar Las Vegas, "Solar Power - The 7 Main Types of Photovoltaic (PV) Systems - Universal Solar Direct." [Online]. Available: https://www.universalsolardirect.com/solar-power-the-7-main-types-of-photovoltaic-pv-systems/

[34] Aladdin Solar LLC., "PV System Types: Grid-Tied, Battery Backup, Off-Grid, Direct PV." [Online]. Available: http://www.aladdinsolar.com/pvsystems.html

[35] National Grid UK, "Grid code." [Online]. Available: http://www2.nationalgrid.com/UK/Industry-information/Electricity-codes/Grid-Code/

[36] Florida Solar Energy Center, "How a PV System Works." [Online]. Available: http://www.fsec.ucf.edu/en/consumer/solar_electricity/basics/how_pv_system_works.htm

[37] J. F. Orgill and K. G. T. Hollands, "Correlation equation for hourly diffuse radiation on a horizontal surface," *Solar Energy*, vol. 19, no. 4, pp. 357–359, 1977.

[38] D. G. Erbs, S. A. Klein, and J. A. Duffie, "Estimation of the diffuse radiation fraction for hourly, daily and monthly-average global radiation," *Solar Energy*, vol. 28, no. 4, pp. 293–302, 1982.

[39] E. L. Maxwell, "A quasi-physical model for converting hourly global to direct normal insolation," pp. 35–46, 1987. [Online]. Available: http://rredc.nrel.gov/solar/pubs/PDFs/TR-215-3087.pdf

[40] P. G. Loutzenhiser, H. Manz, C. Felsmann, P. A. Strachan, T. Frank, and G. M. Maxwell, "Empirical validation of models to compute solar irradiance on inclined surfaces for building energy simulation," *Solar Energy*, vol. 81, no. 2, pp. 254–267, 2007.

[41] A. Louche, G. Notton, P. Poggi, and G. Simonnot, "Correlations for direct normal and global horizontal irradiation on a French Mediterranean site," *Solar Energy*, vol. 46, no. 4, pp. 261–266, 1991.

[42] R. Perez, "Article Dynamic global-to-direct irradiance conversion models," vol. 98, no. 1, pp. 354–369, 2015.

[43] B. Y. Liu and R. C. Jordan, "The interrelationship and characteristic distribution of direct, diffuse and total solar radiation," *Solar Energy*, vol. 4, no. 3, pp. 1–19, 1960. [Online]. Available: http://linkinghub.elsevier.com/retrieve/pii/0038092X60900621

[44] T. M. Klucher, "Evaluation of models to predict insolation on tilted surfaces," *Solar Energy*, vol. 23, no. 2, pp. 111–114, 1979.

[45] R. Perez, P. Ineichen, R. Seals, J. Michalsky, and R. Stewart, "Modeling daylight availability and irradiance components from direct and global irradiance," *Solar Energy*, vol. 44, no. 5, pp. 271–289, 1990.

[46] J. E. Hay, "Calculating solar radiation for inclined surfaces: Practical approaches," *Renewable Energy*, vol. 3, no. 4-5, pp. 373–380, 1993.

[47] International Finance Corporation, "Utility-Scale Solar Photovoltaic Power Plants."

[48] C. Budig, J. Orozaliev, and K. Vajen, "Comparison of Different Sources of Meteorological Data for Central Asia and Russia," *EuroSun 2010*, p. 8, 2010.

[49] T. Mahachi and A. J. Rix, "COMPARISON OF VARIOUS LONG TERM AVERAGED METEOROLOGICAL DATA SOURCES Conference Paper · January 2017," no. February, 2017.

[50] Solar Green Australia, "The Three Types of Solar Cells." [Online]. Available: http://www.solargreen.net.au/the-three-types-of-solar-cells.html

[51] Energy Informative, "Which Solar Panel Type is Best? Mono-, Polycrystalline or Thin Film?" [Online]. Available: http://energyinformative.org/best-solar-panel-monocrystalline-polycrystalline-thin-film/

[52] J. Chase, "Bloomberg New Energy Finance PV Module Maker Tiering System," no. July, pp. 1–4, 2014.

[53] Arup, "First Solar Energy Yield Simulations Module Performance Comparison for Four Solar PV Module Technologies," no. 1, 2015.

[54] C. Deline, A. Dobos, S. Janzou, J. Meydbray, and M. Donovan, "A simplified model of uniform shading in large photovoltaic arrays," *Solar Energy*, vol. 96, pp. 274–282, 2013. [Online]. Available: http://dx.doi.org/10.1016/j.solener.2013.07.008

[55] PVSyst, "PVSyst Software." [Online]. Available: http://www.pvsyst.com/en/software

[56] T. Mahachi, "Energy yield analysis and evaluation of solar irradiance models for a utility scale solar PV plant in South Africa," no. December, 2016.

[57] M. Lalwani, M; Kothari, D.P; Singh, "Investigation of Solar Photovoltaic Simulation Softwares," vol. 1, no. 3, pp. 585–601, 2010.

[58] "Optimum Tilt of Solar Panels." [Online]. Available: http://www.solarpaneltilt.com/

[59] "About Us | Black & Veatch." [Online]. Available: https://www.bv.com/about-us

[60] A. Engineering, "A study into the optimisation and calculation of electrical losses in renewable energy generation," 2014.

[61] M. L. Louazene, D. Korichi, and B. Azoui, "Optimization of global solar radiation of tilt angle for solar panels, location: Ouargla, algeria," *Journal of Electrical Engineering*, vol. 13, no. 1, pp. 106–111, 2013.

[62] X. Gong and M. Kulkarni, "Design optimization of a large scale rooftop photovoltaic system," *Solar Energy*, vol. 78, no. 3, pp. 362–374, 2005.

[63] D. Del Vecchio, "Optimizing a PV Array with Orientation & Tilt | Home Power Magazine." [Online]. Available: https://www.homepower.com/articles/solar-electricity/design-installation/optimizing-pv-array-orie

[64] G. Warner, "Solar energy in South Africa Challenges and opportunities." [Online]. Available: http://www.solarcentury.com/za/media-centre/solar-energy-south-africa-challenges-opportunities/

[65] D. Oliveira, "Northern Cape renewable Energy Mecca." [Online]. Available: http://www.engineeringnews.co.za/article/northern-cape-renewable-energy-mecca-joemat-pettersso

[66] W. F. Holmgren, R. W. Andrews, A. T. Lorenzo, and J. S. Stein, "PVLIB Python 2015," *42nd IEEE PVSC*, pp. 1–5, 2015.

[67] Sandia National Labs and R. Andrews, "PVLIB _ Python Documentation," 2016.

[68] "Project Jupyter | About." [Online]. Available: http://jupyter.org/about.html

[69] Python Software Foundation, "About Python." [Online]. Available: https://www.python.org/about/

[70] PVSyst, "PVSyst Software Development." [Online]. Available: http://www.pvsyst.com/en/software/software-development

[71] NREL SAM U.S. Department of Energy Office of Energy Efficiency and Renewable Energy, "System Advisor Model (SAM) Release Notes." [Online]. Available: https://sam.nrel.gov/sites/default/files/content/updates/releasenotes.html

[72] W. F. Holmgren, "PVLib-python release notes," 2016. [Online]. Available: https://github.com/pvlib/pvlib-python/releases

[73] SAM Analysis Options, "SAM Help - Analysis Options." [Online]. Available: https://www.nrel.gov/analysis/sam/help/html-php/index.html?samul_write_a_simple_script.ht

[74] Z. Ren, S. Jacques, S. Bissey, N. Batut, A. Schellmanns, and A. Caldeira, "PVLab: an innovative and flexible simulation tool to better size photovoltaic units," *Renewable Energies and Power Quality Journal*, vol. 1, no. 12, 2014. [Online]. Available: http://www.icrepq.com/icrepq%2714/241.14-Ren.pdf

[75] "SAM Open Source | System Advisor Model (SAM)." [Online]. Available: https://sam.nrel.gov/opensource

[76] PVLib-python, "PVLib-python Modules." [Online]. Available: http://pvlib-python.readthedocs.io/en/latest/modules.html

[77] A. P. Dobos, "LK Scripting Language Reference," pp. 1–46, 2015.

[78] Timeanddate, "Seasons: Meteorological and Astronomical." [Online]. Available: https://www.timeanddate.com/calendar/aboutseasons.html

[79] D. Chung, C. Davidson, R. Fu, K. Ardani, and R. Margolis, "U.S. Photovoltaic Prices and Cost Breakdowns : Q1 2015 Benchmarks for Residential , Commercial , and Utility-Scale Systems," *National Renewable Energy Laboratory*, no. September, p. 42, 2015. [Online]. Available: http://www.nrel.gov/docs/fy15osti/64746.pdf

[80] K. Trabish, Herman, "Better, More Bankable Solar PV Installation Designs From Any Computer? | Greentech Media." [Online]. Available: https://www.greentechmedia.com/articles/read/better-faster-bankable-solar-pv-installation-design

[81] BEW, "Bew Engineering." [Online]. Available: http://bewengineering.co.uk/

[82] SunPeak, "SunPeak's solar installation technology; East West panel orientation | SunPeak." [Online]. Available: https://www.sunpeakpower.com/sunpeak-technology-details

[83] A. Mellit, S. A. Kalogirou, L. Hontoria, and S. Shaari, "Artificial intelligence techniques for sizing photovoltaic systems: A review," *Renewable and Sustainable Energy Reviews*, vol. 13, no. 2, pp. 406–419, 2009.

[84] D. Gómez-Lorente, I. Triguero, C. Gil, and A. E. Estrella, "Evolutionary algorithms for the design of grid-connected PV-systems," *EXPERT SYSTEMS WITH APPLICATIONS*, 2012.

[85] S. Sinha and S. Chandel, "Review of recent trends in optimization techniques for solar photovoltaic-wind based hybrid energy systems," *Renewable and Sustainable Energy Reviews*, vol. 50, pp. 755–769, 2015. [Online]. Available: http://linkinghub.elsevier.com/retrieve/pii/S1364032115005006

[86] S. Sreedhar and D. Jagadeesh, "A Review on Optimization Algorithms for MPPT in Solar PV System under Partially Shaded Conditions," pp. 23–32, 2016.

[87] a. Kornelakis and E. Koutroulis, "Methodology for the design optimisation and the economic analysis of grid-connected photovoltaic systems," *IET Renewable Power Generation*, vol. 3, no. July 2008, p. 476, 2009.

[88] A. Kornelakis, "Multiobjective Particle Swarm Optimization for the optimal design of photovoltaic grid-connected systems," *Solar Energy*, vol. 84, pp. 2022–2033, 2010.

[89] A. Kornelakis and Y. Marinakis, "Contribution for optimal sizing of grid-connected PV-systems using PSO," *Renewable Energy*, vol. 35, no. 6, pp. 1333–1341, 2010. [Online]. Available: http://dx.doi.org/10.1016/j.renene.2009.10.014

[90] D. Weinstock and J. Appelbaum, "Optimal Solar Field Design of Stationary Collectors," *Journal of Solar Energy Engineering*, vol. 126, no. 3, p. 898, 2004. [Online]. Available: http://solarenergyengineering.asmedigitalcollection.asme.org/article.aspx?articleid=1457085

[91] D. Szubert, "Lire la première p a rtie de la thèse," 2015. [Online]. Available: http://ethesis.inp-toulouse.fr/archive/00002416/02/perez_gallardo_partie_2_sur_2.pdf

[92] D. A. Coley, "An Introduction to Genetic Algorithms for Scientists and Engineers."

[93] K. Yoon and C.-L. Hwang, *Multiple attribute decision making: an introduction*, 1995. [Online]. Available: http://books.google.com/books?hl=en&lr=&id=Fo47SWBuEyMC&oi=fnd&pg=PP8&dq=Multip

[94] C. Doctorale, "0Rïsentïe Et Soutenue Par," *Sciences-New York*, pp. 0–180, 2011.

[95] C. Azzaro-pantel, E. Nationale, G. Hernandez-rodriguez, F. Morales-mendoza, L. Pibouleau, C. Azzaro-pantel, S. Domenech, and A. Ouattara, "Applications of Metaheuristics in Process Engineering," no. April, 2014. [Online]. Available: http://link.springer.com/10.1007/978-3-319-06508-3

[96] M. Boix, L. Montastruc, L. Pibouleau, C. Azzaro-Pantel, and S. Domenech, "A multiobjective optimization framework for multicontaminant industrial water network design," *Journal of Environmental Management*, vol. 92, no. 7, pp. 1802–1808, 2011.

[97] A. S. Milani, A. Shanian, R. Madoliat, and J. A. Nemes, "The effect of normalization norms in multiple attribute decision making models: A case study in gear material selection," *Structural and Multidisciplinary Optimization*, vol. 29, no. 4, pp. 312–318, 2005.

[98] A. Çelen, "Comparative analysis of normalization procedures in TOPSIS method: with an application to Turkish deposit banking market," *Informatica*, vol. 25, no. 2, pp. 185–208, 2014.

[99] Folsom Labs, "Mechanical Design." [Online]. Available: https://www.folsomlabs.com/modeling/design/mechanical

[100] International Renewable Energy Agency, *Solar Pv in Africa: Costs and Markets*, 2016, no. September.